

FUNCTIONAL ANALYSIS OF A NOVEL MUTATION IN THE CD70 GENE
LEADING TO PRIMARY IMMUNODEFICIENCY DISEASE

by
SEDEN BEDİR

Submitted to the Graduate School of Engineering and Natural Sciences
in partial fulfilment of
the requirements for the degree of Master of Science

Sabancı University
July 2020

FUNCTIONAL ANALYSIS OF A NOVEL MUTATION IN THE CD70 GENE
LEADING TO PRIMARY IMMUNODEFICIENCY DISEASE

APPROVED BY:

Prof. Dr. Batu Erman
(Thesis Supervisor)

Asst. Prof. Dr. Tolga Stl
(Thesis Co-supervisor)

Prof. Dr. Selim etiner

Prof. Dr. Ahmet zen

Prof. Dr. Safa Barıř

DATE OF APPROVAL: 28/07/2020

SEDEN BEDİR 2020 ©

All Rights Reserved

ABSTRACT

FUNCTIONAL ANALYSIS OF A NOVEL MUTATION IN THE CD70 GENE LEADING TO PRIMARY IMMUNODEFICIENCY DISEASE

SEDEN BEDİR

Molecular Biology, Genetics and Bioengineering, MSc. Thesis, July 2020

Thesis Supervisor: Prof. Dr. Batu Erman

Thesis Co-Supervisor: Assist. Prof. Dr. Tolga Sütlü

Keywords: Co-stimulation, CD70 deficiency, EBV, lymphoproliferative disorder, primary immunodeficiency disease, lentiviral vectors, transduction, flow cytometry

Immunity is the broad definition that embodies all protective mechanisms employed by the body against pathogens. T cell activation is central to a functional immune response, as T cells are fully activated by antigen-specific-interactions, co-stimulation, and instructive cytokines, according to the three-signal hypothesis. Primary immunodeficiencies (PIDs) are the heterogenous group of congenial immune system defects that result in either partial or complete loss of immune responses against pathogens. Individuals with the PIDs are highly prone to recurrent infections. Epstein-Bar virus (EBV) is a ubiquitous oncogenic virus that is mostly asymptomatic, yet it can cause lymphoproliferative disorders (LPDs) in individuals with genetic defects. In this thesis, we identified a novel point mutation in the CD70 gene that leads to EBV-associated PID. The CD27/CD70 signalling pathway was previously shown to be responsible for the expansion and maintenance of EBV-specific CD8⁺ T cells, and humoral immunity. To analyze further, we generated stable cell lines through HIV-1 based lentiviral vector production, and transduction to transfer the wild-type and mutant CD70 proteins to K-562 and Namalwa cell lines. We performed cell surface and intracellular staining experiments to investigate wild-type and mutant CD70 gene products with flow cytometry. We also aimed to construct an *in vitro* functional assay employing CD27-Fc fusion protein production to evaluate the functionality of the identified CD70 mutations. Overall, we report a novel mutation in the CD70 gene that causes CD70 deficiency that can potentially contribute to the diagnosis of the suspected PID cases.

ÖZET

CD70 GENİNDEKİ PRİMER İMMÜN YETERSİZLİK HASTALIĞINA SEBEP OLAN YENİ BİR MUTASYONUN FONKSİYONEL ANALİZİ

SEDEN BEDİR

Moleküler Biyoloji, Genetik ve Biyomühendislik, Yüksek Lisans Tezi, Temmuz 2020

Tez Danışmanı: Prof. Dr. Batu Erman

Tez Eş-Danışmanı: Dr. Öğr. Üyesi Tolga Sütü

Anahtar Kelimeler: Ko-stimulasyon, CD70 eksikliği, EBV, lenfoproliferatif hastalık, primer bağışıklık yetmezlik, lentiviral vektörler, transdüksiyon, akış sitometrisi

Bağışıklık vücudu patojenlerden koruyan tüm mekanizmaların genel bir tanımıdır. T hücrelerinin aktivasyonu fonksiyonel bağışıklık tepkilerinin oluşturulması için temel bir rol oynar, ve T hücrelerinin aktivasyonu üç-sinyal hipotezine göre antijen-spesifik etkileşimler, ko-stimulasyon ve yardımcı sitokinler sayesinde olur. Primer bağışıklık yetmezlikleri (PIY), bağışıklık sisteminin kısmi veya tam olarak fonksiyonunu doğuştan gelen mutasyonlar sebebiyle kaybetmesiyle ortaya çıkar. PIY tanılı bireyler yinelenen enfeksiyonlara yatkındır. Epstein-Bar Virus (EBV) tümöre neden olan yaygın bir virüstür. bu virüs çoğunlukla asemptomatiktir, fakat genetik bozukluğu olan bireylerde lenfoproliferatif hastalıklara neden olabilir. Bu çalışmada, CD70 geninde EBV-ilişkili PIY'e neden olan yeni bir nokta mutasyonu keşfettik. CD27/CD70 sinyal yolağının, EBV'ye özgün CD8+ T lenfosit hücrelerinin çoğalması, sürdürülebilirliği ve humoral bağışıklık için önemi önceden gösterilmiştir. Bu mutant CD70 molekülünün etkilerini daha detaylı araştırmak için, HIV-1 temelli lentiviral vektörlerin üretimi ve transdüksiyonu ile yabancı-tip ve mutant CD70 proteinlerini K-562 ve Namalwa hücre hatlarına aktardık. Akış sitometrisi ile hücre yüzeyi ve içeri boyayarak yabancı-tip ve mutant CD70 proteinlerinin ifadesini araştırdık. Ek olarak, CD27-Fc füzyon proteini üretip belirlediğimiz mutasyonların *in vitro* fonksiyonel analizini sınavan bir yöntem geliştirmeyi amaçladık. Sonuç olarak, CD70 geninde CD70 eksikliğine sebep olan yeni bir mutasyonu tespit ettik, bu çalışma PIY şüphesi olan bireylerde teşhis için katkı sağlayabilecek niteliktedir.

ACKNOWLEDGEMENTS

Firstly, I would like to express my sincerest gratitude to my thesis supervisor Prof. Dr. Batu Erman for his continuous guidance, encouragement, and support during my thesis period. I have developed myself substantially thanks to the fruitful scientific discussions we had with my supervisor. Therefore, I would like to thank him for providing me with this opportunity to study within a genuinely rewarding scientific environment. I also would like to thank my co-supervisor Assist. Prof. Dr. Tolga Sütü for his scientific guidance, and support throughout my studies. I would like to express my deep gratitude to him, since he has provided me with this great opportunity to join his lab during a critical step of my career. I am truly honored to complete my thesis under supervision of both Prof. Batu Erman and Assist. Prof. Tolga Sütü. I would like to thank all jury members of mine Prof. Dr. Ahmet Özen, Prof. Dr. Safa Barış and Prof. Dr. Selim Çetiner for accepting to be in my thesis jury, and their contribution to my thesis with their feedbacks. Working within a kind and supportive lab environment had great impacts over my scientific development and interpersonal skills. Therefore, I would like to thank my current and former labmates Sarah Barakat, Melike Gezen, Liyne Noğay, Gülin Baran, Pegah Zahedimaram, Sofia Piepoli and Ronay Çetin. I have truly enjoyed working with you and your friendship, and thank you very much for your kindness, help and continuous support throughout my studies. I would like to especially thank Ronay Çetin for his great contribution to my thesis and the experiments he has conducted. The experiments he has performed were PBMC isolation, TOPO cloning for the mutation identification and their sanger sequencing, cloning wild-type and mutant CD70 into lentiviral backbones. I also would like to thank Işık Kantarcıoğlu for her contribution to my thesis, as she performed CD70 homology modelling. I would also thank Sütü Lab members Dr. Başak Özata, Ayhan Parlar, Ertunga Eyüpoğlu, Elif Çelik, Cevriye Pamukcu, Lolai Ikromzoda and Didem Özkazanç Ünsal for their help in my studies. I also would like to state that figures in this study were created with BioRender.com through my student monthly promo account, and they were exported under a paid subscription. I will always remember my gorgeous friends who have made my life happier every day on and off campus. I would like to express my heartfelt gratitude to my best friends Yusuf Ceyhun Erdoğan, Zeynep Çokluk, Büşra Ülger, İpek Bedir and Berk Uluğ for their endless friendship and support no matter what. I would like to thank my sweetest family, who has loved me and supported me every day of my life. I am looking forward to the next chapter of my life!

To my beloved sister...

Canım ablama...

TABLE OF CONTENTS

LIST OF TABLES	x
LIST OF FIGURES	xi
LIST OF SYMBOLS AND ABBREVIATIONS	xiii
1. INTRODUCTION	1
1.1. Immune System at a Glance.....	1
1.2. T Cell Activation at the Immunological Synapse.....	3
1.2.1. Antigen Recognition	7
1.2.2. Co-stimulation and Instructive Cytokines.....	9
1.3. The TNF/TNFR Superfamilies of Signalling Molecules.....	13
1.3.1. The Basis of Signal Transduction in the CD27/CD70 Pathway.....	17
1.4. Primary Immunodeficiency Diseases	21
1.4.1. Epstein-Barr Virus Infection and Primary Immunodeficiency Diseases ..	26
2. AIM OF THE STUDY.....	30
3. MATERIALS & METHOD	32
3.1. Materials.....	32
3.1.1. Chemicals	32
3.1.2. Equipment	32
3.1.3. Solution and Buffers	32
3.1.4. Growth Media.....	33
3.1.5. Molecular Biology Kits.....	34
3.1.6. Enzymes	34
3.1.7. Antibodies	34
3.1.8. Bacterial Strains.....	34
3.1.9. Mammalian Cell Lines.....	34
3.1.10. Plasmids and Oligonucleotides.....	35
3.1.11. DNA and Protein Molecular Weight Markers.....	41
3.1.12. DNA Sequencing	41

3.1.13. Software, Computer-based Programs, and Websites.....	41
3.2. Methods.....	43
3.2.1. Bacterial Cell Culture.....	43
3.2.2. Mammalian Cell Culture.....	45
3.2.3. Lentiviral Vector Production, Transduction and Flow Cytometry.....	46
3.2.4. Isolation of Human PBMCs and Total RNA.....	48
3.2.5. Vector Construction.....	49
3.2.6. Mammalian Expression Vector Construction.....	51
4. RESULTS.....	59
4.1. Mutation Identification in the CD70 Gene.....	59
4.2. Genetic Modification by Lentiviral Vectors and Flow Cytometry.....	63
4.3. Cloning Strategy for Human CD27-Fc Chimeric Protein Production.....	74
5. DISCUSSION.....	76
6. BIBLIOGRAPHY.....	79
APPENDIX A.....	92
APPENDIX B.....	93
APPENDIX C.....	94
APPENDIX D.....	94
APPENDIX E.....	95
APPENDIX F.....	96

LIST OF TABLES

Table 1.1 Topological and genomic features of CD27 and CD70 molecules	17
Table 1.2 Ten clinical symptoms considered as the warning signs of immunodeficiencies	22
Table 1.3 PID classification and main disorders belonging to adaptive and innate immune systems	23
Table 1.4 Genetic mutations that create susceptibility/resistance to viral infections	25
Table 3.1 List of plasmids	35
Table 3.2 List of oligonucleotides	39
Table 3.3 List of computer-based programs, software and websites	41

LIST OF FIGURES

Figure 1.1 Cells of innate and adaptive immunity.....	1
Figure 1.2 T cell cytotoxicity against a variety of pathogens.....	3
Figure 1.3 Brief overview of the immunological synapse	5
Figure 1.4 TCR signaling pathway	6
Figure 1.5 Structure of the TCR complex and MHC-restricted antigen recognition.....	8
Figure 1.6 Molecules responsible for co-stimulation: co-stimulatory receptors and their ligands	10
Figure 1.7 Three-signal hypothesis at the APC-T cell interface	11
Figure 1.8 Cytokines drive naïve CD4+ T cell fates.....	12
Figure 1.9 Mode of action for TNF/TNFR SFs.....	15
Figure 1.10 Bidirectional signalling through TNF/TNFR SFs.....	16
Figure 1.11 Life cycle of EBV in primary and persistent infections	27
Figure 1.12 Genetic mutations of CD8+ T cells causing susceptibility to EBV-driven PIDs.....	29
Figure 3.1 Isolation of PBMCs.....	49
Figure 4.1 Total RNA isolation and cDNA synthesis from PBMCs	60
Figure 4.2 The principle behind TOPO cloning, and gel images showing the diagnostic digests of TOPO cloned constructs.....	61
Figure 4.3 Sanger sequencing results for full-length amplified CD70 gene of the patient and his father.....	62
Figure 4.4 Updated exon and domain map of human CD70	62
Figure 4.5 Demonstration of principle of complementation, and self-inactivating lentiviral vectors.....	63
Figure 4.6 Cloning strategy for lentiviral vector construction to clone CD70wt and CD70mut into LeGO-iG2-puro and LeGO-iT2-puro backbones	64

Figure 4.7 Experimental steps of lentiviral vector construction for the stable expression of CD70wt and CD70mut in LeGO-iG2-puro and LeGO-iT2-puro backbones	65
Figure 4.8 Diagnostic digest results for lentiviral constructs with CD70wt and CD70mut in LeGO-iG2-puro and LeGO-iT2-puro backbones	65
Figure 4.9 Flow cytometry analysis for the generation of stable cell lines of K-562 and Namalwa cells.....	67
Figure 4.10 Flow cytometry analysis for CD70 detection on the cell surface of K-562 and Namalwa stable cell lines	68
Figure 4.11 MFI ratio plot, and values indicating the relative gene expression levels of CD70 in the stable cell lines of K-562 and Namalwa cells.....	69
Figure 4.12 Homology modelling of CD70 monomer and homotrimer	69
Figure 4.13 Flow cytometry histograms demonstrating intracellular staining for the stable cell lines of K-562	70
Figure 4.14 Flow cytometry analysis for CD70 detection on the cell surface of K-562 stable cell lines with a different antibody clone	71
Figure 4.15 Flow cytometry analysis for CD70 detection on the cell surface of Namalwa cells through single and double stainings.....	72
Figure 4.16 Site-directed mutagenesis, and cloning epitope-tagged CD70 expression cassettes into the LeGO-iG2-puro backbone	73
Figure 4.17 Experimental steps of lentiviral vector construction for the stable expression of epitope-tagged CD70wt, and CD70mut proteins in the LeGO-iG2-puro backbone ..	74
Figure 4.18 Cloning strategy for ligating two inserts in a single backbone for CD27-Fc fusion protein production	75

LIST OF SYMBOLS AND ABBREVIATIONS

α	Alpha
β	Beta
γ	Gamma
ϵ	Epsilon
κ	Gamma
γ	Kappa
ζ	Zeta
μg	microgram
μl	Microliter
μM	Micromolar
ADA	Adenosine deaminase
ALR	AIM2-like receptor
AP-1	Activator protein-1
APC	Allophycocyanin
APC	Antigen presenting cell
APRIL	A proliferation-inducing ligand
CaCl_2	Calcium chloride
CDR	Complementary determining region
CIAP	Calf intestinal alkaline phosphatase
CID	Combined immunodeficiency
CLR	C-type lectin receptor
CMV	Cytomegalovirus
CRD	Cysteine-rich domain
CO_2	Carbon dioxide
CVID	Common variable immunodeficiency
cSMAC	Central SMAC
cIAP	Cellular inhibitor of apoptosis-1
DAG	Diacylglycerol
DD	Death domain
ddH ₂ O	Distilled water
dSMAC	Distal SMAC
DMEM	Dulbecco's Modified Eagle Medium
DMSO	Dimethylsulfoxide
DNA	Deoxyribonucleic acid
DPBS	Dulbecco's phosphate-buffered saline
EBV	Epstein-Bar virus
<i>E. coli</i>	Escherichia coli
EDTA	Ethylenediaminetetraacetic acid
ER	Endoplasmic reticulum
FACS	Fluorescence activated cell sorter
FBS	Fetal Bovine Serum
GC	Germinal center
GFP	Green fluorescent protein
GM-CSF	Granulocyte-macrophage colony-stimulating factor
HBS	HEPES buffered saline

HLH	Hemophagocytic lymphohistiocytosis
ICAM-1	Intercellular adhesion molecule 1
ID	Immunodeficiency
IFN	Interferon
IL	Interleukin
IS	Immunological synapse
ITAM	Immunoreceptor tyrosine-based activation motif
KO	Knock-out
LeGO	Lentiviral gene ontology vectors
LFA-1	Lymphocyte function-associated antigen 1
LCMV	Lymphocytic choriomeningitis virus
LCL	Lymphoblastoid cell line
LPD	Lymphoproliferative disease
LTR	Long terminal repeat
MAPK	Mitogen-activated protein kinase
MEF	Mouse embryonic fibroblast
MHC	Major histocompatibility complex
MI	Milileter
mM	Milimolar
MOI	Multiplicity of infection
NFAT	Nuclear factor of activated T cells
NF κ B	Nuclear factor kappa B
NLR	Nucleotide-binding oligomerization domain-like receptor
NK	Natural killer cell
HSC	Hematopoietic stem cell
pMHC	Peptide-MHC complex
PAMP	Pathogen-associated molecular pattern
PBMC	Peripheral bone mononuclear cell
PID	Primary immunodeficiency disease
PRR	Pathogen recognition receptor
rpm	Rounds per minute
rSAP	Shrimp alkaline phosphatase
RAG	Recombination-activating gene
RCC	Renal cell carcinoma
RIG-I	Retinoic acid-inducible gene-I-like receptors
RPMI	Roswell Park Memorial Institute
sCD27	Soluble CD27
SCID	Severe combined immunodeficiency disorder
SF	Superfamily
SMAC	Supramolecular activation cluster
SID	Secondary immunodeficiency
T _H	Helper T cell
Tconv	Conventional T cell
Treg	Regulatory T cell
TCR	T cell receptor
TF	Transcription factor
TIL	Tumor infiltrating lymphocyte
THD	TNF homology domain
TNF- α	Tumor necrosis factor alpha
TNF	Tumor necrosis factor

TNFRF	Tumor necrosis factor receptor
TGF- β	Transforming growth factor beta
TRAF	TNFR-associated factor
TRAIL	TNF-related apoptosis-inducing ligand
VSV-G	Vesicular stomatitis virus G
XLA	X-linked agammaglobulinemia
WT	Wild-type

1. INTRODUCTION

1.1. Immune System at a Glance

The immune system has fascinatingly evolved to defend host from the world of rapidly-changing pathogens. Central function of the immune system is to differentiate between self and non-self along with healthy and unhealthy cells, and mount effective molecular defense mechanisms to further prevent or minimize the effects (Mostardinha & De Abreu, 2012). Immune system is further classified as innate and adaptive immune systems (Figure 1.1.). The Innate immune system has been described as the first line of defense against foreign molecules or organisms. To achieve this, the innate immune system exploits inflammatory signaling, complement activation, and physical barriers including mucous and skin layers to create an inhibitory environment after the initial encounter with a pathogen, which are disease-producing agents including bacteria and viruses. Upon this niche created by innate immune cells, recruitment and activation of adaptive immune cells are initiated so that inflammatory responses can be generated.

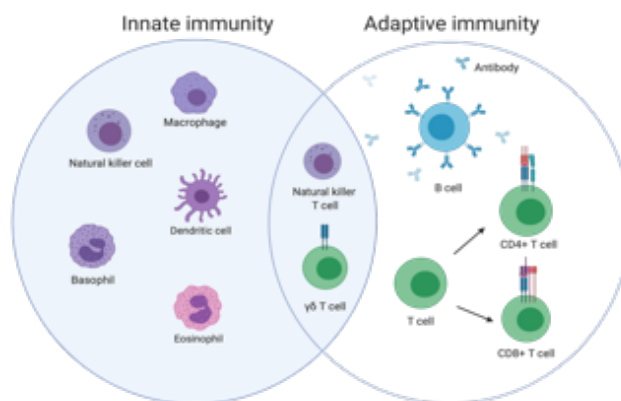


Figure 1.1 Cells of innate and adaptive immunity

Schematic representation of cells functioning in innate and adaptive immunity, together with cell types working at the interface of the two systems.

Innate immune responses are quick and robust responses that are mediated by dendritic cells, macrophages together with the help of non-professional cells such as fibroblasts (Jang et al., 2015). Pathogen-associated molecular patterns (PAMPs) are defined as the conserved molecular structures that do not belong to the host organism. Lipopolysaccharide is a very well-characterized example of PAMPs, that belongs to the outer membrane of gram-negative bacteria (Cochet & Peri, 2017). Recognition of PAMPs in the cytoplasm, endosomes or on the cell membrane is mediated by pattern recognition receptors (PRRs). Toll-like receptors (TLRs), nucleotide-binding oligomerization domain-like receptors (NLRs), C-type lectin receptors (CLRs) and retinoic acid-inducible gene-(RIG-)I-like receptors (RLRs) are the main types of PRRs found on innate immune cells (O. Takeuchi & Akira, 2010). Signaling through PRRs converge on Activator Protein-1 (AP-1), Nuclear Factor kappa B (NF κ B) and mitogen-activated protein kinase (MAPK) to upregulate the genes responsible for pro-inflammatory cytokines and chemokines including tumor necrosis factor alpha (TNF- α), interleukin-6 (IL-6), and IL-1 to drive enhanced cell survival, metabolic activity and inflammation to recruit adaptive immune cells to the site of infection (Liu, Zhang, Joo, & Sun, 2017).

Adaptive immunity is the second line of defense besides innate immunity. The adaptive immune system is responsible for the generation of antigen-specific immune responses through the action of recombination-activating gene (RAG) dependent formation of specific lymphocyte receptors which recognize the major histocompatibility complex (MHC) (Lovely & Sen, 2016). Adaptive immunity also generates immunologic memory upon primary infection so that a strong immune response can be achieved after secondary infection within a shorter time span (Bonilla & Oettgen, 2010). T cells and B cells are the cells of adaptive immune system, which both have unique antigen-specific receptors, and are derived from hematopoietic stem cells (HSCs) from the bone marrow. The basic workflow of the adaptive immune system is that T cells respond to antigen-presenting cells (APCs) through their T cell antigen receptors (TCRs) to develop into effector T cells along with the B cells differentiating into plasma cells to produce antibodies. T cells mature in the thymus (Spits, 2002), whereas B cells mature in the bone marrow (Nagasawa, 2006).

1.2. T Cell Activation at the Immunological Synapse

The adaptive immune system plays the fundamental role in defending the host from pathogens and unhealthy cells through their antigen-specific receptors and immunologic memory. T cells are classified into major classes according to their cell surface expression of co-receptors, and TCR types. In terms of co-receptor expression, T cell subsets are defined as cytotoxic (CD8+) and helper (CD4+) T cells (Golubovskaya & Wu, 2016). CD8+ T cells express a heterodimeric cell surface molecule CD8 (CD8 α , CD8 β) and perform cellular immunity through cytolytic activity towards intracellular pathogens (Thakur, Mikkelsen, & Jungersen, 2019), and also contribute to tumor immunosurveillance (Ribatti, 2017) (Figure 1.2). CD4+ T cells express a single polypeptide chain called CD4, and function in regulation of immune responses.

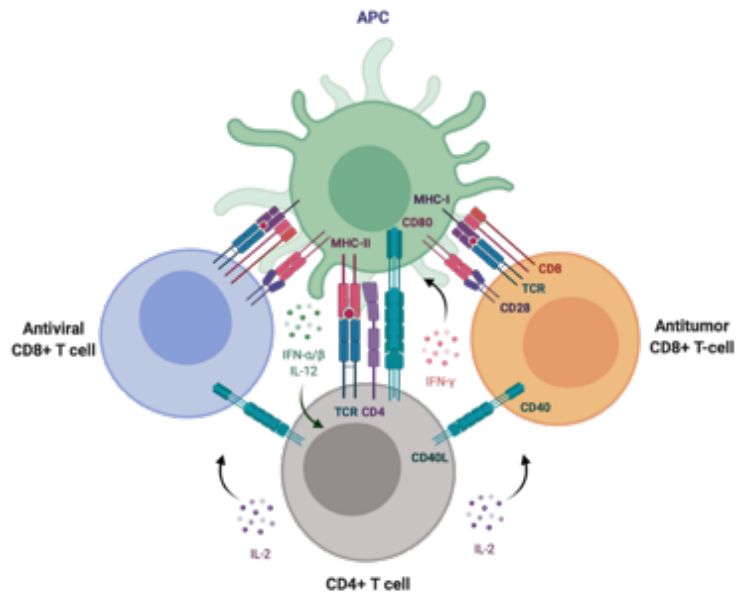


Figure 1.2 T cell cytotoxicity against a variety of pathogens

Cytotoxic T cell immunity against viruses by CD8+ T cell (blue) and cancer (orange) through MHC-restricted antigen presentation and recognition on APCs. CD4+ T cells (grey) aid CD8+ cells by producing IL-2 and IFN- γ to drive effector functions when they are exposed to IFN- α/β and IL-12.

Full activation of T cells can only be achieved by a sustained signal. The concept of immunological synapse (IS) as a molecular machine explains the mechanisms underlying sustained T cell activation signals. Dynamic cell-cell interactions coordinate bidirectional intercellular communication between T cells and APCs. ISs are formed at the sites of intercellular communication between lymphocytes and APCs. Firm contacts by the IS is robustly triggered upon the recognition of peptide-MHC complex (pMHC) by the TCR. Accordingly, ISs are generated by the coordinated action of TCRs and a ring of adhesion molecules.

Generation of an IS requires three main stages (Grakoui et al., 1999). In stage 1 junction formation occurs, in which lymphocyte function-associated antigen 1 (LFA-1) integrin creates a fulcrum that anchors the central part of the nascent IS so that outermost ring of the T cell membrane is brought in close proximity to the other cell's membrane with cytoskeletal protrusions (Walling & Kim, 2018). Hence, LFA-1 participates in initiating the IS. Stage 2 involves MHC peptide transport, whereby TCR complexes interact with MHC-peptide complexes and these complexes are transported towards the center of the IS by actin-mediated transport (Dustin, 2014). Stage 3 is the stabilization stage where clustered TCR-pMHC complexes are further stabilized, and referred as central supramolecular activation cluster (cSMAC) and the ring that contains LFA-1 as peripheral cluster (pSMAC) (Lin, Miller, & Shaw, 2005). Distal SMAC (dSMAC) is the outermost layer that ensures the proper mechanical forces are distributed along the synapse, and its members are mainly CD45, CD44 and CD43 (Alarcón, Mestre, & Martínez-Martín, 2011).

The molecular events controlling IS formation are not only dependent on antigenic interactions but also adhesive interactions and co-stimulatory ligands such as LFA-1/ICAM-1 and B7/CD28 respectively (Dustin, 2002). LFA-1 and intercellular adhesion molecule 1 (ICAM-1) are pSMAC components on the T cell and on the APCs respectively. The components of the cSMAC in the T cell and APC are TCR/CD3, CD27, CD28, 4-1BB and OX40; MHC, CD70, CD80/CD86, 4-1BBL, OX40L, respectively (Onnis & Baldari, 2019). All of these non-antigenic molecules are responsible for the creation of a network that initiates and prolongs the strong T cell activation signals by intercellular adhesion so that effector functions can be achieved. An armed effector T cell

is characterized by its array of *de novo* synthesized molecules, which are mainly cytotoxins, cytokines and membrane-associated proteins (A. Takeuchi & Saito, 2017).

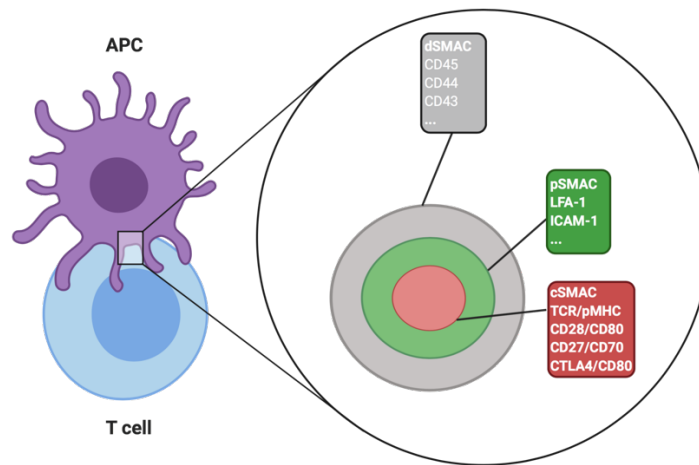


Figure 1.3 Brief overview of the immunological synapse

The interface indicating an IS between a T cell (purple) and an APC (blue). Cross-sectional representation of the IS having cSMAC (red), dSMAC (grey) and pSMAC (green). The molecules in the respective supramolecular clusters are shown in the corresponding colors.

CD8⁺ T cells carry out their killing function by the action of its cytotoxic granules secreted from the endocytic compartments, and are therefore referred to as killer T cells. Cytolytic vesicles are transported to the cell surface upon formation of the IS to secrete perforin and granzyme into the intercellular space (Janas, Groves, Kienzle, & Kelso, 2005). Perforin is a hydrophobic molecule that exerts its function by creating holes in target cells to disrupt their structural integrity. Granzyme proteases induce apoptosis in target cells by activating intracellular apoptotic machinery. In addition to these, CD8⁺ cells also release interferon gamma (IFN- γ) (Bhat, Leggatt, Waterhouse, & Frazer, 2017).

The second subset of T cells, namely CD4⁺ T cells amplify the effector responses of CD8⁺ T cells and other lymphocytes (Eagar & Miller, 2013). The first functional type of helper T cells (T_{H1}) secrete IFN- γ , tumor necrosis factor alpha (TNF- α), CD40 ligand (CD40L), TNF- β , granulocyte-macrophage colony-stimulating factor (GM-CSF), IL-3 and IL-2. T_{H1} cells usually activate macrophages (Romagnani, 1992). T_{H2} cells secrete CD40L, IL-3, IL-4, IL5, IL-10, GM-CSF, transforming growth factor beta (TGF- β), and activate mainly B cells (Cowan, 2017). The concerted activities of the aforementioned molecules in the IS render T cells fully activated. The activated T cells undergo signalling

through their T cell receptor complex. Immunoreceptor tyrosine-based activation motifs (ITAMs) of the TCR complex are responsible for initiating signalling. ITAMs are found in the intracellular tails of CD3 molecules, and their phosphorylation recruits other adaptor and scaffold proteins (Love & Hayes, 2010). TCR signaling results in the translocation of JUN, FOS, nuclear factor of activated T cells (NFAT), AP-1 and NFκB transcription factors to the nucleus, resulting in gene transcription necessary for inflammatory responses, cell survival and cytokines secretion (Conley, Gallagher, & Berg, 2016). The molecular pathways in T cell activation are outlined in Figure 1.4.

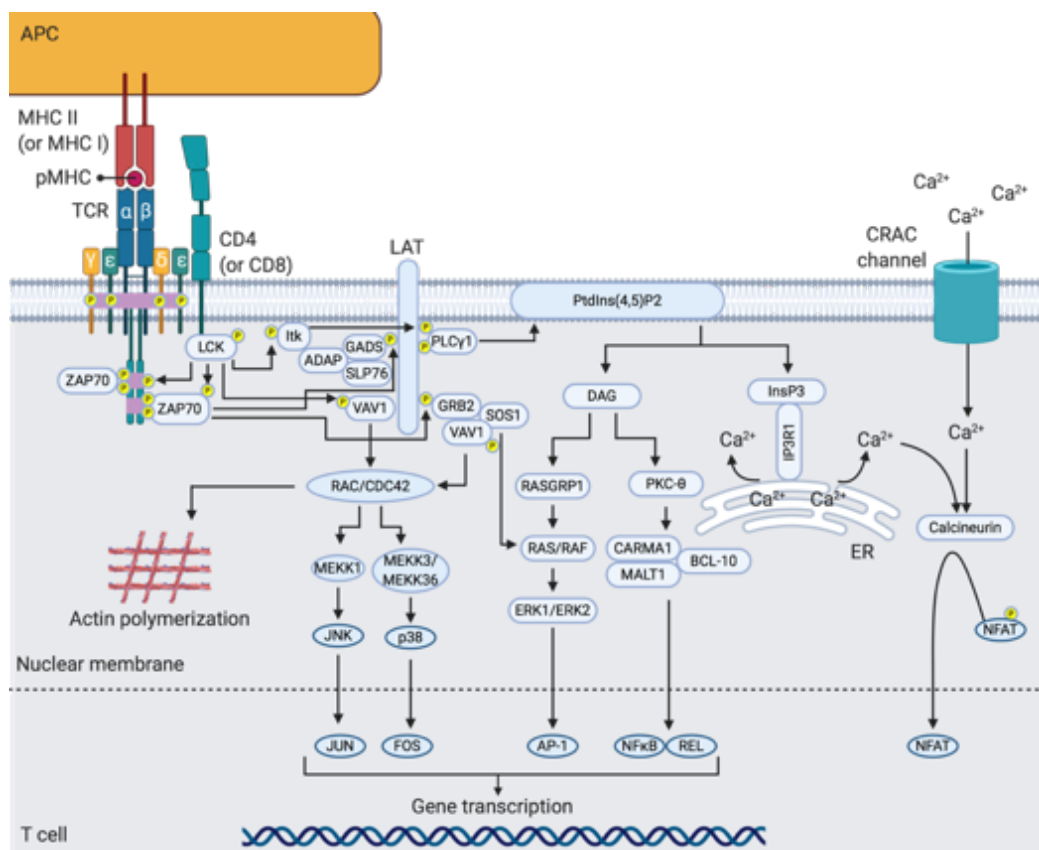


Figure 1.4 TCR signaling pathway

Main events underlying the TCR signalling network. Antigen loaded MHC molecules initiate the TCR signalling. LCK is recruited to the intracellular domains of co-receptor molecules. ITAMs on CD3 molecules are phosphorylated by LCK, which in turn recruits ZAP70. ZAP70 phosphorylates LAT, which serves as an active signalosome with docking sites for other molecules. After this step, signalling is carried out in three diversified branches that involves Ca^{2+} -calcineurin, mitogen-activated protein kinase (MAPK) and NFκB. Calcium signaling modulation and diacylglycerol (DAG) action play important roles for transcription factor activation. The coordinated actions of transcription factors activates target genes and promotes actin polymerization to render T cells armed to function towards pathogens.

1.2.1. Antigen Recognition

TCR was initially described as the disulphide-linked glycosylated heterodimer ($\alpha\beta$) that are present on the cell surface of mouse and human T cells. Cloning of the highly variable TCR $\alpha\beta$ chains later demonstrated that $\alpha\beta$ TCR genes share sequence homology and diversity to immunoglobulins (Wälchli et al., 2011). TCR genes have variable (V), diversity (D), joining (J) and constant (C) regions that go through somatic recombination (Ma et al., 2016). Another type of TCR having $\gamma\delta$ TCR genes was also discovered as the lesser portion of the peripheral T cells but more prominent members within mucosal tissues, so that the term $\gamma\delta$ T cell was coined after $\alpha\beta$ T cell (Zhao, Niu, & Cui, 2018).

TCR complex is basically composed of CD3 chains (δ , ϵ , γ , ζ), and TCR $\alpha\beta$ as the integral membrane proteins (Reinherz, 2014) (Figure 1.5A). The CD3 δ , CD3 ϵ and CD3 γ chains are members of the C-type immunoglobulin superfamily, therefore they are closely related to each other. On the other hand, CD3 ζ protein is not genetically related to the rest of CD3 chains as it is located on a different chromosome. CD3 ζ is also structurally unrelated due to its long intracellular and short extracellular chains, unlike other CD3 chains. $\alpha\beta$ TCR chains are linked to CD3 (ϵ , δ , γ) chains in a non-covalent manner. Each CD3 chain contains signal transduction motifs (Bettini et al., 2017) as other immune cell receptors (Fc and B cell receptors) contain. Signal transduction motif found in the CD3 chains are ITAMs, displayed in orange rectangles in Figure 1.5A. ITAMs have a conserved motif (YxxL/I), and this motif is separated by 6 and 8 amino acids in the intracellular tail (Love & Hayes, 2010). Three copies of ITAMs are present in CD3 (ϵ , δ , γ) and one copy of ITAM is present in CD3 ζ .

The TCR $\alpha\beta$ ectodomains have a 3D structure similar to immunoglobulin Fab fragments. Hypervariable chains of $\alpha\beta$ TCR are aligned to $\alpha 1$ and $\alpha 2$ helices of antigen-bound MHC molecules. Hypervariable loop of $\alpha\beta$ TCR referred complementary determining region 3 (CDR3) has a pivotal location on the interface of pMHC and TCR (Borg et al., 2005). CDR3 is therefore the most important hypervariable loop contributing to pMHC interaction, whereas CDR1 and CDR2 are more involved in the interactions between $\alpha 1$ and $\alpha 2$ helices of the nascent MHC molecules (Chlewicki, Holler, Monti, Clutter, &

Kranz, 2005; Garcia & Adams, 2005). The simplified structure of a TCR complex is outlined in Figure 1.5A.

MHC restriction refers that an $\alpha\beta$ TCR can only recognize peptides upon their binding the the corresponding MHC molecules so that T cells can distinguish between self and non-self molecules (La Gruta, Gras, Daley, Thomas, & Rossjohn, 2018). This combined need of recognition is the fundamental ground in T cell responses. This phenomenon was discovered with the works on lymphocytic choriomeningitis virus (LCMV) as a model organism by the ground-breaking work by Rolf Zinkernagel and Peter Doherty (Zhou, Ramachandran, Mann, & Popkin, 2012; Zinkernagel & Doherty, 1997). In this experimental set-up, LCMV-specific CD8⁺ T cells from two different strains (strains A and B) were reported to be only demonstrate specific killing for the same strain. Other immune cells such as B cells, $\gamma\delta$ T cells and NK cells do not follow the rules of MHC restriction recognition (Lowdell, Lamb, Hoyle, Velardi, & Grant Prentice, 2001).

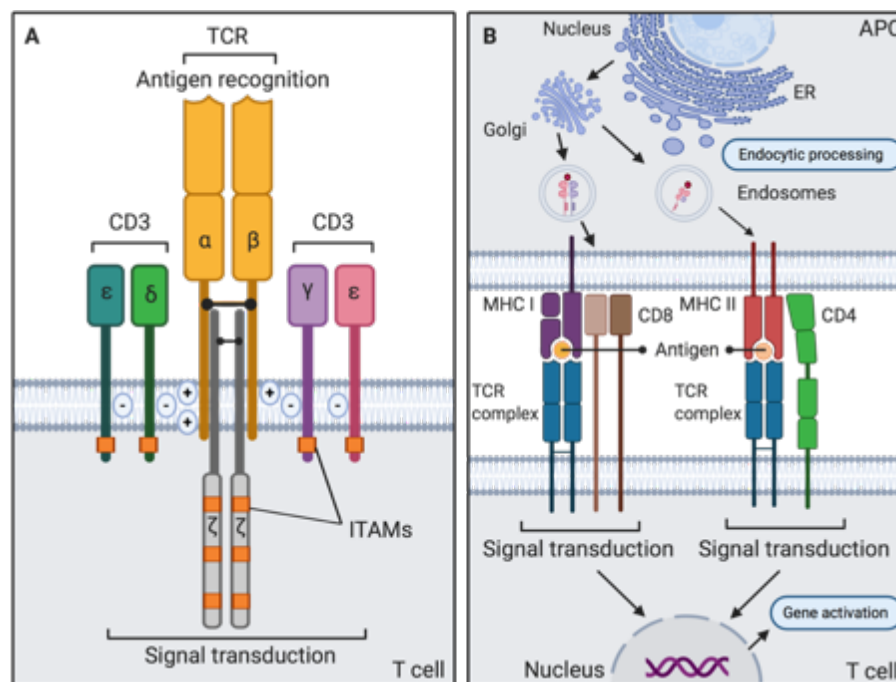


Figure 1.5 Structure of the TCR complex and MHC-restricted antigen recognition

Structure of the $\alpha\beta$ TCR complex: members are α and β chains of the TCR (yellow); CD3 ϵ (dark green, pink), CD3 δ (light green), CD3 γ (purple), CD3 ζ (grey), ITAMs (orange), disulphide bonds (black lines) (A). The process of antigen presentation to cell surface through endocytic processing leads to cell surface appearance of pMHCs (MHC I or MHC II). TCRs recognize peptides on MHC I (red) or MHC II (purple) along with the corresponding co-receptors CD8 heterodimer (brown) and CD4 (green). Signaling through TCRs with pMHCs initiates activation of target genes.

1.2.2. Co-stimulation and Instructive Cytokines

Co-signalling receptors on T cells drive cell fate decisions. T cell co-signalling receptors is the collective term for co-stimulating receptors and co-inhibitory receptors. The classical two-signal model of immune cell activation suggests that T cells can only be activated through the concerted function of pMHCs and co-stimulatory molecules. The antigenic recognition is referred as the signal 1 for T cell activation where IS arranged to be generated. Upon formation of pMHC-TCR complex, co-stimulatory molecules are required as the signal 2. Many studies have showed that the presence of only signal 1 results in anergy (Yamamoto, Hattori, & Yoshida, 2007; Zheng, Zha, & Gajewski, 2008), in which T cells are able to recognize the antigen but lose their ability to eliminate them. Therefore, anergy is also described as the functional hyporesponsiveness. This finding resulted in the fact that a T cell can only be activated by the combined effect of two signals together. Co-signalling molecules are known to overlap spatiotemporally with TCRs within the IS to exhibit their effects in a synergistical way (Yokosuka et al., 2008). The dynamic distribution of SMACs ensures the co-signalling molecules to interact with their corresponding ligand. Accordingly, co-signalling molecules have been suggested to support IS by contributing to the fulcrum of molecules physically (Hivroz & Saitakis, 2016). Co-signaling molecules may also be dispersed in different microclusters (Dustin & Groves, 2012), and bring molecules into close proximity together with their downstream signalling motifs.

The discovery of B7/CD28 axis shed light on the co-stimulatory pathways and two-signal hypothesis was stemmed from this. A study showed the impaired proliferation of T cells against antigens and alloantigens in CD27-deficient mice, and these responses were not restored with exogenous IL-2 administration (Green et al., 1994). B7-transfected accessory cells also did not serve as co-stimulatory signal for T cells of CD28-deficient mice in the same study. Consequently, CD28 is referred as the principal co-stimulatory receptor, and expressed constitutively on T cells, and its discovery led to exploration of its ligands B7 family members B7-I (CD80) and B7-II (CD86) (Kaempfer et al., 2013). The repertoire of co-signalling receptors is subject to be shaped according to tissue microenvironment, hence it is very diverse (Chen & Flies, 2013). Furthermore, the availability of ligands has also been reported to vary from nonlymphoid to lymphoid

tissues, which explains the fundamental difference in T cell activation in periphery and in lymphoid tissue. Although B7/CD28 axis is the most elucidated pathway, it has been shown that there are other co-stimulatory molecules as well.

The main co-signalling families on T cells are immunoglobulin superfamily (IgSF) and TNF receptor superfamily (TNFR) (Sharpe, 2009). IgSF members are further classified into B7/CD28, TIM and CD2-SLAM families; TNFR members are grouped into Type V and Type L families (Simons et al., 2019). Major co-signalling molecules and their corresponding ligands on T cells and APCs are shown in Figure 1.6.

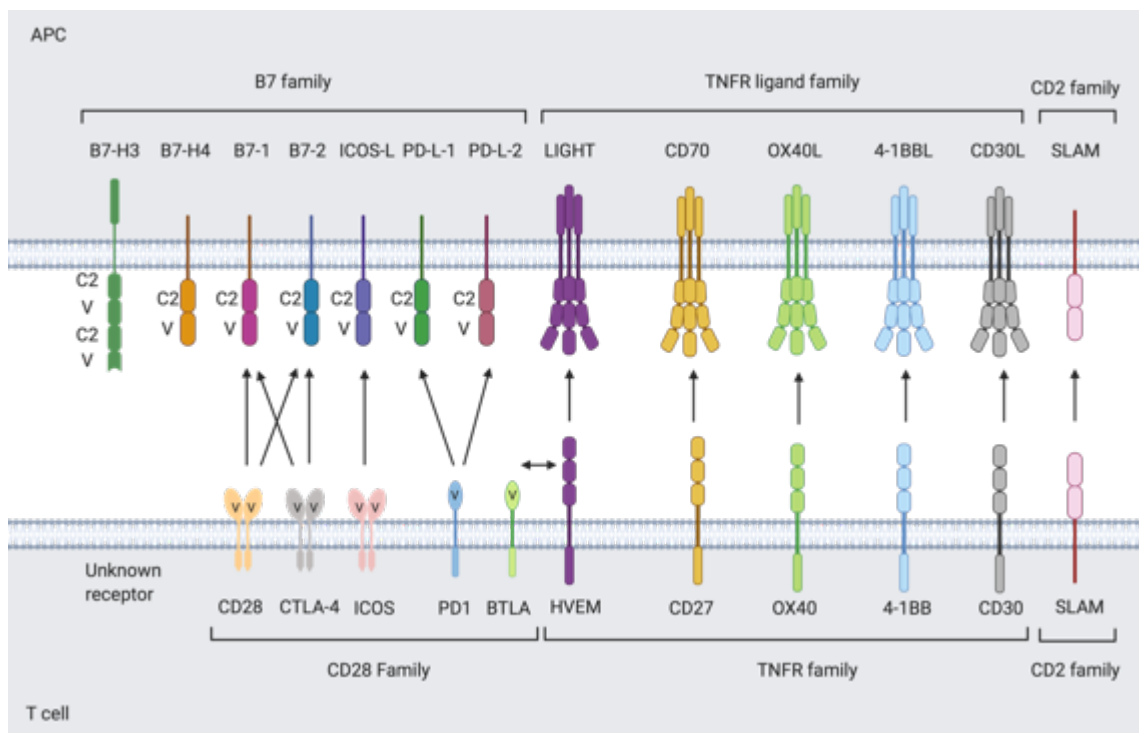


Figure 1.6 Molecules responsible for co-stimulation: co-stimulatory receptors and their ligands

Schematic representation of co-stimulatory molecules and their ligands on T cells and APCs. Co-signalling receptor families are CD28, TNFR and CD2 families; ligands belong to B7, TNFR ligand and CD2 families, respectively. Arrows show the interaction partners. BTLA, B and T lymphocyte attenuator; C2, constant type-2 immunoglobulin-like domain; CTLA, cytotoxic T lymphocyte antigen; HVEM, herpes virus entry mediator; SLAM, signalling lymphocyte activation molecule; V, immunoglobulin-like variable domain.

As the understanding of T cell activation have proceeded, two-signal model has been replaced with the three-signal model, in which the positive regulatory role of cytokine environment has also been considered. Three-signal model for T cell activation states that

instructive cytokines also function in the full activation of T cells, along with the first two cells (Figure 1.7). Introduction of the signal 3 integrates multiple positive and negative regulatory pathways for T cell fate (Sckisel et al., 2015).

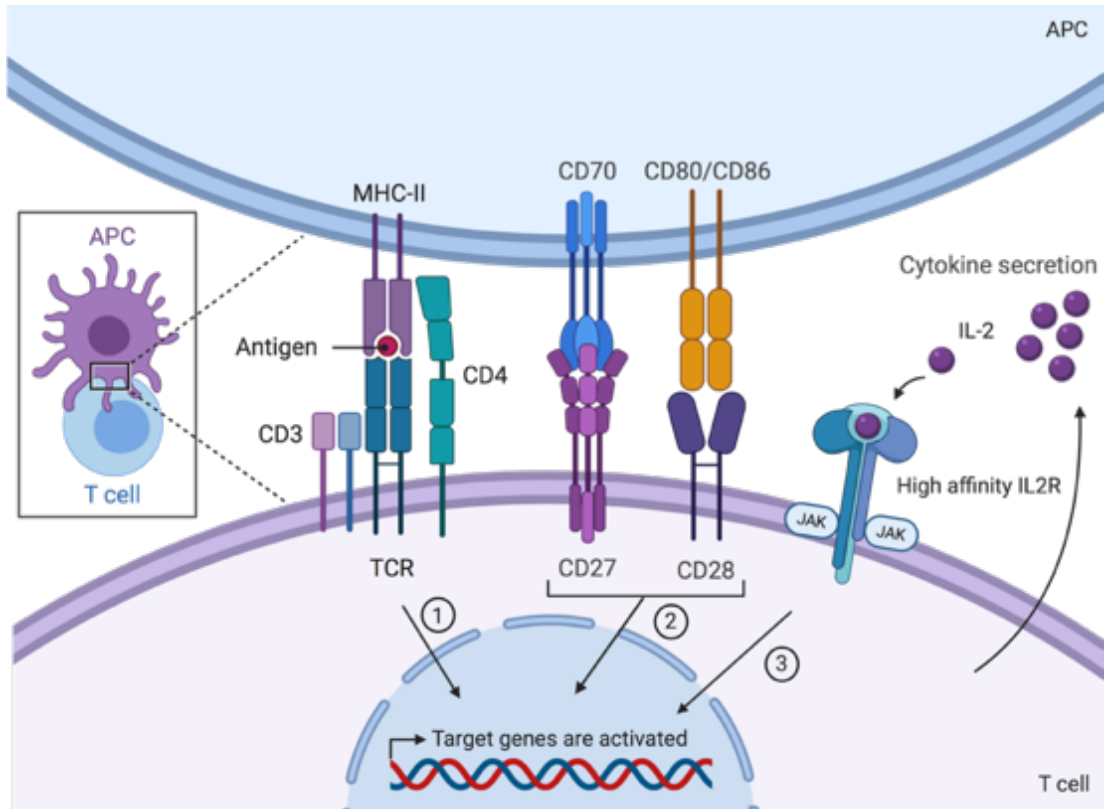


Figure 1.7 Three-signal hypothesis at the APC-T cell interface

A closer look into APC-T cell interface: three-signal hypothesis for T cell activation. Signal 1 represents the antigen-specific interactions between pMHC and TCR. Signal 2 is the positive signal received from co-stimulatory receptors and their ligands. Third signal denotes instructive cytokines where cytokines trigger production of cytokines in a positive feedback loop, IL-2 and JAK/STAT pathway is demonstrated as an example here.

Cytokines are the glycoproteins which are utilized for cell communication by immune cells, and they are secreted by both innate and adaptive immune system cells (Ray, 2016). Cytokines have been shown to drive naïve T cell fate decisions into effector helper T cell subset cells in the presence of corresponding cytokines (Figure 1.8). Therefore, signal 3 is also referred as polarization signal. Interferons also play essential roles for immune cell development and cytotoxic responses. For instance, NK and CD4⁺ T cells are responsive to IL12 as they have IL-12 receptors on their cell surface (Lovett-Racke & Racke, 2018). IL-12 has positive regulatory functions to differentiate naïve CD4⁺ T cells into T_H1 cells.

NK and T_H1 cells secrete IFN- γ . The increased levels of IFN- γ drives the initiation of inflammatory cascade by producing chemokines, cytokines and matrix metalloproteases (S. H. Lee, Kwon, Kim, Jung, & Cho, 2017). IL-4 is considered as the T_H2-polarizing cytokine. Helper T cell polarization is only mediated in the presence of polarizing cytokines. A mutual property of the polarizing cytokines is that they should be provided to the naïve T cells so that a positive feedback loop can be formed to augment helper T cell responses. Since naïve T cells and DCs are not responsible for the secretion of the polarizing cytokine secretion, the three-cell model for helper T cell activation originates from this (Corthay, 2006). In this model, polarizing cytokines are secreted from another immune cell in close proximity: $\gamma\delta$ T and NK cells as the IFN- γ -secreting cells to initiate T_H1 polarization; NK T, $\gamma\delta$ T, eosinophils, mast cells and basophils as the IL-4-secreting cells to promote T_H2 polarization (Corthay, 2006).

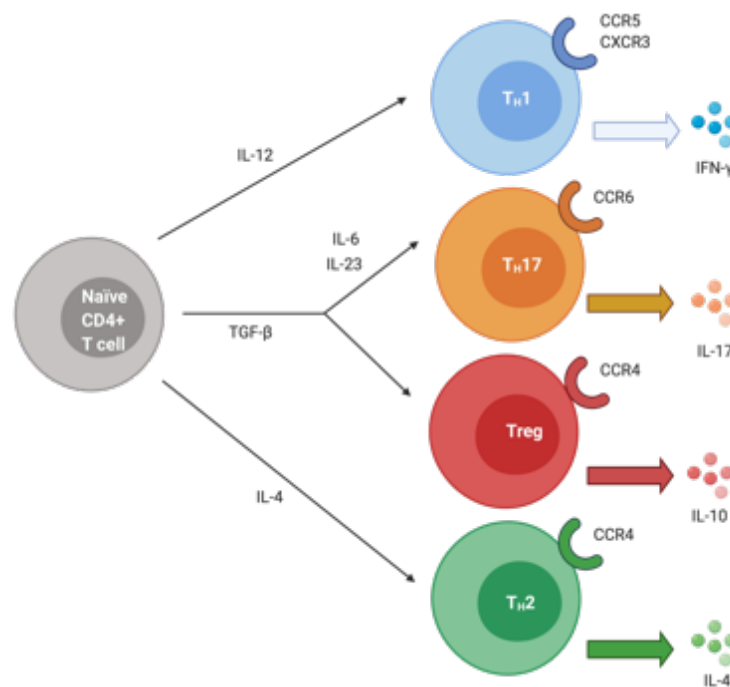


Figure 1.7 Cytokines drive naïve CD4+ T cell fates

Naïve T cell polarization into helper T cell subsets: T_H1, T_H2, T_H17, and Treg cells in the presence of polarizing cytokines. Polarized subsets further express distinct chemokine receptors, cytokines and interleukins to mediate immune responses. Arrows indicate the secreted cytokines, and expressed chemokine receptors are shown upon polarization. CCR, C-C chemokine receptor; CXCR, C-X-C chemokine receptor.

The effect of cytokines over immune cells as the environmental cues has been reported to cause changes in the DNA binding of transcription factors (TFs) (Lambert et al., 2018;

van Schoonhoven, Huylebroeck, Hendriks, & Stadhouders, 2020). As TFs have the essential functions to maintain cell fate decisions and lineage progression into specialized effector programs, cytokines also have key roles in immune cell development as well (Nutt & Kee, 2007; Radtke, MacDonald, & Tacchini-Cottier, 2013; Robinette & Colonna, 2016). Abnormalities in the inflammatory cytokine levels through epigenetic regulation have been implicated in human malignancies such as in tumor tissue (Yasmin et al., 2015), which potentially interferes with the tumor immunosurveillance of the immune system (S. Lee & Margolin, 2011; Mumm & Oft, 2008). Collectively, cytokines play an indispensable role for T cell activation and proper immune system functioning.

1.3. The TNF/TNFR Superfamilies of Signaling Molecules

Tumors that have been surrounded with a bacterial infection was observed to be cleared out sporadically. This phenomenon was attributed to bacterial secretions that might contribute to formation of hemorrhagic necrotic tumors and eventually tumor disappearance. This factor was historically termed as tumor necrosis factor alpha (TNF- α) in the 1970s (Drutskaya, Efimov, Kruglov, Kuprash, & Nedospasov, 2010; Old, 1985). Over the course of scientific advances, it was found out that TNF- α and lymphotoxin- α (LT- α) are actually released by the patient's immune system cells, mainly macrophages and T cells, to eliminate bacterial invaders.

The TNF superfamily functions by interacting TNF receptor (TNFR) superfamily (SF). TNF/TNFR superfamilies are evolutionarily conserved molecules that are found in both vertebrates and invertebrates such as arthropods and chordate species (Quistad & Traylor-Knowles, 2016). For instance, the primitive forms of TNF/TNFR axis including eiger-wangen pathway are shown to mediate host immune defense against pathogens (Mabery & Schneider, 2010) and cell development and death (Vidal, 2010) in *Drosophila melanogaster*. In higher vertebrates, TNF/TNFR SFs perform many physiological functions in the cellular context including oncogenesis and immune homeostasis (Roca et al., 2008), and have many members due to whole genome duplication (Kinoshita,

Biswas, Kono, Hikima, & Sakai, 2014) and translocation events (Morrow & Cooper, 2012).

Signaling of TNFs is mediated by the type I transmembrane proteins TNFSFRs. After the discovery of TNF- α and LT- α , sequence homology analysis revealed other members of TNF SF members including: TNF- α , CD30L, FasL, CD27L, OX40L, LT- β , B cell activating factor (BAFF), 4-1BBL, TNF-related apoptosis-inducing ligand (TRAIL), glucocorticoid-induced TNFR family-related gene ligand (GITRL), a proliferation-inducing ligand (APRIL), and receptor activator of NF κ B ligand (RANKL). TNFR SF is mainly separated into three classes: death receptors, TRAF-interacting receptors, and decoy receptors. The TNFRs to the aforementioned ligands are demonstrated in Figure 1.9. Some TNFs have been implicated to bind more than one TNFRs as well.

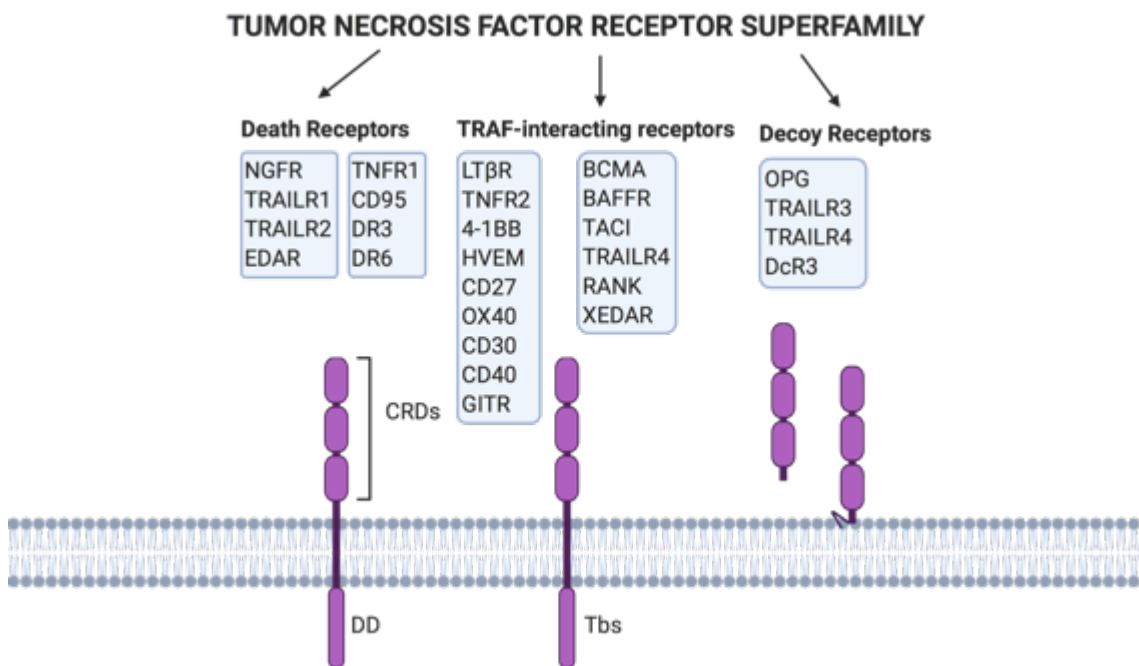


Figure 1.8. Classification of TNFR SF and its main family members

Schematic representation of main classes of TNFR SF members: death receptors, TRAF-interacting receptors, and decoy receptors. CRD, cysteine-rich domain; DD, death domain.

Ligand-receptor crystal structures including CD40-CD40L and OX40-OX40L have shown that 3:3 ratio is favoured for the interaction between TNF-TNFR SFs. Therefore, it has been figured out that trimerization takes place for the ligand-receptor connections, as outlined in Figure 1.9. TNF is composed of 19 known ligands that are type II

transmembrane proteins (Xu et al., 2017). TNFs have an extracellular TNF homology domain (THD). Most of the TNFs are also found in the soluble form, as metalloproteases cleave their extracellular domain. TNFs have been shown to bind to the cysteine-rich domain (CRD) of the TNFRs, which is located on the N terminus of TNFRs. Six cysteine residues are present in a typical CRD, and these cysteines are responsible for the creation of disulphide bonds. THD domain has been implicated to have essential functions in the trimerization of TNFs, as the membrane-bound TNFs are converted into soluble proteins by metalloproteases. Solubilization process of TNFs was reported to be crucial for some TNFs including EDA. However, it creates loss-of-function for some other TNFs like FasL. TNF SF members are predominantly expressed by the immune system cells, particularly found on the cell surface of APCs including macrophages, DCs, B cells (Croft, 2009). Additional to APCs; NK cells, basophils, T cells, mast cells, endothelial cells, smooth muscle cells, and thymic epithelial cells have been reported to express TNFs.

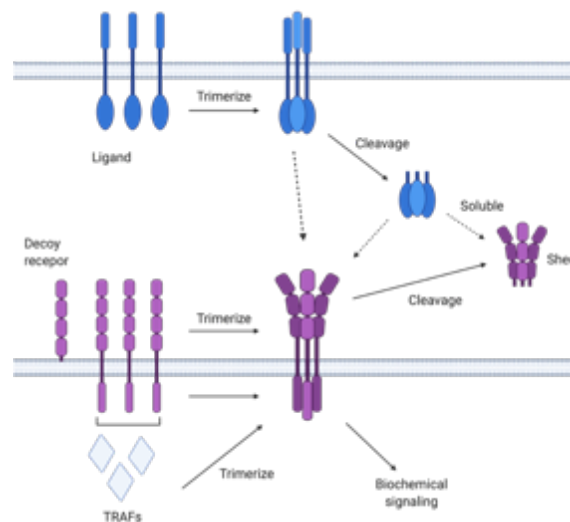


Figure 1.9. Mode of action for TNF/TNFR SFs

TNF/TNFR SF members undergo trimerization prior to their interaction with each other. Their association triggers cleavage events, and TRAF recruitment to induce biochemical signalling. Decoy receptors lack of cytoplasmic tails, whereby they function as signalling inhibitors.

TNFR SF members are classified under type I transmembrane proteins. However, some members of TNFRs are classified as type III transmembrane proteins including BAFF receptor (BAFF-R), and transmembrane activator and calcium modulator and cyclophilin ligand interactor (TACI). TNFRs are structurally divided into two groups: death receptors

and non-death receptors in terms of death domain (DD) presence in the cytoplasmic tail (Wajant, 2003), which is a conserved structure at a size of 80 amino acids. Death receptors generate and further recruit membrane-proximal scaffolding complex to promote apoptosis by caspase activity. Non-death receptors convey the signal by recruiting TRAFs to integrate different signalling axes, contributing to cytokine production and cell proliferation (Itoh & Nagata, 1993).

TNF/TNFR SF members have been demonstrated to create bidirectional signals through forward and reverse signalling (Qu, Zhao, & Li, 2017). Delivered signals in both directions may generate outcomes including cell proliferation, survival, inflammation and death based on how the signal is integrated with the other pathways in the cells, as explained in the Figure 1.10 (Sun & Fink, 2007). Since reverse signalling conveys co-stimulatory signals, and leads to altered cell fate decisions, it plays important role in the generation of immune response.

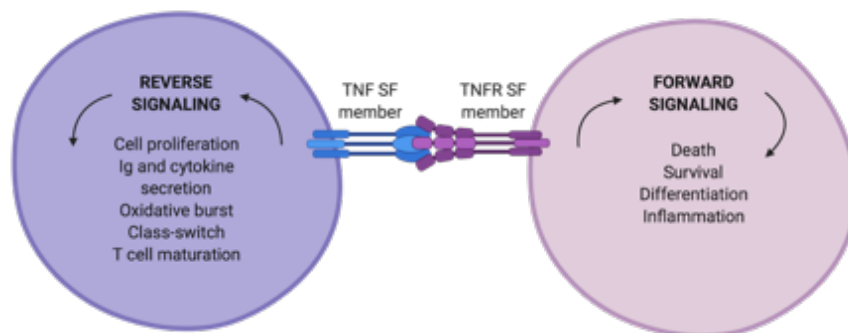


Figure 1.10. Bidirectional signalling through TNF/TNFR SFs

Bidirectional signalling is composed of receptor-mediated forward, and ligand-mediated reverse signalling in an equilibrium to favour cell survival and differentiation.

Majority of TNF/TNFR SF expression is carried out by cells of the immune system. Activation of the immune system triggers expression of these receptor-ligands to induce the cell survival and differentiation into effector phenotypes to generate effective immune responses. This co-stimulatory property of TNF/TNFR members have crucial impacts over T cell activation and development (Watts, 2005). These molecules are also implicated to contribute to maintenance of lymphoid tissue and its development through activating inflammatory axis NF κ B. Major co-stimulatory receptor-ligands are CD27/CD70, CD40/CD40L, OX40/OX40L, 4-1BB/4-1BBL, and CD30/CD30L.

Accordingly, the aberrant expressions of TNF/TNFR SF co-stimulatory molecules have been shown to contribute to autoimmunity, immunodeficiency, chronic infections, cancer, and other inflammatory diseases (Martínez-Reza, Díaz, & García-Becerra, 2017; Yang et al., 2019). Accordingly, TNF/TNFR SF members are potential therapeutic targets. For instance, blockade of TNF- α impaired the development of colorectal carcinogenesis in mice upon chronic colitis (Popivanova et al., 2008).

1.3.1. The Basis of Signal Transduction in the CD27/CD70 Pathway

CD27 (TNFRSF7) is a member of TNFR SF of co-stimulatory signalling molecules, and at a size of 263 amino acids. CD27 is a single-pass type I membrane homotrimeric glycoprotein that has CD70 as its ligand at the size of 193 amino acids. CD27 has one incomplete and two complete CRD domains in its N-terminus. CD70 (TNFSF7) is a TNF SF member type II homotrimeric co-stimulatory ligand that is found on activated cells of lymphoid lineage mainly on T cells, DCs, NK cells and B cells, thymic epithelial cells, and other APCs (Wu, Anasetti, & Yu, 2019). The transient availability of the ligand provides fine-tuning of the CD27/CD70 signalling axis. However, constitutive expression of CD70 is observed on some tumors such as large B cell lymphoma and B cell chronic lymphocytic leukemia (Lens et al., 1999). Constitutive expression of CD27 is detected on B cells, NK cells, Treg cells, and naïve T cells. Main features of CD27 and CD70 are shown in Table 1.1 below.

Table 1.1. Topological and genomic features of CD27 and CD70 molecules

	CD27	CD70
Topology		
Topological domain (extracellular)	20-191	39-193
Transmembrane (helical)	192-212	18-38
Topological domain (cytoplasmic)	213-260	1-17
Length (aa); MW (kDa)	260 aa; 29 kDa	193 aa; 50 kDa
Genomic context		
Location	12p13.31	19p13.3
Exon count	6	4

The expression of CD27 was reported to be disappeared on cell differentiation and activation of T cells, yet memory cells continue to have CD27 on their surfaces. CD27/CD70 pathway has gained attention because of its contribution in the immunity or tolerance decisions in immune cells. A study showed that Tregs were depleted in the CD27 deficient mice, but the amount of conventional T cells (Tconv) were not changed (Wasiuk et al., 2017). CD27 was demonstrated to contribute to Treg development through the prevention of apoptosis. These findings suggest that CD27/CD70 signaling axis contributes to autoimmunity by modulating Tregs. Another study shows that single knockout (KO) mice for CD27 and CD28 had impaired CD8+ T cell-mediated immune response against influenza, and double KO mice did not mount an immune response (Hendriks, Xiao, & Borst, 2003; Munitic, Kuka, Allam, Scoville, & Ashwell, 2013). This study points out the complementary role of CD28 and CD27 through their ligands B7 family members and CD70, respectively. CD27 signaling is reported to be more involved in the survival of effector and memory cells, CD28 signaling has more profound effects on the cell cycle entry of primed T cells. Additional to these, germinal center responses are highly dependent on CD27 expression as well, as it is regarded as B cell memory and maturation marker (Agematsu, Hokibara, Nagumo, & Komiyama, 2000). As B cells turn into plasma cells, their CD27 expression elevates remarkably due to priming to DCs so that germinal center (GC) resident are found to be CD27+ (Arens et al., 2004).

Studies employing CD70-deficient mice or anti-CD70 blocking antibodies have led to impaired T cell responses upon viral infections. The impaired effects were mainly on CD8+ antigen-specific responses that leads to reduced viral elimination, not on the CD4+ T cell immune responses. Therefore, CD70 molecule has been implicated to have a role in robust immune response generation. Tight regulation of CD70 is crucial for CD27/CD70 signalling. Overexpression of CD70 by demethylation of its promoter region in the CD4+ T cells has been reported in systemic sclerosis and systemic lupus erythematosis patients, leading to autoimmunity (H. Y. Jiang et al., 2012). Besides its effects on autoimmunity, overexpressed CD70 expression levels especially in the non-lymphoid tissues have been linked to solid tumors and hematological malignancies. Renal cell carcinoma (RCC) (Jilaveanu et al., 2012), Epstein-Barr virus induced cancers, and lymphomas are examples of this . Constitutive CD70 expression has also been associated with autoimmunity and B cell lymphoma. The proposed mechanisms of CD70

involvement in tumor tissue is that its expression leads to enhanced tumor cell survival and expansion (Ge et al., 2017). To test this hypothesis, leukemic stem cell proliferation was impaired significantly through CD70 blockade by employing an anti-CD70 antibody (Riether et al., 2015). The interaction between CD27 on the tumor infiltrating lymphocytes (TILs) and CD70 on the cancer cells in the context of tumor microenvironment has been shown (Julie Jacobs et al., 2018). By taking everything into consideration, CD70 has been suggested to be targeted in an anti-cancer vaccine strategy (Starzer & Berghoff, 2020). CD70 is also shown to function in viral infections in a pathogen-dependent manner. An example for this is that CD70 expression has been pronounced as the initiator of early cytokine releases by providing T_H1 polarization to promote adaptive immunity in mice against murine cytomegalovirus (CMV) (Allam, Swiecki, Vermi, Ashwell, & Colonna, 2014). To contribute more, T_H17 effector polarization is also prevented to boost CD8⁺ T cell responses by CD27/CD270 signalling.

CD70 deficiency was linked to many human diseases, mainly immunodeficiencies such as combined immunodeficiency and primary immunodeficiencies. It has been shown that the lack of CD70 and CD27 cause EBV-driven lymphoproliferative diseases in the immunodeficient individuals that have genetic mutations (Abolhassani et al., 2017; Munitic et al., 2013). This leads to reduced elimination of EBV-infected cells through affecting both CD8⁺ T cells and NK cells, and also memory T cells, as the receptors 2B4 and NKG2D are downregulated (Abolhassani et al., 2017).

Activation of the CD27/CD70 signaling pathway begins with the recruitment of TNF-associated factor-2 (TRAF-2) and TRAF-5 to the cytoplasmic tail of the CD70-bound CD27 receptor, whereby CD27 is cleaved by metalloproteases to have soluble CD27 (sCD27) (J. Jacobs et al., 2015). TRAF2 and TRAF5 are similar proteins, which share a conserved TRAF domain at their C-termini. TRAFs function as signal transducers for many TNFR SF members including CD27, CD40, and RANK. JNK, MAPK, classical and alternative NFκB activations are achieved through TRAF signalling (Xie, 2013). Single KOs of TRAF2 or TRAF5 did not show remarkable impairment in mouse embryonic fibroblasts (MEFs) (Au & Yeh, 2007). However, double KO of TRAF2 and TRAF5 significantly dismantled NFκB activation. This shows the redundancy between TRAF2 and TRAF5, where TRAF2 is predominant compared to TRAF5 due to its constitutive expression. Additional to TRAF recruitment, NFκB-inducing kinase (NIK)

is also recruited to CD27. After adaptor recruitments to CD27, E3 ligases cellular inhibitor of apoptosis-1 (cIAP1) and cIAP2 in conjunction with TRAFs mediate the NIK degradation. By activating these MAPK, Akt and NFκB pathways, CD27/CD70 axis leads to gene activation for cell survival, proliferation, anti-apoptotic and inflammatory proteins. Additional to all of these, CD27 association with SIVA1 protein has been suggested to lead to apoptosis with less understood mechanisms (Py, Slomianny, Auberger, Petit, & Benichou, 2004). The CD27/CD70 signalling axis is schematically outlined in Figure 1.10.

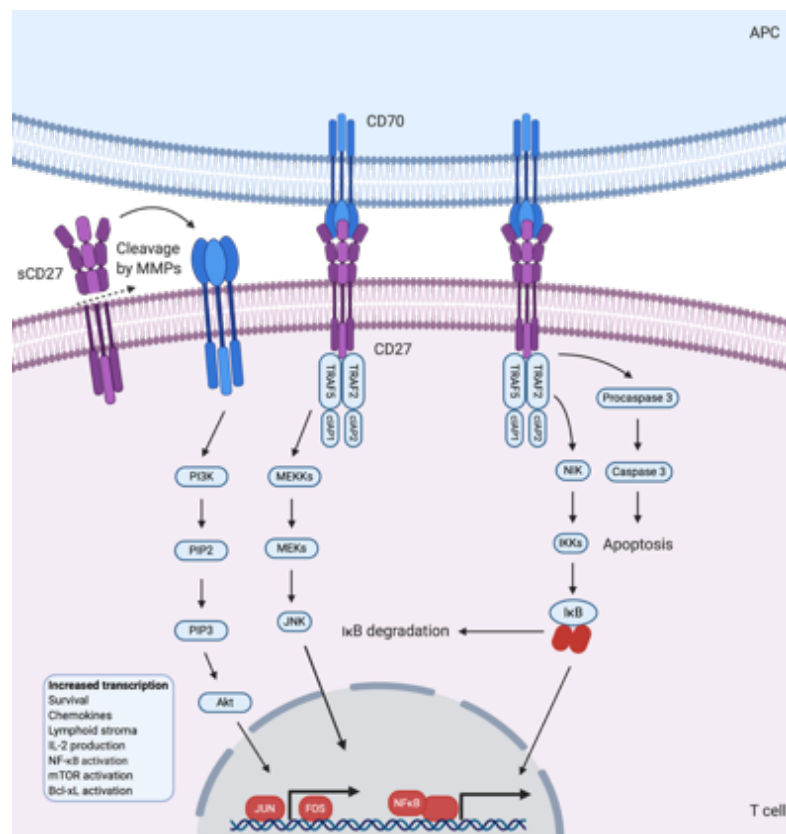


Figure 1.10 The CD27/CD70 Signaling Pathway

Recruitment of TRAFs to cytoplasmic tail of homotrimeric CD27 after interacting with its homotrimeric ligand CD70 starts the signal transduction. Gene activation is achieved with TFs JUN, FOS, NFκB to be translocated to the cell nucleus. TFs drive gene transcriptions required for cell survival and proliferation.

1.4. Primary Immunodeficiency Diseases

Immunodeficiency (ID) is as a condition in which the immune system cannot mount effective immune responses towards pathogens and other malignancies, due to the complete absence or severely compromised state of immune system. Immunodeficiencies are mainly classified into two groups: primary and secondary immunodeficiencies. Primary immunodeficiency (PID) is defined as a broad group of diseases that stem from genetic mutations of individuals that render them to have life-threatening and serious infectious because of genetic defects. PIDs are rare diseases also referred as the inborn errors of immunity, as the different branches of immune system are genetically impaired congenitally (J. L. Casanova & Abel, 2005). The diseases are usually associated with a susceptibility to autoinflammation, autoimmunity, cancer and lymphoproliferative diseases. Secondary immunodeficiency (SID) is an acquired condition over time based on environmental conditions, and other diseases (Notarangelo, 2010). For instance; malnutrition, immunosuppression with corticosteroids, cancer, and chronic infections including acquired immunodeficiency syndrome (AIDS) are key contributors to SID development and progression. The prevalence of SIDs are found to be more than PIDs. According to studies, selective IgA deficiency has the highest prevalence with the ratio of 1:223 to 1:1000 based on the specific ethnic population (Yel, 2010). The fatal disease severe combined immunodeficiency (SCID) has a rarer pattern with a prevalence of 1:100.000 for newborns in the USA (Francisco et al., 2015).

Patients with PIDs usually have obvious warning symptoms related to their rare condition. Ten clinical symptoms are accepted as the warning signs according to The Jeffrey Modell Foundations (Table 1.2) (McCusker & Warrington, 2011). Since these diseases are caused by genetic abnormalities, there is no established way to avoid them. Although the symptoms can be quite obvious, PIDs commonly have very variable clinical manifestations depending on the genetic background of the individuals. However, patients with PIDs usually develop susceptibility to infections, and undergo multiple severe infections, which are termed as routine infections (Raje & Dinakar, 2015). The elevated infection susceptibility is a hallmark for PIDs.

Table 1.2. Ten clinical symptoms considered as the warning signs of immunodeficiencies (McCusker & Warrington, 2011)

1	≥ 8 ear infections in a year
2	≥ 2 serious sinus infections within 1 year
3	≥ 2 months on antibiotics without significant effect
4	≥ 2 pneumonias within 1 year
5	Failure of an infant to grow normally or gain weight
6	Recurrent, deep skin or organ abscesses
7	Persistent thrush in mouth or on the other parts of the skin, after age 1
8	Requirement for intravenous antibiotics to clear infections
9	≥ 2 deep-seated infections
10	A family history of PID

Many PIDs are detected in the early life due to the severity of the conditions. Because of the heterogeneity of the symptoms, specialized testing by clinical immunologists is essential. PIDs are subdivided into main classes depending on the defective compartment of the immune system: adaptive immunity or innate immunity disorders (Table 1.3) (McCusker, Upton, & Warrington, 2018).

Adaptive immunity defects are concerned with the defects in B and T cells. B cells are responsible for the antibody production to create humoral immune responses (Rosenzweig & Holland, 2011). Therefore, defects related to the development of maturation of B cells are referred as B cell (humoral) IDs. Cellular immunity is governed by T cells in the body. Defects at any step for a naïve T cell to form an effector T cell is referred as T cell (cellular) IDs. Production of antibodies is dependent on functional T cell responses; cellular IDs usually lead to combined immunodeficiencies (CIDs).

Innate immunity is described as the first line of defense towards pathogens. The defects associated with innate immunity causes delays in the inflammatory and immune responses, as innate immune cells are responsible for the activation of adaptive immune cells. Innate immune system has many components such as complement system, phagocytes and DCs. Therefore, defects at any component might cause severe outcomes in terms of infection. Innate immune system has many components such as complement

system, phagocytes and DCs.

Table 1.3 PID classification and main disorders belonging to adaptive and innate immune systems (McCusker et al., 2018)

Classification of PIDs
Adaptive Immunity Disorders
T cell (cellular) Immunodeficiency
<ul style="list-style-type: none"> • AIRE mutations • IFN-γ/IL-12
B cell (antibody-mediated) Immunodeficiency
<ul style="list-style-type: none"> • CVID • Selective IgA deficiency • Specific antibody deficiency • IgG isotype deficiency • XLA
CID
<ul style="list-style-type: none"> • Ataxia telangiectasia • DiGeorge syndrome • Wiskott-Aldrich syndrome • SCID <p>T⁻, B⁺ -γc deficiency -JAK3 deficiency</p> <p>T⁻, B⁺ -ADA deficiency -RAG1/2 deficiency</p>
Innate Immunity Disorders
Phagocyte defects
<ul style="list-style-type: none"> • Chronic granulomatous disease • Leukocyte adhesion deficiency
Complement defects
<ul style="list-style-type: none"> • C3 and regulatory components • Deficiency in early complement pathway components (C1q, C1r, C2, C4)

- Deficiency in late complement pathway components (C5, C6, C7, C8, C9)

The clinical representations of CIDs and T cell IDs is highly patient-specific. For instance, patients might be neutropenic or lymphopenic. The most serious version of CIDs leads to SCID. In patients with SCID, there is a fundamental absence of immune response and T cells (Notarangelo, 2016). SCID are therefore subdivided into subclasses based on the presence of B cells (T⁻, B⁺; T⁻, B⁻). SCID patients commonly have chronic diarrhea and opportunistic infections, thus cannot survive within the first year of their lives. The curative strategy for SCID is bone marrow transplantation (Buckley, 2011). Ataxia telangiectasia, DiGeorge syndrome, Wiscott-Aldrich syndrome, X-linked lymphoproliferative diseases are other CIDs that progress less serious than SCID, and they present later clinical manifestations in the childhood (Kobrynski, 2006). B cell IDs result in deficiency of antibodies. This heterogeneous class of IDs are especially defined by the elevated tendency to have bacterial infections of respiratory tract (*Haemophilus influenzae* and *Streptococcus pneumoniae*) (McCusker & Warrington, 2011). There are currently a more than 20 B cell IDs. For instance; common variable immunodeficiency (CVID), IgA deficiency, and X-linked agammaglobulinemia (XLA) are examples of it. The diminished levels of serum IgGs (IgG, IgA and IgM) as well as circulating B cells are the warning signs. Phagocyte disorders are usually characterized by the serious fungal or bacterial infections on the internal organs, respiratory tracts, and other parts of the skin (Rosenzweig & Holland, 2004). Hyper IgE syndrome and chronic granulomatous disease (CGD) are widespread examples PIDs related to innate immunity. On the other hand, complement deficiencies are quite rare, which are related to systemic autoimmune disorders.

With the advancement in next generation sequencing technologies including whole exome and genome sequencing technologies, diagnosis of PIDs have been accelerated. In the 2000s, the definition of inborn errors of immunity have been augmented, as provided with the discoveries on both mendelian and non-mendelian genetic bases of infectious diseases (J.-L. Casanova & Su, 2020). Accordingly, accumulating body of knowledge discovered some genetic defects causing susceptibility to viral pathogens (Table 1.4).

**Table 1.4 Genetic mutations that create susceptibility/resistance to viral infections
(J.-L. Casanova & Su, 2020)**

Outcome	Pathogen (condition)	Gene
Susceptibility	Rhinovirus (severe pneumonia)	IFIH1
	Influenza virus (severe pneumonia)	IRF7
		IRF9
		TLR3
	Herpes simplex virus 1, influenza virus, norovirus (brainstem encephalitis)	DBR1
	Herpes simplex virus 1 (encephalitis)	UNC93B1
		TLR3
		TRIF
		TRAF3
		TBK1
		IRF3
		SNORA31
	Beta-papillomavirus (skin warts and cancer)	TMC6
		TMC8
		CIB1
	Hepatitis A virus (fulminant hepatitis)	IL18BP
	Human herpes virus-8 (Kaposi sarcoma)	TNFRSF4
	Eppstein-Barr virus (hemophagocytosis, lymphoproliferation, lymphoma, hypogammaglobulinemia)	SH2D1A
		XIAP
		ITK
		MAGT1
		CD27
		CD70
Varicella-zoster virus (disseminated disease)	POL3A	
	POLR3C	
Live attenuated measles or yellow fever vaccine (disseminated disease)	IFNAR1	
	IFNAR2	
	STAT2	
	IRF9	

	Cytomegalovirus (disseminated disease)	NOS2
Resistance	Human immunodeficiency virus	CCR5
	Norovirus	FUT2

1.4.1. Epstein-Bar Virus and Primary Immunodeficiency Diseases

Epstein-Bar virus (EBV) is a widespread γ -herpes virus that is the first characterized human oncovirus. Initial identification of EBV was performed from biopsy cells from a Burkitt's lymphoma patient (Epstein et al., 1963; O'Connor, 1987; Shabani, Nichols, & Rezaei, 2016). EBV is classified into two types: type 1 and type 2. Genomic studies revealed that those two types are quite similar yet the difference is in the EBNA genes. A study demonstrated that type 1 EBV can induce B cell proliferation more because of higher EBNA2 expression, which increases cellular CXCR7 and LMP1 levels (Cancian, Bosshard, Lucchesi, Karstegl, & Farrell, 2011).

EBV has a tropism to infect B cells and epithelial cells. EBV-associated malignancies are commonly observed in people that has immunosuppression; such as patients with PIDs, AIDS patients, and solid organ transplantation patients. EBV is linked to gastric carcinomas, nasopharyngeal carcinoma, diffuse B cell lymphoma, Hodgkin lymphoma, and lymphoproliferative diseases (LPD) of T and NK cells (Shannon-Lowe & Rickinson, 2019). EBV enters the body through epithelial surfaces. Latency of EBV is characterized by varying gene expression levels after primary infection. Hence, EBV life cycle is separated into four latency types (latency 0-III), and determined by epigenetic modifications including histone modifications and CpG methylation, so that primary infection is followed by persistent infection. EBV life cycle is depicted in Figure 1.11. EBV usually goes undetected in healthy people as it stays dormant because of its distinct latency programs. For instance, CpG promoter methylation is responsible for maintaining lytic phase genes silent and staying in the latency phases (Bergbauer et al., 2010). When, EBV lytic phase is activated; changes in transcription factor accessibility, triggering tumor development because of the silencing of tumor suppressor genes are observed. For instance, enhancer looping of myc gene provides enhanced cell survival and metabolic activities allowing tumor support (S. Jiang et al., 2017). In an immunocompetent person

with seropositive EBV condition, monitoring of EBV is carried out by CD8⁺ T cells. In immunocompetent patients, EBV is able to proliferate because of reduced CD8⁺ T cells. This leads to the reduction in EBV-specific CD8⁺ T cell numbers.

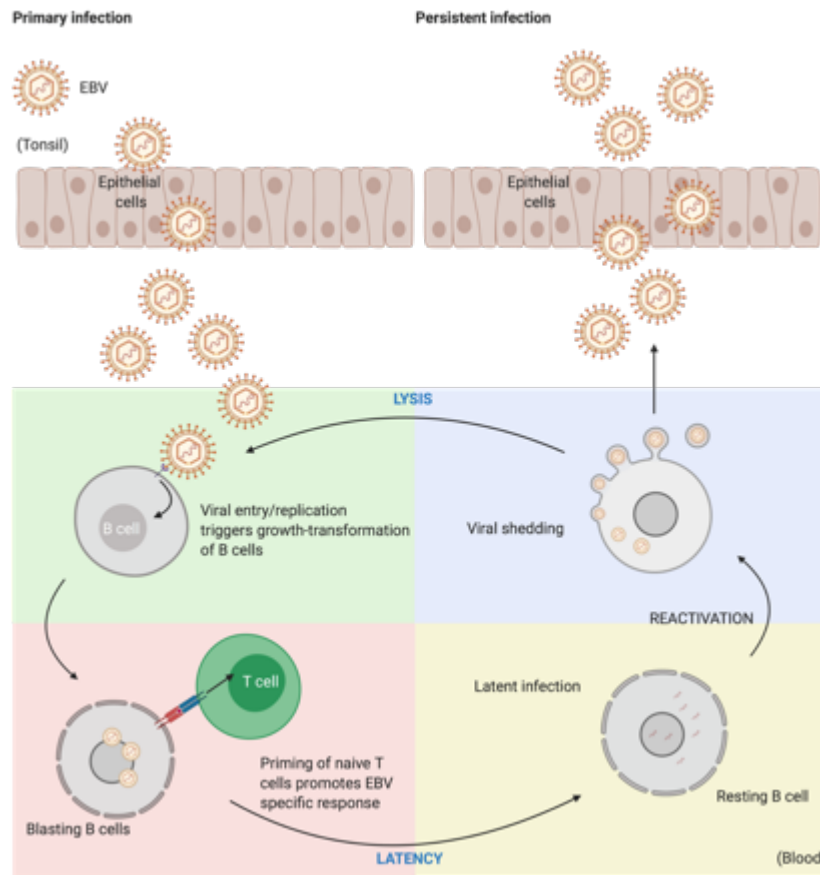


Figure 1.11. Life cycle of EBV in primary and persistent infections

EBV life cycle starts with its entry to body through epithelial surfaces as the first step by direct fusion. Multiple viral proteins facilitate viral entry to cells through glycoprotein complexes gB and gH/gL. The entry routes are different for epithelial cells and B cells. EBV entry into B cells also require gp42 and gp350, which are necessary for B cell fusion as it binds to MHC II. Transformation of B cells results in the formation of lymphoblastoid cells (LCLs). Naïve T cells differentiates into memory and CD8⁺ T cells in order to combat transformed cells. This infection is kept under control by the cytolytic activity of T cells, this stage is referred as latency. When latency is broken, with the impact of different stimuli such as environmental cues, resting B cells begins to be a host for viral replication, new virions are released through viral shedding, and this step is referred as the lytic stage.

Inherited IDs have been indicated to set individuals at high susceptibility in term of LPDs that are induced by EBV. LPDs are usually classified as malignant and non-malignant

LPDs of B lymphoma, and virus-associated hemophagocytic syndrome. The mutations that render individuals susceptible to LPDs are mainly ITK, XIAP, MAGT1, CTPS1, CD27, CD70, CORO1A, SH2D1A (SAP) and RASGRP1 (Latour & Winter, 2018). Deficiencies in the aforementioned mutations have been reported and characterized in the EBV-associated LPDs. Studies regarding these mutations have revealed the essential pathways that are fundamental for the immunity towards EBV. Expansion of EBV-specific T cells is carried out by the CD27/CD70 pathway, which represents a vital axis for this purpose. RASGRP1 and CTPS1 are also enhances expansion as well. MAGT1-mediated NKG2D and SLAM receptor pathways provide the cytotoxicity for NK and T cells against EBV-infected B cells (Latour & Fischer, 2019).

TNF/TNFR SF members constitute important co-stimulatory molecules for T cell activation. CD27, CD70 and 4-1BB deficiencies in immunocompetent individuals with EBV-induced LPDs have been previously reported (Abolhassani et al., 2017; Alosaimi et al., 2019; Caorsi et al., 2018; Izawa et al., 2017). CD70 deficiency was found in total six individuals, which are homozygous carriers of the corresponding mutations. B cell lymphoproliferation and EBV-driven Hodgkin's lymphoma was observed in five patients. Inflammatory symptoms with viral encephalitis, reduced serum Ig levels were also found out. An additional study by (Abolhassani et al., 2017), demonstrated that memory CD8⁺ T cells had reduced expressions of NKG2D and 2B⁺ in the patients with CD70 deficiency. Clinical manifestation of CD27 deficiency also quite similar to CD70 deficiency (Alkhairy et al., 2015; Izawa et al., 2017; Salzer et al., 2013; Van Montfrans et al., 2012). 18 patients have been pronounced to have EBV-linked LPDs including non-Hodgkin's and Hodgkin's lymphoma and polyclonal proliferation of B cells. EBV-associated hemophagocytic lymphohistiocytosis (HLH) was also among the LPDs observed.

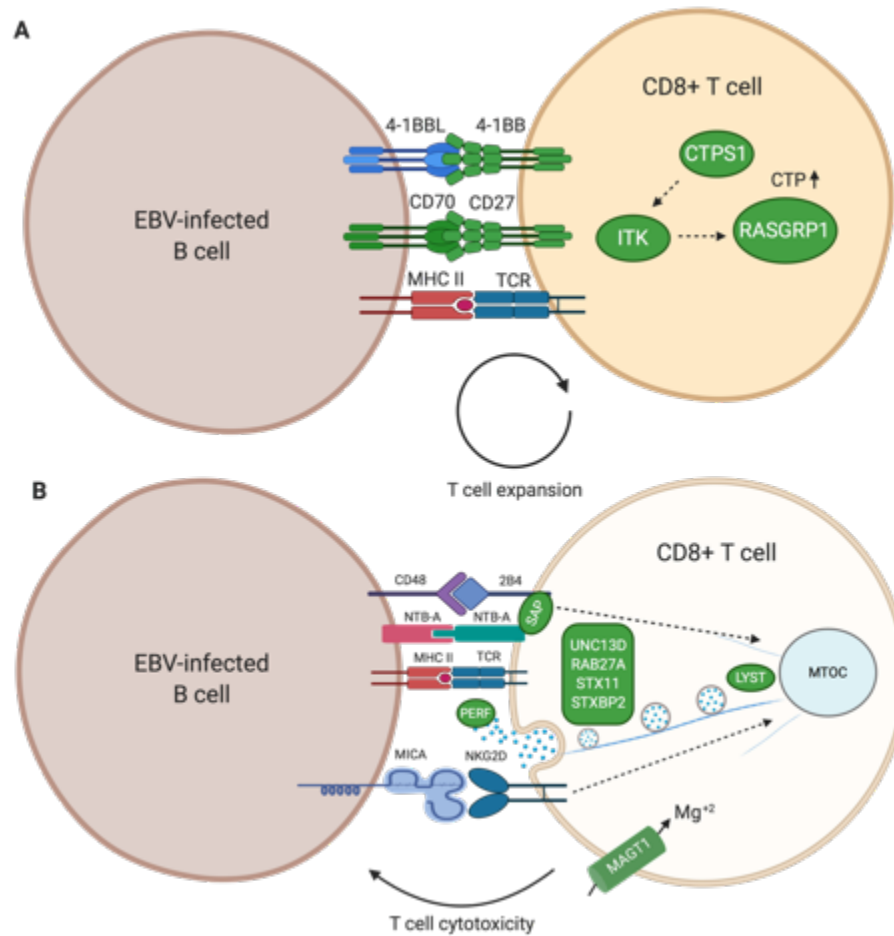


Figure 1.12 Genetic mutations of CD8+ T cells causing susceptibility to EBV-driven PIDs

Important signalling pathways required for immunity towards EBV infected cells is depicted. Defects in the CD8+ T cell expansion (A) and cytotoxicity (B) towards EBV-infected B cells. Mutated proteins are demonstrated in green.

2. AIM OF THE STUDY

The immune system has evolved to carry out protective, specific, and robust responses towards pathogens, and unhealthy cells. The immune system is responsible for the creation of strong and long-lasting defense mechanisms that protect individuals through adaptive and innate immunity. In this context, defense against viral infections is mediated by the concerted activity of interacting cells, cell products and tissues in a strictly regulated manner. Primary immunodeficiencies (PIDs) are a heterogeneous group of immune disorders, that stem from genetic defects leading to partial or complete loss-of-function. Epstein-Bar virus (EBV) is a widespread human gammavirus that is usually asymptomatic in immunocompetent individuals, but causes severe conditions in immunodeficient individuals. The CD27/CD70 co-stimulatory pathway activates T lymphocytes and is required to combat EBV.

In the first part of this study, we aimed to identify a novel genetic mutation in the CD70 gene that causes PID. A patient with this mutation exhibited an EBV-driven lymphoproliferative disease. To investigate the genetic causes, we isolated peripheral blood mononuclear cells (PBMCs) from the patient and his parents to clone and sequence the CD70 gene. We identified a point mutation in the third exon of CD70.

Next, we wanted to investigate the functional outcomes of this mutation. Accordingly, the second part of this study focuses on the cell surface and intracellular expression of wild-type and mutant CD70 proteins. To investigate this, we use pseudotyping-mediated lentiviral vector production, and transduction to generate stable cell lines of K-562 and Namalwa cells. We also expressed epitope-tagged CD70 from lentiviral constructs to address cell surface expression.

Tumor necrosis family (TNF) member CD70 is a unique ligand of tumor necrosis family receptor (TNFR) family member CD27. The homotrimeric interaction between these receptors initiate T cell co-stimulatory signalling. In the third part of this thesis, we employ a cloning strategy to produce CD27-Fc fusion proteins for use as an activator of CD70. In conclusion, our aim was to identify and characterize a novel mutation causing CD70 deficiency, which leads to PID. Our work adds important details to the literature because it reports a novel genetic defect. The diagnosis of PIDs are challenging, and very important to prevent recurrent severe infections. Our study demonstrates the identification and characterization of this mutation and describes the functional significance of CD70 mutations in PIDs.

3. MATERIALS & METHODS

3.1. Materials

3.1.1. Chemicals

All the chemicals used in this thesis are displayed in Appendix A.

3.1.2. Equipment

All the equipments used in this thesis are displayed in Appendix B.

3.1.3. Solutions and Buffers

Agarose gel: 1 g of agarose powder was dissolved within 100 mL of 0.5X TBE buffer by applying heat in a microwave to achieve 1% (v/v) agarose gel. 0.002% (v/v) ethidium bromide was added to the solution.

Calcium Chloride (CaCl₂) Solution: 60 mM CaCl₂ (dilution from 1M stock solution), 15% glycerol and 10 mM PIPES (pH 7.0) were combined and total volume was filled up to 500 mL with ddH₂O. The solution was filtered with 0.22 μM filter and stored at 4 °C.

HBS solution (2X): 280 mM NaCl, 50 mM HEPES, and 1.5 mM Na₂HPO₄ were mixed, pH was maintained at 7.1 with 10 M NaOH. The solution was filtered with 0.22 μM filter and stored at -20 °C.

Permeabilization Buffer: In order to prepare 50 ml of permeabilization buffer, 5 ml of 10X saponin (0.01% w/v saponin in ddH₂O) was added 5 ml of 10X PBS and total volume was completed to 50 ml with ddH₂O.

Permeabilization and Fixation Buffer: To prepare 10 ml of permeabilization and fixation buffer: 2.5 ml of 4% PFA w/v was added 1 ml of 10X saponin, 1 ml of PBS and total volume was completed to 10 ml with ddH₂O.

Tris-Borate-EDTA (TBE) Buffer: 27.5 g boric acid, 54 g Tris-Base, and 20 mL of 0.5 M EDTA (pH 8.0) were dissolved within 1L of ddH₂O to prepare 5X TBE buffer stock solution. Working solution (0.5X) was achieved by diluting the stock with a ratio of 1 to 10.

3.1.4. Growth Media

Luria Broth (LB): 20 g of LB powder was added 1 L of ddH₂O and sterilized by autoclaving at 121 °C for 15 minutes to prepare 1L 1X LB medium. Ampicillin at the final concentration of 100 µg/mL or kanamycin at the final concentration of 50 µg/mL was added upon cooling down the medium and only prior to use for antibiotic selection.

LB-Agar: 35 g LB-Agar powder was added 1 L of ddH₂O and autoclaved 121 °C for 15 minutes for the preparation of 1L 1X agar medium. The corresponding antibiotic was added to agar medium upon cooling down to 50 °C. Ampicillin at the final concentration of 100 µg/mL or kanamycin at the final concentration of 50 µg/mL was added. 15 mL of LB-Agar solution was transferred to sterile petri dish under laminar flow hood. Petri dishes were stored at 4 °C.

Complete DMEM Medium: HEK293FT cells were cultured in DMEM supplemented with 10% (v/v) heat-inactivated fetal bovine serum (FBS), 2 mM L-Glutamine, 1 mM Sodium Pyruvate, 0.1 mM MEM non-essential amino acid solution and 25 mM HEPES solution.

Complete RPMI 1640 Medium: K-562 and Namalwa cells were maintained in RPMI 1640 supplemented with 10% (v/v) heat-inactivated FBS, 2 mM L-Glutamine, 1 mM

Sodium Pyruvate, 0.1 mM MEM non-essential amino acid solution, 25 mM HEPES, 1X MEM vitamins.

Freezing Medium: All cell lines were frozen within heat-inactivated FBS having 6% (v/v) Dimethylsulfoxide (DMSO).

3.1.5. Molecular Biology Kits

All commercial molecular biology kits are listed in Appendix C.

3.1.6. Enzymes

DNA modifying, restriction enzymes, polymerases, and their corresponding buffer solutions were obtained from New England Biolabs (NEB).

3.1.7. Antibodies

All flow cytometry antibodies employed are listed in Appendix D.

3.1.8. Bacterial Strains

Escherichia coli (*E.coli*) DH-5 α and Top10 strains were used for transformation and cloning applications.

3.1.9. Mammalian Cell Lines

HEK293FT: Highly transfectable, fast-growing clonal isolate isolated from human embryonic kidney cells transformed with SV40 large T antigen (Invitrogen R70007).

K-562: K-562 cells are human immortalized myelogenous leukemia cell line. They were derived from a 53-year-old female chronic myelogenous leukemia patient in blast crisis (ATCC® CCL- 243™).

Namalwa: Namalwa cells are human Burkitt's lymphoma cell line isolated from a tumor mass of 3-year-old Burkitt's lymphoma patient. (ATCC® CRL-1432™).

3.1.10. Plasmids and Oligonucleotides

All plasmids employed in this thesis are listed in Table 3.1.

Table 3.1 List of plasmids used in this thesis

PLASMID NAME	PURPOSE OF USE	SOURCE
pCR4-TOPO-CD70 FLAG-father	Mammalian plasmid for sequencing of full-length FLAG-tagged CD70 gene from father	Lab construct
pcDNA3.1(+)-CD70 FLAG-patient	Mammalian plasmid for sequencing of full-length FLAG-tagged CD70 gene from patient	Lab construct
pCR4-TOPO-CD70-exon 3-FLAG-patient	Mammalian plasmid for sequencing of third exon of FLAG-tagged CD70 gene from patient	Lab construct
pCR4-TOPO-CD70-exon 3-FLAG-mother	Mammalian plasmid for sequencing of third exon of FLAG-	Lab construct

	tagged CD70 gene from mother	
pCR4-TOPO-CD70-exon 3-FLAG- father	Mammalian plasmid for sequencing of third exon of FLAG- tagged CD70 gene from father	Lab construct
pMDLg/pRRE	<i>Gag/pol</i> encoding plasmid. Third generation lentiviral vector production	Addgene #12251
pRSV-REV	<i>Rev</i> encoding plasmid. Third generation lentiviral vector production	Addgene #12253
pCMV-VSV-g	<i>Env</i> encoding plasmid. Third generation lentiviral vector production	Addgene #8454
LeGO-iG2-puro	Lentiviral construct for eGFP expression with IRES	Kind gift from Prof. Boris Fehse, University Medical Center Hamburg- Eppendorf, Hamburg, Germany
LeGO-iT2-puro	Lentiviral construct for tdTomato expression with IRES	Kind gift from Prof. Boris Fehse, University Medical Center Hamburg- Eppendorf, Hamburg, Germany
CD70wt-LeGO-iG2-puro	Lentiviral construct for the stable	Lab construct

	expression of wild-type CD70 protein with eGFP, IRES and puromycin genes	
CD70mut-LeGO-iG2-puro	Lentiviral construct for the stable expression of mutant CD70 protein with eGFP, IRES and puromycin genes	Lab construct
CD70wt-LeGO-iT2-puro	Lentiviral construct for the stable expression of wild-type CD70 protein with tdTomato, IRES and puromycin genes	Lab construct
CD70mut-LeGO-iT2-puro	Lentiviral construct for the stable expression of mutant CD70 protein with tdTomato, IRES and puromycin genes	Lab construct
RC200410	Subcloning of wild-type CD70 into lentiviral constructs	Kind gift from Prof. Michael Lenardo, NIAD/NIH
RC200410-CD70 (F186del)	Subcloning of wild-type CD70 into lentiviral constructs	Kind gift from Prof. Michael Lenardo, NIAD/NIH
RC200410-CD70 (T111M)	Subcloning of wild-type CD70 into lentiviral constructs	Lab construct

CD70wt-MF-LeGO-iG2-puro	Lentiviral construct for the stable expression of wild-type myc- and FLAG-tagged CD70 protein with eGFP, IRES and puromycin genes	Lab construct
CD70(T111M)-MF-LeGO-iG2-puro	Lentiviral construct for the stable expression of mutant (c. 332C>T) myc- and FLAG-tagged CD70 protein with eGFP, IRES and puromycin genes	Lab construct
CD70(F186del)-MF-LeGO-iG2-puro	Lentiviral construct for the stable expression of mutant (c. delCTT555_557) myc- and FLAG-tagged CD70 protein with eGFP, IRES and puromycin genes	Lab construct
CD27-LeGO-iG2-puro	Subcloning of extracellular domain of CD27 into a mammalian expression plasmid	Lab construct
AbVec2.0-IGHG1	Subcloning of Fc domain of IgG1 into	Addgene #80795

	a mammalian expression plasmid	
pcDNA3.1/myc-His (-) A	Mammalian expression plasmid with CMV promoter and myc- and FLAG epitope tags	ThermoFischer Scientific (V85520)
CD27-Fc-pcDNA3.1/myc-His (-) A	Mammalian expression plasmid for the expression of recombinant CD27-Fc	Lab construct

All oligonucleotides used in this thesis are shown in Table 3.3.

Table 3.2 List of oligonucleotides

OLIGONUCLEOTIDE NAME	SEQUENCE (5' → 3')	PURPOSE OF USE
CD70 cDNA BamHI - Forward	GAGAGGATCCATGCCGGAGGAGGG TTCG	TOPO cloning
CD70 cDNA FLAG EcoRI - Reverse	TTTTGAATTCTCACTTGTCGTCATCG TCTTTGTAGTCGGGGCGCACCCACT G	TOPO cloning
CD70 cDNA no FLAG EcoRI - Reverse	TTTTGAATTCTCAGGGGCGCACCCA CTGCACTCCAAAG	TOPO cloning
CD70 Exon 3 - Forward	TCCTTCCTGCATGGACCAGA	TOPO cloning
CD70 Exon 3 - Reverse	CACTCCCAAAGAAGGTCTCATCAG	TOPO cloning
CD70 SDM - Forward	ATCCAGGTGATGCTGGCCATC	Site-directed mutagenesis

CD70 SDM - Reverse	GTGTACCATGTAGATGCCATC	Site-directed mutagenesis
M13 – Reverse	CAGGAAACAGCTATGAC	Sanger sequencing of pCR4-TOPO constructs
SFFV forward	TGCTTCTCGCTTCTGTTC	Cloning into pcDNA3.1/myc-His (-) A plasmid and Sanger sequencing of LeGO backbones
T7 promoter	TAATACGACTCACTATAGGG	Sanger sequencing of pCMV6-Entry constructs
CD27 ED XhoI - Reverse	ATTCTCGAGGATTCTGATGAAATCGCT	Cloning into pcDNA3.1/myc-His (-) A plasmid
EGRMD Fc XhoI - Forward	TAACTCGAGGGCCGAATGGATCCCA AATCTTGTGACAAAACCT	Cloning into pcDNA3.1/myc-His (-) A plasmid
Fc HindIII - Reverse	TTGAAGCTTTTTACCCGGGGACAGG GA	Cloning into pcDNA3.1/myc-His (-) A plasmid

3.1.11. DNA Weight Marker

DNA ladders used in this thesis are shown in Appendix E.

3.1.12. DNA Sequencing

DNA sequencing services were provided by MCLAB, CA, USA. (<https://www.mclab.com/home.php>).

3.1.13. Software, Computer-based Programs and Websites

All computer-based programs, softwares, and websites in this thesis are provided in Table 3.3.

Table 3.3 List of computer-based programs, software and websites

SOFTWARE, PROGRAM, WEBSITE NAME	COMPANY/WEBSITE	PURPOSE OF USE
Addgene	https://www.addgene.org/	Information for plasmid maps
BD FACSDiva	BD Biosciences	Flow cytometry data acquisition and analysis
CLC Main Workbench v7.9.4	QIAGEN Bioinformatics	Molecular cloning, DNA sequence alignment and analysis

FLOWJo v4	Tree Star Inc. Flow Jo	Flow cytometry data analysis
Human Protein Atlas	https://www.proteinatlas.org	RNA expression levels overview
NCBI BLAST	https://blast.ncbi.nlm.nih.gov/Blast.cgi	Tool for biological sequence similarities
NCBI Primer-Blast	https://www.ncbi.nlm.nih.gov/tools/primer-blast/	Tool for primer design
STRING	https://string-db.org	Tool for protein-protein interactions network
UniProt	https://www.uniprot.org	Topological information about proteins
Visual Molecular Dynamics (VMD)	https://www.ks.uiuc.edu/Research/vmd/	Homology modelling for single CD70 molecule, and its heterotrimers

3.2. Methods

3.2.1. Bacterial Cell Culture

3.2.1.1. Bacterial Growth

Cultures of *E.coli* DH5 α and Top10 strains were carried out in LB medium in the presence of the corresponding antibiotics overnight (12-16 hours) with shaking (221 rpm) at 37 °C for antibiotic selection. Single bacterial colonies were obtained by spreading the bacterial culture on LB Agar plates with the corresponding antibiotic through autoclaved glass beads. Plates were incubated at 37 °C for overnight (12-16 hours) to get single colonies. For long-term storage, glycerol stocks were prepared. 10% (v/v) glycerol was combined with bacterial culture to achieve total volume of 1 ml within cryovials under the laminar flow hood. Glycerol stock cryovials were stored at -80 °C.

3.2.1.2. Preparation of Competent Bacteria

Competent *E.coli* DH5 α or Top10 cells were cultured in 40 ml of LB Broth in a flask (250 ml) in the absence of any antibiotics overnight at 37 °C and shaking (221 rpm). 4 mL from the turbid overnight-culture of 40 ml was inoculated into 400 mL of LB Broth in a flask (2 L) and incubated at 37 °C with shaking (221 rpm) until optical density (OD) has been 0.375. Upon reaching this OD value, the culture was splitted into eight falcon tubes (50 ml) and put on ice for 10 minutes. CaCl₂ solution was used ice-cold and centrifugation steps were carried out at 4 °C throughout the entire protocol. Bacterial culture was then centrifuged at 1600 g for 10 minutes. The supernatants were discarded

and each pellet was dissolved within 10 mL of CaCl₂ solution. Dissolved pellets were centrifuged at 1100 g for 5 minutes. Pellets were resuspended within 10 ml of CaCl₂ solution and kept on ice for 30 minutes. Suspensions were centrifuged at 1100 g for 5 minutes. Pellets were dissolved with 2 mL of CaCl₂/tube and combined in a single falcon tube (50 ml). Suspensions were aliquoted as 200 µL/tube into pre-chilled microcentrifuge tubes. Aliquots were snap-frozen in liquid nitrogen and then stored at -80 °C. Transformation efficiency was assessed by transforming with pUC19 plasmid at varying concentrations. Transformation efficiency was aimed to be in the range of 10⁷-10⁸ cfu/µg.

3.2.1.3. Transformation of Competent Bacteria

Heat-shock transformation was performed in each transformation. Chemically-competent bacteria aliquots were thawed on ice. DNA at a desired concentration was put into competent bacteria aliquots and kept on ice for 30 minutes. Plasmid transformation with purified DNA was transformed with 1 pg-1ng of DNA amount; ligation mixes were transformed with 10-20 µl of volume. Heat-shock step was achieved by keeping cells at 42 °C for 90 seconds followed up with a minute on ice. 800 µl of LB Broth was added each heat-shocked cell, and this step was continued with a subsequent centrifugation at 13,000 rpm for 30 seconds. Bacterial pellets were dissolved in 100 µl of LB Broth from supernatants. Spreading of these suspensions was done to LB-agar plates with the appropriate antibiotic for selection, and the plates were incubated at 37°C overnight (12-16 hours).

3.2.1.4. Isolation of Plasmid DNA

Plasmid DNA from competent *E.coli* DH5α and Top10 was performed according to alkaline lysis method for mini preparations, demonstrated in Molecular Cloning: A Laboratory Manual (Sambrook et al.). Midi preparations were carried out with the commercial Macharey Nagel Midiprep kit, based on the manufacturer's instructions. Isolated plasmid DNA from mini preparations was assumed to be 200 ng/µL.

Concentration and purity values of isolated plasmid DNA from midi preparations were measured by a NanoDrop S-spectrophotometer.

3.2.2. Mammalian Cell Culture

3.2.2.1. Maintenance of Cell Lines

293FT cells were cultured in complete DMEM medium within sterile tissue culture flasks with filtered caps at 37 °C and 5% CO₂ levels. Cell splitting was performed when cell confluency was reached to 80-90%. Cells were rinsed with sterile PBS, trypsin-EDTA (0.25%) was added to cells to achieve cell detachment from flasks. To do so, cells were incubated for 5 minutes at 37 °C, 5% CO₂. After confirming cell detachment by visual inspection, cells were resuspended within complete DMEM. Cell splitting was performed at a 1:5 splitting ratio in 2-3 days. K-562 and Namalwa cells were cultured in complete RPMI 1640 medium at a density 300.000 cells/ml and incubated at 37 °C, 5% CO₂. Cells were splitted when they reached to 1,000,000 cells/mL in every 2-3 days in complete RPMI 1640 within sterile tissue culture flasks.

3.2.2.2. Cryopreservation of Cells

Cells of any cell line were split to a confluence around 40% for 293FT cells and to a cell density of 500,000 cells/ml for Namalwa and K-562 cells. 293FT and K-562 cells were frozen as 3x10⁶ cells/vial and Namalwa cells were frozen as 4x10⁶ cells/vial the next day. To do so, cells were spun down at 300 g for 5 minutes. For each vial, 0.5 ml of FBS was added to dissolve cell pellets, and incubated at 4 °C for 15-20 minutes. 12% (v/v) DMSO in FBS was prepared fresh at the same time as the freezing medium. 0.5 ml of ice-cold 12% (v/v) DMSO in FBS was mixed with 0.5 ml of cell suspension in FBS to reach 1 ml of total volume/vial at a final 6% (v/v) DMSO concentration. Cryovials were incubated within a freezing container having isopropanol at -80 °C for a day. Cryovials were then transferred to liquid nitrogen tank for long-term storage.

3.2.2.3. Thawing Frozen Mammalian Cells

Cells in cryovials from liquid nitrogen tank was brought to room temperature. Falcon tubes (15 ml) were added 4 ml of FBS for each vial. 1 ml of frozen cell suspension was transferred to the 4 ml of FBS very slowly. Cells were spun down at 300 g for 5 minutes and cell pellet was resuspended in complete media, and cells were visually inspected the day after the thawing process.

3.2.3. Lentiviral Vector Production, Transduction and Flow Cytometry

3.2.3.1 Lentiviral Vector Production

VSV-G pseudotyped third generation lentiviral vectors were produced in 293FT cells. To do so, 100-mm dishes added 3 ml of Poly-L-Lysine solution (0.1% w/v in H₂O) solution for each dish for coating purposes. After incubation for 10 minutes at RT, dishes were washed with 5 mL of sterile ddH₂O to eliminate the residues of poly-L-Lysine solution, and plates were left with their lids open under laminar flow hood. When dishes were dried out, each poly-L-Lysine coated dish was seeded with 5 x 10⁶ 293FT cells. Calcium phosphate co-transfection was performed using 3.75 µg of pMDLg/pRRE, 2.25 µg of pRSV-REV and 1.5 µg of pCMV-VSV-G together with 7.5 µg of gene of interest plasmid (LeGO-iG2-puro & LeGO-iT2-puro backbones). Upon preparing the plasmid DNA mixes, the final mix was added 50 µl of 2.5 M CaCl₂ solution, and total volume was completed to 500 µl with sterile ddH₂O. 500 µl of plasmid mixes and 500 µl of 2X HBS were combined together while bubbling and kept at RT for 15 minutes. Culture media of transfection dishes were replaced with DMEM-Glutamax (supplemented with 25 µM chloroquine). Transfection mixes were added to dishes in a dropwise manner while gently swirling the dishes. Transfection dishes were incubated at 37 °C, 5% CO₂ for 10 hours. Upon completion of 10 hours, cell culture media was replenished with DMEM Glutamax. Cell culture supernatant with infectious particles were harvested after 24 and 36 hours of incubations by passing through filters with a pore size of 0.45 µm into falcon tubes. An aliquot volume of 100 µl of the corresponding infectious particles was spared for further titration purposes. Harvested infectious particles were stored at -80 °C until

further use in transduction purposes.

3.2.3.2. Virus Titer Determination

In order to calculate infectious particles per ml, 0.5×10^5 293FT cells/well was seeded into 24-well plates and incubated at 37 °C, 5% CO₂ for 5-6 hours until cells are attached to the well plate surface. Serial dilutions were prepared to achieve different concentrations of harvested viral supernatants. Serial dilutions were applied to each well with proteamine sulfate (8 µg/ml). Culture media was replenished with DMEM after 16 hours of incubation. Flow cytometry analysis was performed after two days of incubation. Multiplicity of infection (MOI) calculations were done according to the percentages of fluorochrome expressing populations.

3.2.3.3. Lentiviral Transduction

Lentiviral transductions were carried out in sterile T25 tissue culture flasks and 6-well plates. K-562 and Namalwa cells were undergo lentiviral gene transfer. All transductions were carried out in the presence of proteamine sulfate (8 µg/ml). To do so, proteamine sulfate (8 µg/ml) and 1 ml of the corresponding viral supernatants were combined. Cell suspensions were then added at the specified ratio: 1×10^6 cells/flask, 0.5×10^5 cells/well for T25 flask and 6-well plate respectively. Cells were then incubated for overnight (16 hours) at 37 °C, 5% CO₂. Cells were spun down at 300 g for 5 minutes in order to eliminate non-integrated infectious particles and proteamine sulfate residues the next day. Cells were kept in the same culture conditions and fluochrome expression percentages were determined by flow cytometry. In order to obtain homogenous cell populations with transgene expressions, cells were added puromycin (8 µg/ml) until entire population has shifted to fluochrome-positive expression state.

3.2.3.4. Flow cytometry

In order to evaluate transgene expression, cell surface and intracellular staining protocols were applied. Surface staining of K-562 and Namalwa cells were performed as follows: cells were rinsed once with PBS and centrifuged at 300 g for 5 minutes. Upon removal of supernatant; cell pellet was added the corresponding antibody, gently mixed using vortex and incubated on ice at dark for 30 minutes. After the completion of incubation time, cells were washed twice with 500 µl of PBS and proceeded to data acquisition in FACS buffer (0.5% v/v FBS in PBS). For intracellular staining; cells were washed, cell pellets were added 250 µl of permeabilization and fixation buffer dropwise while mixing with vortex, and incubated on ice for 15 minutes as the fixation step. Cells were then washed with 1 ml of permeabilization buffer twice. Cell pellets were added the corresponding antibody and incubated on ice for 30 minutes at dark. Cells were then washed with 2 ml of permeabilization buffer and proceeded to flow cytometry in FACS buffer. All data were acquired with BD Biosciences LSR Fortessa and analyzed with FlowJo software.

3.2.4. Isolation of Human PBMCs and Total RNA

3.2.4.1. Isolation of Human PBMCs

Isolation of human PBMCs were performed based on differential migration of cells based on their sedimentations under centrifugal force. To do so, Histopaque was used to create density-gradient centrifugation environment, which has Ficoll as the synthetic polymer of sucrose. Blood samples of patient, mother and father were diluted at a 1:1 ratio. Diluted blood samples were added onto Histopaque layer at a 45° angle very slowly and without bubbling in a falcon tube (15 ml). Tubes were centrifuged at 400 g for 20 minutes with slow acceleration and deceleration rates. PBMC layer was carefully pipetted through plasma layer and transferred to round bottom tube, as blood layers after successful separation were shown in Figure 3.1 below. Sterile PBS was added, tube was mixed by inverting up and down gently and centrifuged at 300 g for 5 minutes to pellet cells.

Supernatants were eliminated and cell pellets were washed again. Cell pellets were then resuspended in complete RPMI 1640 media supplemented with 10% v/v FBS. Cells were counted and some of them were frozen for cryopreservation.

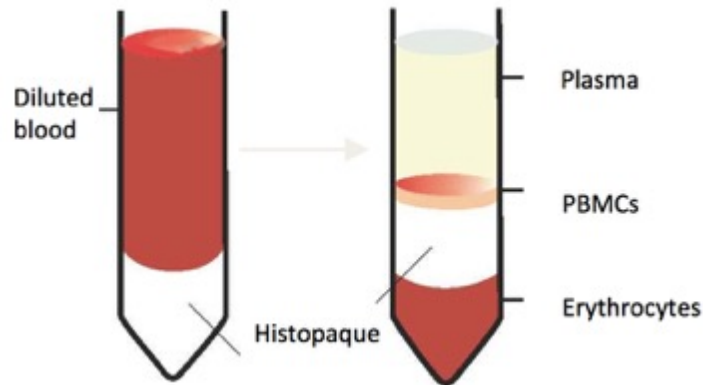


Figure 3.1 Isolation of PBMCs

Schematic representation of density gradient-based separation of blood cells

3.2.4.2. Nucleic Acid Isolation

Isolation of total RNA and genomic DNA was both carried out from previously isolated peripheral blood mononuclear cells (PBMCs) of patient, mother and father. Total RNA isolation was performed with TRIzol reagent, Invitrogen according to manufacturer's protocol. Genomic DNA isolation from PBMCs of patient, mother and father was performed by the PureLink Genomic DNA Mini Kit, ThermoFischer. Synthesis of cDNA was carried out with

3.2.5. Vector Construction

Restriction enzyme digestion:

Restriction enzyme digestion reactions were set up in PCR tubes by combining the DNA amount, enzymes and their compatible buffers. Incubation at the optimal temperatures for enzymes was carried out in Thermal Cycler for 1-3 hours.

Dephosphorylation of 5' phosphate groups:

In order to prevent self-annealing of plasmid DNA backbones, 5' phosphate groups were eliminated upon single or double restriction digestion through the use of alkaline phosphatases. Alkaline phosphatases employed are either calf intestinal alkaline phosphatase (CIAP) or shrimp alkaline phosphatase (rSAP).

Agarose gel electrophoresis and DNA extraction:

Separation and subsequent visualization of products obtained after restriction digestion reactions, PCR and other plasmid DNA were done by agarose gel electrophoresis. Agarose gels were prepared and agarose percentage, [0.7 to 2% w/v] was determined based on the size of DNA fragment within 100 ml of 0.5X TBE. Agarose gel solution was heated in a microwave for total dissolution, 2 μ l of ethidium bromide (0.0002% v/v). Then, the agarose solution was solidified by pouring into gel tray. DNA samples were mixed with gel loading dye prior to loading to gel. Electrophoresis was performed by supplying 100 V constant voltage for 45-90 minutes within 0.5X TBE buffer. After separation of DNA fragments, fragments at the expected size was quickly extracted from the agarose gel under UV light to prevent the potential mutagenic effects of UV light to DNA. Purification of gel was performed with a commercially available kit.

Ligation:

All ligation reactions except TOPO clonings were set up with 1:3 vector to insert ratio according to 100 ng vector DNA, and T4 DNA Ligase and its compatible buffer (NEB) were utilized. TOPO cloning ligation mixes were set up according to manufacturer's instructions for five minutes at room temperature. Ligations reactions were performed either at 16°C overnight (16 hours) or at 25°C for two hours. Vector-only ligation was also carried out in each step to evaluate self-ligation of dephosphorylated vector ends as a negative control and all ligation mixes were transformed to either *E.coli* DH5 α or Top10 competent cells.

3.2.6. Mammalian Expression Vector Construction

3.2.6.1. Vector Construction by TOPO Cloning

In order to identify mutation through blunt end cloning, Thermo Fischer Zero Blunt TOPO PCR Cloning Kit for Sequencing was employed for fast and efficient cloning of PCR products. With the purpose of mutation identification, pCR4-TOPO-CD70 FLAG-

father, pCR4-TOPO-CD70 FLAG-patient, and pcDNA3.1(+)-CD70 FLAG-patient constructs were cloned. For TOPO cloning experiments, pCR4-TOPO was the backbone. As the initial work, PCR amplification was performed to create CD70 cDNA inserts with C-terminal FLAG tag together with BamHI and EcoRI restriction sites. Q5 High Fidelity DNA Polymerase was employed in all PCR reactions. Gradient PCR was performed to determine the ideal annealing temperature prior to cloning. Then, PCR reactions were set on ice as follows for the insert amplification as follows:

5X Q5 Reaction Buffer	5 μ l
10 mM dNTPs	0.5 μ l
10 μM Forward Primer (CD70 cDNA BamHI - Forward)	1.25 μ l
10 μM Reverse Primer (CD70 cDNA FLAG EcoRI - Reverse)	1.25 μ l
Template cDNA (1 ng)	1 μ l
Q5-High-Fidelity DNA Polymerase (2,000 units/ml)	0.25 μ l
ddH₂O	Up to 25 μ l

TOPO reaction reagents were mixed according to manufacturer's instructions and incubated at room temperature for five minutes. The recipe are as follows:

Reagent	Volume
PCR product (father, patient)	4 μ l
Salt solution	1 μ l
pCR4-TOPO vector	1 μ l
Final volume	6 μ l

For cloning into pcDNA3.1(+), restriction digestions were performed at 37°C for two hours in order to proceed to ligation step:

	pcDNA3.1(+)	Insert (father, patient)
DNA	1 µg	PCR product
10X CutSmart Buffer	3 µl	3 µl
BamHI-HF	1 µl	1 µl
EcoRI-HF	1 µl	1 µl
ddH₂O	Up to 30 µl	Up to 30 µl

Dehydroxylation of 5' phosphate groups were achieved using CIAP enzyme (Fermentas), which was only applied to digested pcDNA3.1 (+) backbone. CIP treatment was applied for 30 minutes at 37 °C with the compatible CIAP buffer as follows:

Digested pcDNA3.1(+) backbone	30 µl
CIAP (20,000 U/ml)	3 µl
10X CIAP Buffer	5 µl
ddH₂O	Up to 50 µl

Double-digested vector was distinguished from the uncut vector by agarose gel electrophoresis. The corresponding band was excised from the gel and followed by the DNA purification protocol. At the same time, reaction mix was applied NucleoSpin Gel and PCR Clean-up kit in order to have efficient enzymatic reactions in the upcoming steps. Ligation reaction was set with 3:1 insert to vector ratio. Both pCR4-TOPO-CD70 FLAG-father and and pcDNA3.1(+)-CD70 FLAG-patient plasmids were transformed into *E.coli* DH5α competent cells. Single bacterial colonies were isolated from the plates. Mini preparation protocol was applied to isolate plasmid DNAs. Ligations were verified with diagnostic digestions and Sanger sequencing.

Upon the mutation identification in the third exon of the CD70 gene (c. 332C>T), exon 3 of the CD70 gene was PCR-amplified from genomic DNA (gDNA) template according to this recipe:

5X Q5 Reaction Buffer	5 μ l
10 mM dNTPs	0.5 μ l
10 μM Forward Primer (CD70 cDNA BamHI - Forward)	1.25 μ l
10 μM Reverse Primer (CD70 cDNA FLAG EcoRI - Reverse)	1.25 μ l
Template gDNA (20 ng)	1 μ l
Q5-High-Fidelity DNA Polymerase (2,000 units/ml)	0.25 μ l
ddH₂O	Up to 25 μ l

PCR-amplified products of patient, mother and father were cloned into pCR4-TOPO backbones through TOPO cloning as described in the previous TOPO cloning. At the end, pCR4-TOPO-CD70-exon 3-FLAG-patient, pCR4-TOPO-CD70-exon 3-FLAG-mother and pCR4-TOPO-CD70-exon 3-FLAG-father constructs were obtained. Diagnostic digests and Sanger sequencing were performed in order to check the presence of the mutation in the RNA level for the mother, father and patient.

3.2.6.2. Site-directed Mutagenesis

Epitope tagged mutant CD70 (CD70mut; c. 332C>T; p. T111M) ORF was aimed to be constructed. RC200410 plasmid encodes FLAG- and myc-tagged wild-type CD70 (CD70wt) in pCMV6-Entry backbone. C-terminus FLAG-and myc-tagged CD70 (T111M) plasmid was constructed by constituting 332th C to T in the CD70wt containing construct RC200410. To incorporate insertions into double-stranded plasmid DNA, site-directed mutagenesis (SDM) was applied in three steps using NEB Q5 Site-Directed Mutagenesis Kit. Mutagenic primers were designed according to substitution purposes, forward primer had the mutagenic T, indicated in red below. Primers were designed back-to-back to obtain exponential plasmid DNA amplification.

Step I included the exponential amplification of the RC200410 plasmid using mutagenic primers. Following reagents were assembled in a PCR tube as follows:

	25 µl reaction	Final conc.
Q5 Hot Start High-Fidelity 2X Master Mix	12.5 µl	1X
10 µM Forward Primer: ATCCAGGTGATGCTGGCCATC	1.25 µl	0.5 µM
10 µM Reverse Primer GTGTACCATGTAGATGCCATC	1.25 µl	0.5 µM
Template DNA (1 ng)	1 µl	1-25 ng
ddH₂O	9 µl	

Gel product was loaded on a gel in order to check its integrity before leading to step II. Upon confirmation of the product integrity, step II was performed. Step II is the kinase, ligase and DpnI (KLD) treatment. Treatment of kinase and ligase allows the ends of the amplified DNA to be rejoined, DpnI is included to have the only *in vitro* amplified DNA fragments. DpnI is a type IIM restriction enzyme that cleaves methylated and hemimethylated sequences through methylated adenosines (^mA) in dam sequences. The use of DpnI allows the digestion of the DNA amplified by bacteria. KLD treatment reaction was set in a PCR tube as below, and the tube was incubated at RT for five minutes:

	Volume	Final Conc.
PCR product	1 µl	
2X KLD reaction buffer	5 µl	1X
10X KLD enzyme mix	1 µl	1X
ddH₂O	3 µl	

After 5 minutes, 5 µl of the KLD mix was transformed into *E.coli* Top10 competent cells. Plates were incubated overnight. Mini preparation protocol was done to isolate plasmid DNA from single cell colonies. Plasmid integrity was controlled with diagnostic digest and DNA was sent to Sanger sequencing for the mutation detection.

3.2.6.3. Lentiviral Vector Construction

To be able to generate stable cell lines for wild-type and mutant (T111M) CD70 expression, VSV-G pseudotyped third generation lentiviral vectors were aimed to be produced. For this purpose, LeGO-iG2-puro and LeGO-iT2-puro plasmids were used, which have eGFP and tdTomato as the fluorochromes, respectively.

CD70wt was PCR-amplified from a single colony of wild-type CD70 containing pCR4-TOPO-CD70 FLAG-father. Mutant CD70 was amplified from pCR4-TOPO-CD70 FLAG-patient plasmid. PCR reactions for insert amplifications were as follows:

5X Q5 Reaction Buffer	5 μ l
10 mM dNTPs	0.5 μ l
10 μM Forward Primer (CD70 cDNA BamHI - Forward)	1.25 μ l
10 μM Reverse Primer (CD70 cDNA no FLAG EcoRI – Reverse)	1.25 μ l
Template gDNA (20 ng)	1 μ l
Q5-High-Fidelity DNA Polymerase (2,000 units/ml)	0.25 μ l
ddH₂O	Up to 25 μ l

PCR products were run on 1% agarose gel to check their integrity. DNA at the desired size were excised from the agarose gel and digested with BamHI-HF and EcoRI-HF enzymes for an hour at 37°C. LeGO-iG2-puro and LeGO-iT2-puro were also digested with the same enzymes and PCR-cleaned up. Ligation reaction was arranged to have 3:1 insert to vector ratio. Ligation was done for two hours at 25°C. Ligation mixes were transformed to *E.coli* DH5 α competent cells.

In order to investigate CD70 cell surface expression, myc- and FLAG-tagged CD70 expression cassettes [CD70wt, CD70mut(F186del) and CD70mut (T111M)] were cloned into LeGO-iG2-puro backbone. Expression cassettes were transferred from the corresponding RC200410 plasmids in the pCMV6-Entry backbone. To do so, restriction digestions were carried out. Insert plasmids were first incubated at 25 °C for an hour. After an hour, BamHI enzyme was added to the tubes and incubated one more hour at 37°C.

	LeGO-iG2-puro	RC200410 (CD70wt)	RC200410 (CD70mut; F186del)	RC200410 (CD70mut; T111M)
DNA	1 µg	1 µg	1 µg	1 µg
10X CutSmart Buffer	5 µl	3 µl	3 µl	3 µl
BamHI-HF (20,000 U/ml)	1 µl	1 µl	1 µl	1 µl
SmaI (20,000 U/ml)	-	1 µl	1 µl	1 µl
StuI (20,000 U/ml)	1 µl	-	-	-
ddH₂O	Up to 50 µl	Up to 30 µl	Up to 30 µl	Up to 30 µl

Digested backbone LeGO-iG2-puro was treated with rSAP enzyme in order to achieve the removal of 5' phosphate ends according to the recipe below and then the enzyme inactivation was done at 65°C for 5 minutes:

Digested LeGO-iG2-puro	1 µg
rSAP enzyme (1,000 U/ml)	1 µl
10X CutSmart Buffer	6 µl
ddH₂O	Up to 60 µl

Dephosphorylated backbone and insert-containing plasmids were separated on 1% Agarose gel electrophoresis. DNA fragments at the corresponding sizes were isolated from the gel. Purified DNAs were used in ligation reactions with the ligation ratio 3:1 insert to vector, ligation reaction took place at 16°C for 16 hours. Transformations into *E.coli* DH5α were performed. Plasmid DNA was isolated by mini preparation. DNAs were digested for diagnostic digest reactions and sent to Sanger sequencing.

3.2.6.4. Vector Construction for Human CD27-Fc Production

CD27 and CD70 are family members of the tumor necrosis factor family (TNF) and CD27 is the interaction partner of CD70. Therefore, interaction of recombinant human CD27-Fc chimeric proteins with the mutant CD70 proteins would indicate the functional assessment of the mutations. Within this scope, three-way cloning methodology was used to construct plasmid DNA encoding CD27-Fc protein, which is CD27-Fc-pcDNA3.1/myc-His (-) A. Extracellular domain (ED) of CD27 (1-192 aa) from the CD27-LeGO-iG2p, and Fc region starting with EGRMD linker sequence from the AbVec2.0-IGHG1 were PCR amplified with the compatible sticky ends:

	Insert 1 (CD27 ED)	Insert 2 (EGRMD-Fc)
5X Q5 Reaction Buffer	5 µl	5 µl
10 mM dNTPs	0.5 µl	0.5 µl
10 µM Forward Primer (SFFV)	1.25 µl	-
10 µM Forward Primer (CD27 ED XhoI)	-	1.25 µl
10 µM Reverse Primer (EGRMD Fc XhoI)	1.25 µl	-
10 µM Reverse Primer (Fc HindIII)	-	1.25 µl
Template DNA (1 µg)	CD27-LeGO-iG2-puro	AbVec2.0-IGHG1
Q5-High-Fidelity DNA Polymerase (2,000 units/ml)	1 µl	1 µl
ddH₂O	Up to 50 µl	Up to 50 µl

PCR products were run on a 1% Agarose gel, DNA fragments at the desired sizes were excised from the gel and purified and eluted in 15 µl. Digestion reactions were performed at 37°C for two hours:

	pcDNA3.1/myc-His (-) A	Insert 1	Insert 2
DNA	2.5 µg	15 µl	15 µl
10X CutSmart Buffer	5 µl	5 µl	5 µl
BamHI-HF (20,000 U/ml)	1 µl	1 µl	-
XhoI (20,000 U/ml)	-	1 µl	1 µl
HindIII-HF (20,000 U/ml)	1 µl	-	1 µl
ddH₂O	Up to 50 µl	Up to 50 µl	Up to 50 µl

Digested backbone pcDNA3.1/myc-His (-) A was then treated with rSAP for the removal of 5' phosphate groups to prevent self-ligation, as described below. Then, ligation reaction was set with 3:3:1 ratio, having insert 1:insert 2:vector. Ligation was done for 2 hours at 25°C. Upon ligation, ligation mixes were transformed into *E.coli* DH5α competent cells.

4. RESULTS

4.1. Mutation Identification in the CD70 Gene

In 2017, a male patient was diagnosed as a Hodgkin's lymphoma and PID at Marmara University Medical School Hospital in Istanbul. The patient presented with severe varicella infection, viral encephalitis, memory B cells and EBV-specific effector memory CD8⁺ T cells reduced, normal T cell proliferation, reduced EBV-specific cytotoxic T cells. The patient's and his parent's blood samples were analyzed by whole genome sequencing with approval from Marmara University Ethics committee and a homozygous mutation in the CD70 gene of the patient was identified. The parents were both heterozygous for the same mutation. To confirm these results, this thesis project aimed to clone, re-sequence and express these mutant gene products. We performed total RNA isolation from PBMCs from the patient and his parents. RNA samples were run on an agarose gel with different volumes (1 μ l, 2 μ l) in order to check RNA quality by assessing their integrity (Figure 4.1A). We found that RNA samples were intact because they had the expected bands corresponding to the eukaryotic RNA migration pattern (5S, 5.8S, 18S and 28S) and a corresponding smear indicating intact mRNA.

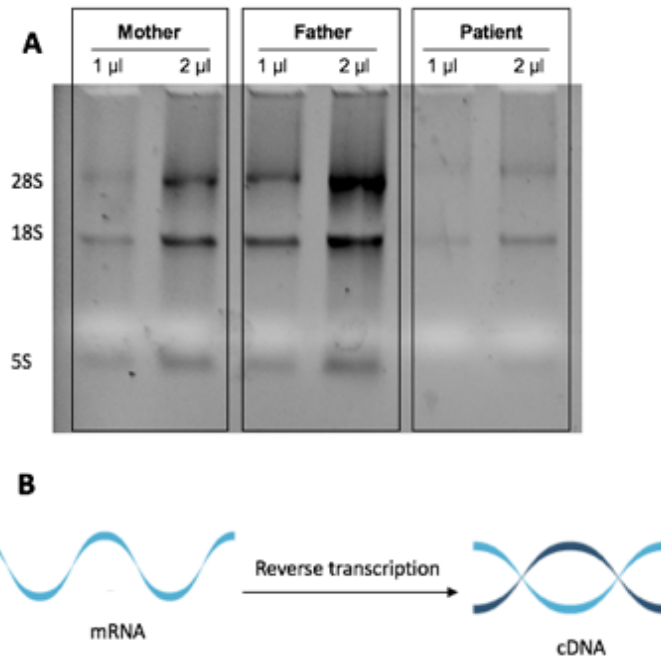


Figure 4.1 Total RNA isolation and cDNA synthesis from PBMCs

Separated RNA samples from patient and his parents displayed on 1% agarose gel.

We performed a reverse transcription reaction from total RNA to obtain cDNA for cloning from the patient and his father. CD70 gene was PCR amplified by adding FLAG tag to C-terminus, and CD70-FLAG sequences from the patient and his father were cloned into the pCR4-TOPO backbone. TOPO cloning reaction was ligation-independent, it uses the inherent ability of DNA topoisomerase to cleave and rejoin blunt-ended DNA, as demonstrated in Figure 4.2 (A). Upon cloning, we performed diagnostic digestion with BsaI enzyme to confirm the presence of the inserts in the vector (Figure 4.2 B and C). The digestion with BsaI has three different possibilities for the insert orientation: no insert (1615 and 2349 bp), positive correct insert (511, 1615 and 2468 bp) and positive insert in reverse orientation (991, 1615 and 1988 bp). We confirmed the positive inserts in reverse orientation with the 3rd and 8th colonies for patient and his father, respectively. Then, we cloned CD70 FLAG cDNA from the patient into the pcDNA3.1(+) backbone to obtain the pcDNA3.1(+)-CD70 FLAG-patient plasmid.

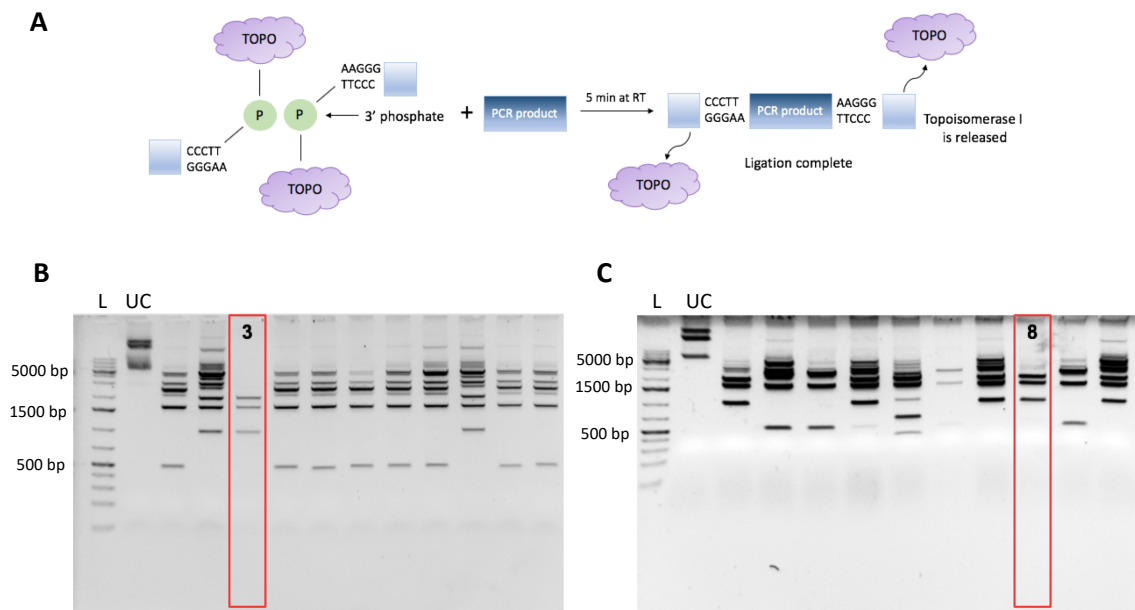


Figure 4.2 The principle behind TOPO cloning, and gel images showing the diagnostic digests of TOPO cloned constructs

The principle behind TOPO-based cloning (A) Diagnostic digest results of pCR4-TOPO-CD70 FLAG-father (B) and pCR4-TOPO-CD70 FLAG-patient (C) with BsaI restriction enzyme indicating the inserts at reverse orientation.

We performed Sanger sequencing on these plasmids in order to obtain full length CD70-FLAG sequences from the patient and his father by using the constructs pCR4-TOPO-CD70 FLAG-father and pcDNA3.1(+)-CD70 FLAG-patient. Sequencing revealed two single nucleotide polymorphisms (SNP) at the 332nd and 345th positions. Every colony from patient's cDNA and half of the colonies from the parental cDNA contained these SNPs indicating that both of the alleles of the patient, and only one of his father's alleles contained these c.332C>T and c.345C>T SNPs and the father's second allele was wild-type. We determined that the mutation was in the third exon of the human CD70 gene (Figure 4.3), corresponding to the extracellular domain of the protein. The mutation c.332C>T causes threonine to be converted to methionine as the 111th amino acid (p. T111M). The second mutation that we have identified c.345C>T was a silent mutation; therefore, we did not focus on that specifically in this study.

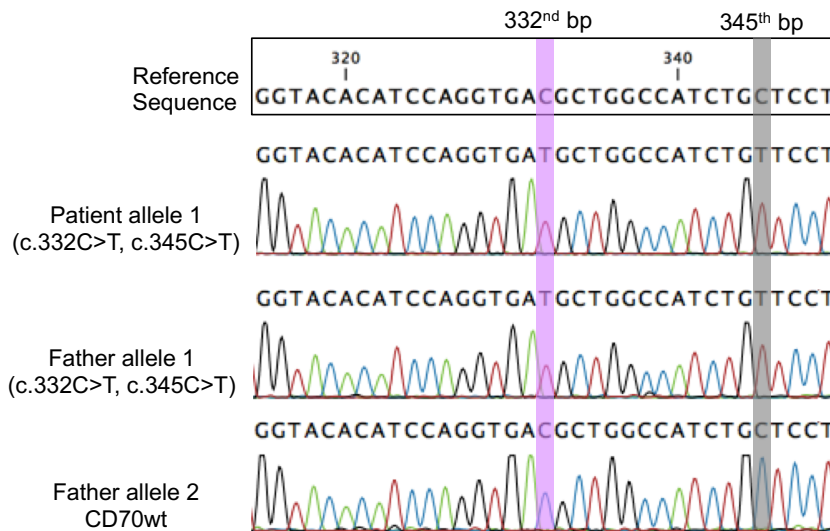


Figure 4.3 Sanger sequencing results for full-length amplified CD70 gene of the patient, and his father

Sequencing results for pcDNA3.1(+)-CD70 FLAG-patient and pCR4-TOPO-CD70 FLAG father indicating the presence of CD70wt and mutant alleles (c.332C>T and c.345C).

We figured out that this mutation was inherited with an autosomal recessive pattern. Collectively, we confirmed the mutations identified by whole exome sequencing by our collaborator through our Sanger sequencing results, where CD70 was among the candidate genes to be investigated further. The previously identified mutations in the third exon of CD70 gene (c.250delT and c.555-557delCTT) that were associated with lymphoproliferative diseases are indicated with a black arrow in Figure 4.4. Along with the previous mutations, we identify a novel point mutation (c.332C>T) associated with EBV-driven PIDs in the third exon of the CD70 gene, as demonstrated with red arrows.

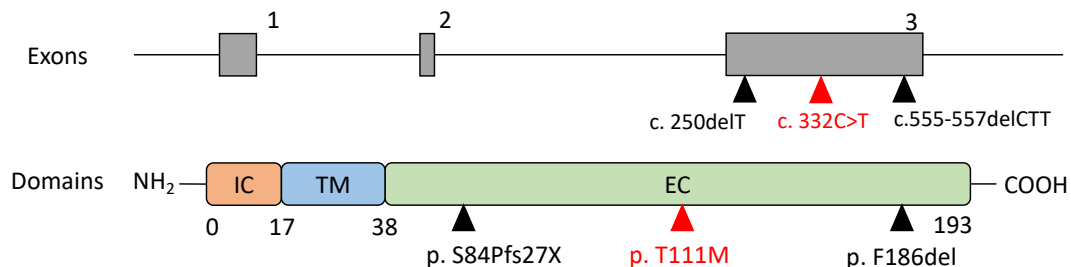


Figure 4.4 Updated exon and domain map of human CD70

Schematical representation of mutations linked to LPDs and PIDs. Black arrows indicate previously identified deletion mutations (c.250delT and c.555-557delCTT) and red arrows indicate the mutation identified by us (c.332C>T).

4.2. Genetic Modification by Lentiviral Vectors and Flow Cytometry

To investigate the mutation further, we cloned these WT and mutant CD70 cDNA's into HIV-1 based lentiviral vectors. We generated VSV-G pseudotyped HIV based virions to infect and express these cDNAs in different human cell lines. This system works based on the principle of complementation, whereby packaging plasmids were co-transfected with a self-inactivating vector having the gene-of-interest. The use of a self-inactivating vector with a deletion in the 3'LTR ensures to have replication-incompetent vectors for safety purposes, as demonstrated in Figure 4.5. Gag/pol encodes the proteins of viral matrix, capsid and nucleoproteins together with reverse transcriptase and integrase, as the latter ones are essential for provirus integration to the genome. Env plasmid encodes for VSV-G due to its specificity for LDL receptor (LDLR), which is used for fusion.

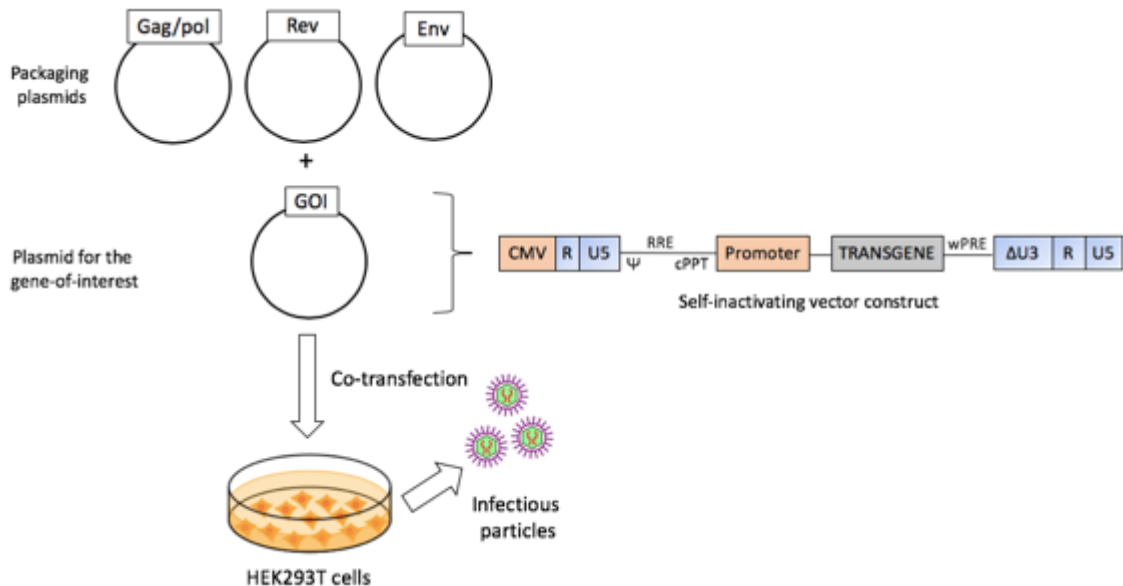


Figure 4.5 Demonstration of the principle of complementation, and self-inactivating lentiviral vectors

The working principle behind the production of 3rd generation VSV-G-pseudotyped SIN lentiviral vectors.

We amplified wild-type and mutant CD70 (T111M) cDNAs using PCR amplified from donor plasmids without the C-terminal FLAG tag (Figure 4.6 A), and cloned these upstream of an internal ribosome entry site (IRES) element in the LeGO-iG2-puro and LeGO-iT2-puro backbones to achieve protein expressions from bicistronic IRES vectors under the control of a spleen focus forming virus (SFFV) internal promoter. The lentiviral construct designs with two different fluorochromes are shown in Figure 4.6 B.

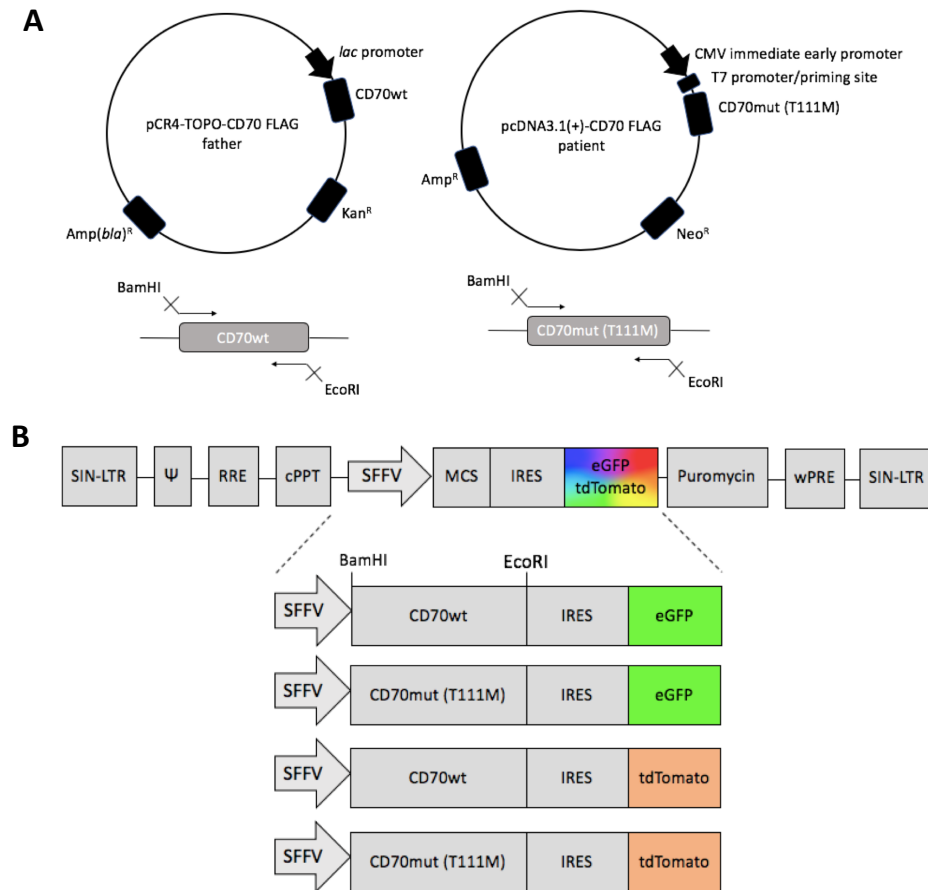


Figure 4.6 Cloning strategy for lentiviral vector construction to clone CD70wt and CD70mut into LeGO-iG2-puro and LeGO-iT2-puro backbones

Donor plasmids with CD70wt and CD70mut were used for the PCR amplification of inserts (A). Lentiviral construct designs for the expression of wild-type and mutant CD70 in the LeGO-iG2-puro and LeGO-iT2-puro backbones (B).

Restriction digestion with BamHI and EcoRI to create matching sticky sites were carried out. DNA fragments were separated with agarose gel electrophoresis and the double digested DNA bands at the desired sizes (Figure 4.7 A, B) were excised. We used extracted bands in cloning applications for the construction vectors in the LeGO-iG2-puro (Figure 4.7 A), and LeGO-iT2-puro (Figure 4.7 B) backbones.

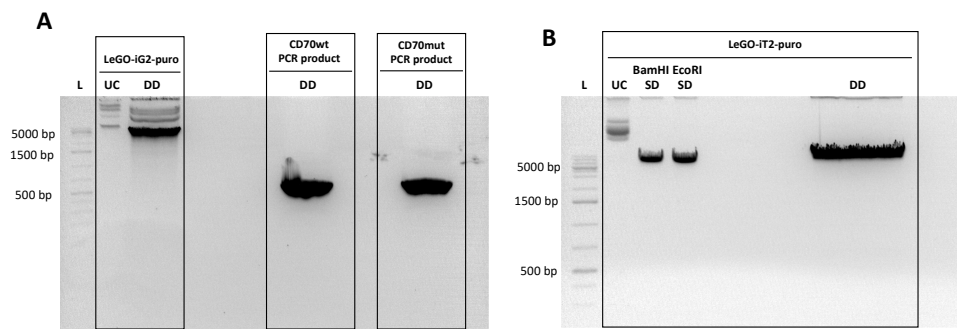


Figure 4.7 Experimental steps of lentiviral vector construction for the stable expression of CD70wt and CD70 mut in LeGO-iG2-puro and LeGO-iT2-puro backbones

Agarose gel image showing DNA fragments of LeGO-iG2-puro, PCR-amplified CD70wt and CD70mut (A) and LeGO-iT2-puro after restriction digestion with BamHI and EcoRI. UC, uncut; DD, double digestion; SD, single digestion.

In order to verify the clones, we performed diagnostic digest reactions with XhoI and NotI enzymes to generate cuts within the inserts (CD70wt and CD70mut). The expected bands sizes upon this double digestion was 475 and 8602 bp for LeGO-iG2-puro backbone, and 475 and 9313 bp for LeGO-iT2-puro. According to the gel images after diagnostic digest, we obtained positive clones for LeGO-iG2-puro (Figure 4.8 A), and LeGO-iT2-puro (Figure 4.8 B) backbones with CD70wt and CD70mut inserts. Since the enzyme cut sites were not able to differentiate between CD70wt and CD70mut, we further confirmed all constructs by Sanger sequencing as well.

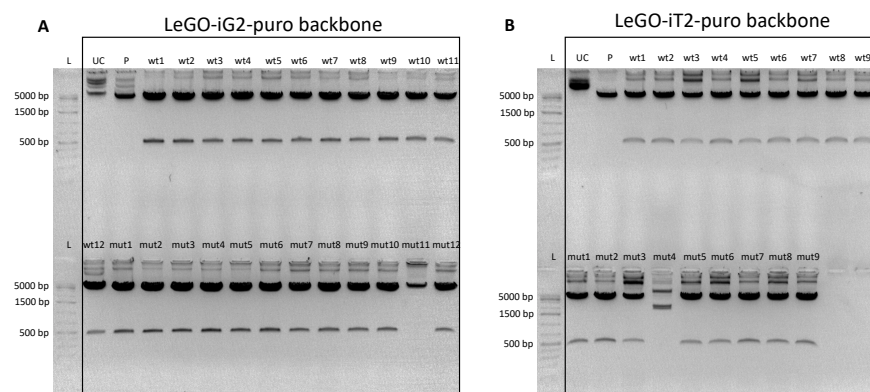


Figure 4.8 Diagnostic digest results for lentiviral constructs with CD70wt and CD70mut in LeGO-iG2-puro and LeGO-iT2-puro backbones

DNA fragments run on agarose gel for CD70wt and CD70mut within LeGO-iG2-puro (A) and LeGO-iT2-puro (B) backbones after XhoI and NotI double digestion. UC, uncut;

P, parental; wt1-12, CD70wt-LeGO-iG2-puro; mut1-12, CD70mut-LeGO-iG2-puro.

To further investigate the functional significance of this mutation, we selected two different human cell lines: K-562 and Namalwa. K-562 cells are chronic myolegenous leukemia (CML) cells that do not express CD70. As the next step, we selected Namalwa cells which are B lymphocytes that were isolated from an EBV positive Burkitt's lymphoma patient. Because Namalwa cells express CD70 endogenously, we aimed to investigate the association of mutant CD70 with its endogenous counterparts, including the homotrimerizations of CD70 molecules.

We transfected K-562 and Namalwa cells through transduction with the lentiviral vectors LeGO-iG2-puro, CD70wt-LeGO-iG2-puro, and CD70mut-LeGO-iG2-puro. In order to obtain stable cell lines with the desired transgene, we further applied puromycin selection for each cell line. During puromycin selection, cells without the lentiviral vector died as they do not encode for the puromycin resistance gene. On the other hand, cells with the lentiviral vectors had puromycin resistance gene, as this gene provided their survival upon puromycin addition to cell culture media. Figure 4.9 displays the histograms indicating the generation of homogenous populations after puromycin selection for both K-562 cells (Figure 4.9 A) and Namalwa (Figure 4.9 B) cells. We used eGFP positivity as a measure of the percentage of the population expressing the CD70 cDNAs because the lentiviral vector contained an IRES-eGFP element after the cDNA. When we first transduced cells, they were positive around 15% in all cell types in terms of eGFP expression indicating the transgene presence (red populations in Figure 4.9). After completion of puromycin selection in around one week, we obtained 100% positive for eGFP expression for all cells (blue populations in Figure 4.9). In this way, we generated stable cell lines of K-562 and Namalwa cells with LeGO-iG2-puro, CD70wt-LeGO-iG2-puro, and CD70mut-LeGO-iG2-puro plasmids.

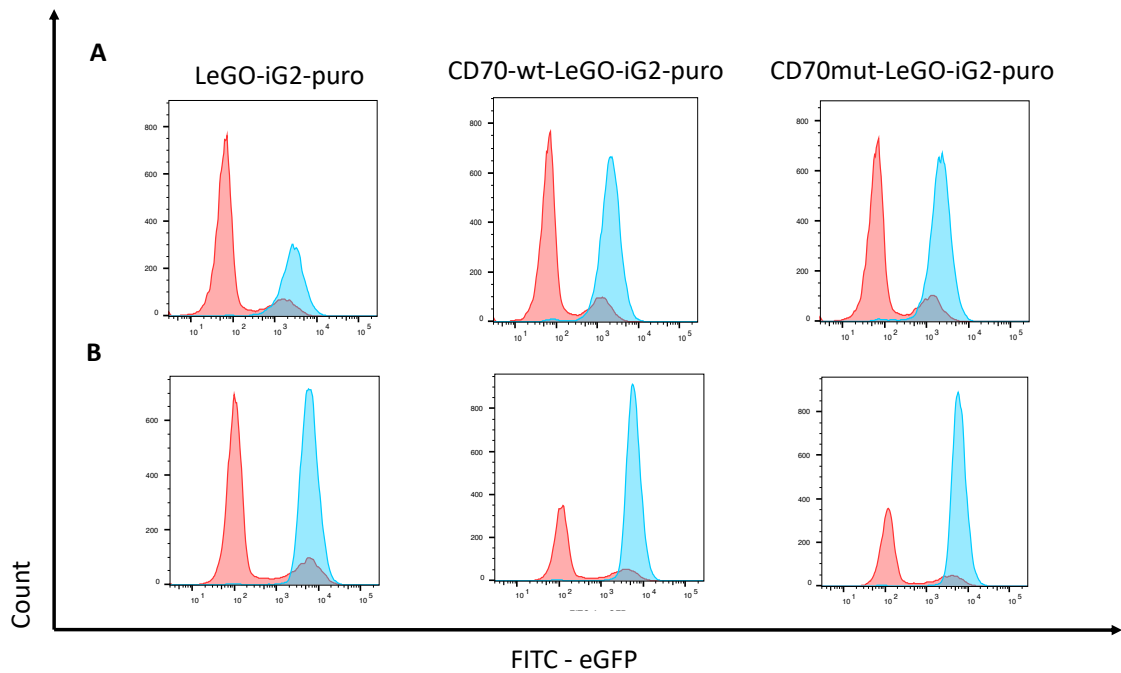


Figure 4.9 Flow cytometry analysis for the generation of stable cell lines of K-562 and Namalwa cells

Histograms showing the lentiviral transduction followed by puromycin selection of both K-562 (A) and Namalwa (B) cells for LeGO-iG2-puro, CD70wt-LeGO-iG2-puro, and CD70mut-LeGO-iG2-puro plasmids. Red, after three days of transduction; blue, after puromycin selection

We used these puromycin selected homogenous populations with the corresponding transgene expression for all experiments in this study. Upon introduction of transgenes and obtaining stable cell lines, we performed cell surface staining with APC-CD70 (red populations), and APC-IgG1 κ isotype control antibodies (blue populations) for both stable cell lines of K-562 (Figure 4.10 A) and Namalwa (Figure 4.10 B) cells. APC-CD70 was from the clone 111-13. According to staining results for K-562 cells; we did not obtain staining for wild-type and K-562-LeGO-iG2-puro cells with CD70 antibody, as they do not express CD70. When we introduced the CD70wt transgene, it resulted in clear staining results, however CD70mut expressing cells did not get stained, and exhibited MFI values in the APC channel close to the MFI value of wild-type cells had for K-562 cells.

For Namalwa cells; we obtained well-stained populations for wild-type cells and LeGO-iG2-puro-introduced cells since they do express CD70 on their cell surface. Introduction of CD70wt to Namalwa cells led to a significant increase in the MFI value, leading to

elevated staining results with the APC-CD70 antibody. Additional to these, Namalwa cells with CD70mut transgene also had an increased MFI value compared to wild-type cells. We attributed this elevated MFI to the appearance of CD70 molecules as homotrimers on the cell surface, pairing up one mutant and two wild-type CD70, and possibly other combinations might be still recognized by the CD70 antibody resulting in the increased fluorescence signal.

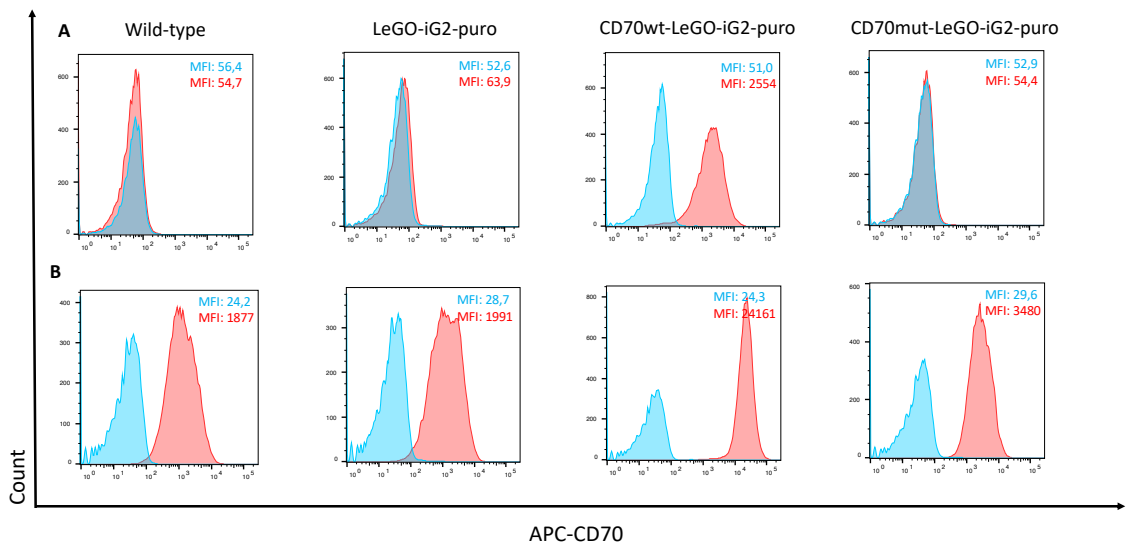


Figure 4.10 Flow cytometry analysis for CD70 detection on the cell surface of K-562 and Namalwa cell lines

Cell surface staining histograms of stable cell lines of K-562 and Namalwa cells with APC-CD70 and APC-IgG1 κ isotype control antibody. Red, APC-CD70; blue, APC-IgG1 κ isotype control antibody.

In flow cytometry analysis, MFI of the positive cells indicate the number of antibody-bound peptides, and hence gives information about relative gene expression using MFI ratio (MFIR) values. In accordance with this, we assessed relative expression levels of wild-type and mutant CD70 through the MFI ratio plot (Figure 4.11 A). We used MFI values from Figure 4.10, MFIRs were calculated by dividing MFI_{stained} to MFI_{isotype} , as values shown in Figure 4.11 B. According to relative expression levels; K-562 cells only had CD70 expression upon transduction, however Namalwa had endogenous CD70 expression. K-562 and Namalwa cells that were transduced with CD70wt-LeGO-iG2-puro had the highest CD70 expression compared to their stable cell line counterparts. Collectively, we obtained Namalwa-CD70wt-LeGO-iG2-puro having the highest CD70 expression levels.

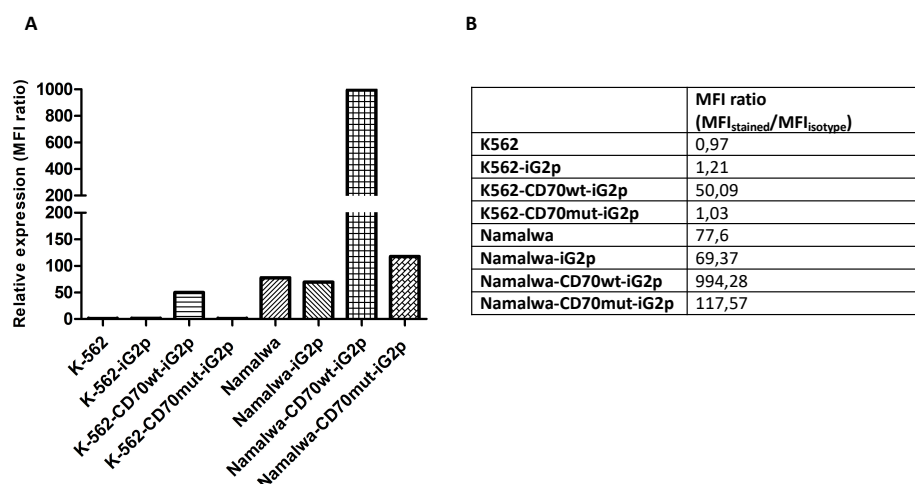


Figure 4.11 MFI ratio plot, and values indicating the relative gene expression levels of CD70 in the stable cell lines of K-562 and Namalwa cells

MFI ratio plot indicating the relative expression levels of CD70wt and CD70mut on cell surface for both K-562, and Namalwa cell lines (A). Table representing the MFI ratio values employed in the plot (B).

In order to assess the location of the mutation (c.332C>T) on the structure of the protein, we performed homology modelling for the wild-type CD70 molecule (70-192 aa), and its homotrimer as shown in Figure 4.12 with VMD software. Single CD70 molecule (side-view) having the mutated residue is shown, and the mutated threonine residue is demonstrated in licorice representation (Figure 4.12 A). Based on the homotrimerization modelling of CD70 molecules (side-view; on the left) (top-view; on the right) (Figure 4.12 B), we concluded that the mutation is at the interface of the monomer interaction, therefore the mutation might interfere the with the formation of stable homotrimers.

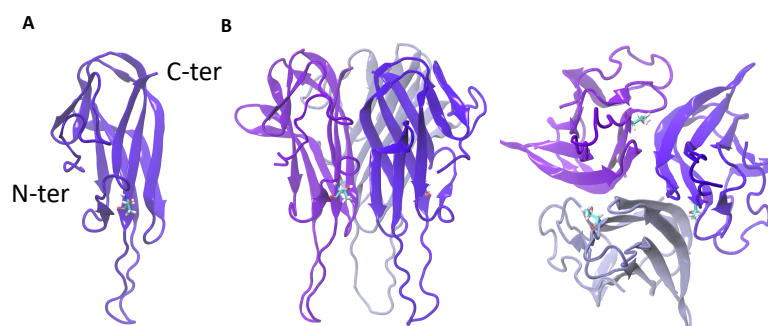


Figure 4.12 Homology modelling of CD70 monomer and homotrimer

CD70 homology modelling showing the 3D structural structure of CD70 molecule (side-view) (A), and its homotrimer (side-view; on the left), and (top-view; on the right) (B). Mutated residue (332nd amino acid) is shown in licorice representation.

We further decided to investigate the intracellular abundance of CD70wt and CD70mut, and have an opinion about antibody recognition of the mutant CD70. Therefore, we decided to perform intracellular staining as intracellular proteins can also be analysed following fixation and permeabilization by flow cytometry with APC-CD70 and APC-IgG1 κ isotype control antibodies. For this purpose, we used a permeabilization buffer with Saponin as a mild detergent to create holes in the cell membrane to create access to intracellular molecules, and PFA solution as the cross-linking fixative agent for fixation purposes. All washing steps were further carried out with permeabilization buffer. We performed intracellular staining with stable K-562 cell lines. According to intracellular staining results (Figure 4.13), we did not detect CD70 for wild-type and LeGO-iG2-puro transduced K-562 cells, which can be reached out from the MFI values as well. However, we did detect CD70 molecules when cells were transduced with CD70wt-LeGO-iG2-puro plasmid, as the MFI value also has elevated to 734 when compared to the wild-type cells. Strikingly, CD70mut-LeGO-iG2-puro transduced K-562 cells were not stained, which indicates either intracellular absence of the protein or unsuccessful antibody recognition. Since we selected these cells with puromycin to obtain 100% eGFP positivity prior the experiment, we attributed that the mutation is highly likely to interfere with the mutated residue (332nd Met), and recognition by the antibody is drastically inhibited.

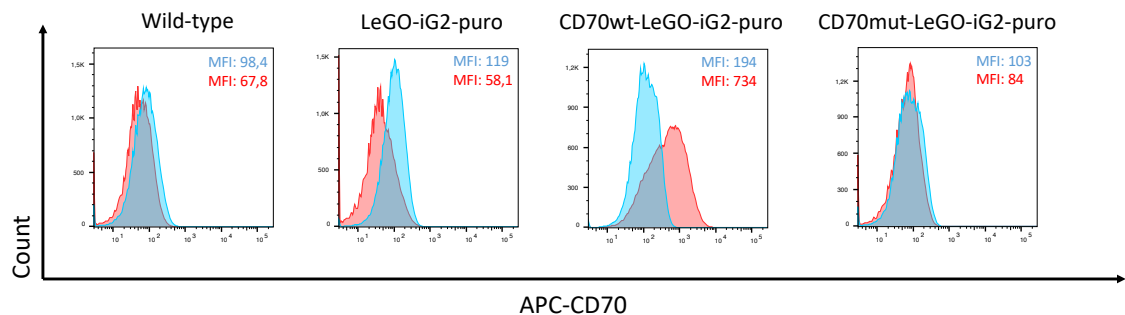


Figure 4.13 Flow cytometry histograms demonstrating intracellular staining for the stable cell lines of K-562

Histograms indicating the intracellular staining with APC-CD70 and APC-IgG1 κ isotype control antibody for K-562 cell lines. Red, APC-CD70; blue, APC-IgG1 κ isotype control antibody.

After obtaining the intracellular signalling histograms implying the impaired recognition of the CD70mut by APC-CD70 antibody, we decided to use a different antibody (PE-CD70) from a different clone (Ki-24) since different antibody clones are likely selected

and raised against different epitopes on the CD70 molecules. We performed cell surface staining with PE-CD70 antibody to stable cell lines of K-562 cells (Figure 4.14). Consistent with the previous data with the APC-CD70 antibody clone, we did not get stained populations for wild-type and LeGO-iG2-puro transduced cells. However, we had significant staining for CD70wt transgene introduced K-562 cells with an MFI value of 12854. Considerably, we obtained very poor staining of CD70mut transgene compared to wild-type and CD70wt expressing K-562 cells. In accordance with our previous results, we also confirm significant impairment in terms of cell surface abundance of CD70mut with PE-CD70 antibody clone as we have done with APC-CD70 antibody clone. Consequently, Figure 4.14 further strengthened our hypothesis stating that this mutation renders impaired cell surface expression of CD70 molecules.

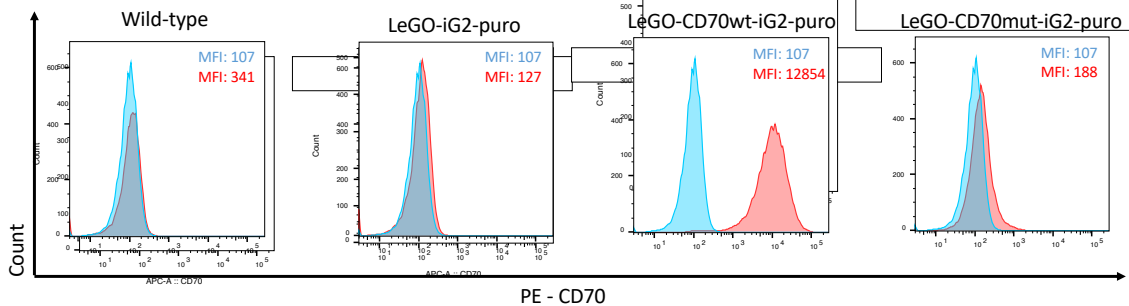


Figure 4.14 Flow cytometry analysis for CD70 detection on the cell surface of K-562 stable cell lines with a different antibody clone

Cell surface staining histograms for K-562 cell lines with PE-CD70 antibody, which belongs to a different antibody clone than the previous APC-CD70 antibody. Red, PE-CD70; blue, unstained cells.

With the aim of further elucidating CD70 epitopes targeted by APC-CD70 and PE-CD70 antibodies, we performed cell surface staining to Namalwa cells this time with double staining together with single stained controls (Figure 4.15). We obtained complete staining of cells from single stained tubes, as demonstrated as +APC-CD70 and +PE-CD70. When we combined these two antibodies in a single tube, both APC and PE signals were acquired. According to our double-stained result, we concluded that these two antibodies target different epitopes on CD70.

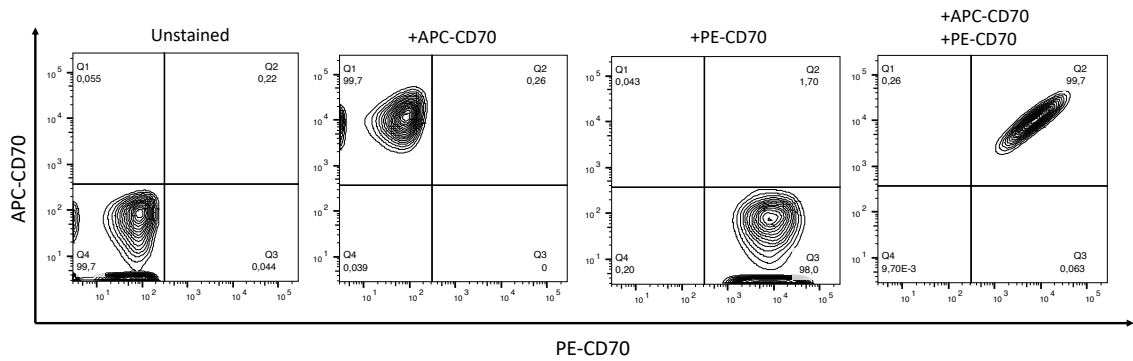


Figure 4.15 Flow cytometry analysis for CD70 detection on the cell surface of Namalwa cells through single and double cell surface stainings

Flow cytometry plots for cell surface staining of Namalwa cells with APC-CD70 and PE-CD70 antibodies. +APC-CD70, and +PE-CD70 indicate the corresponding antibodies included in the single tube for staining.

Cell surface expression of CD70 has a pivotal importance for downstream signalling processes. To support our initial findings about cell surface expression of CD70, we decided to epitope-tag CD70 molecules to detect epitope tag levels with flow cytometry analysis. For this purpose, we used the RC200410 plasmid that encodes myc- and FLAG-tagged CD70 on the C-terminus in our cloning experiment (Figure 4.16). We also employed a previously characterized CD70mut (c.555-557del; p. F186del) by (Abolhassani et al., 2017) in our cloning experiment. To generate our mutated protein CD70mut (c. 332C>T; T111M), we performed site-directed mutagenesis (Figure 4.16 A) to have C to T transition at the 332nd position in the ORF. SDM is a PCR-based technique that can modify DNA sequences through substitutions, small insertions or deletions. We designed primers to obtain primers annealing back-to-back to amplify the entire plasmid (on the top-left, Figure 4.16), we included the mutation in the center of the forward primer to have substitution of a single basepair, and we confirmed the base substitution with Sanger sequencing (on the top-right, Figure 4.16 A). We cloned CD70wt, CD70mut (F186del) and CD70mut (T111M) into the LeGO-iG2-puro backbone so that we could create stable cell lines expressing epitope-tagged CD70 molecules (Figure 4.16 B).

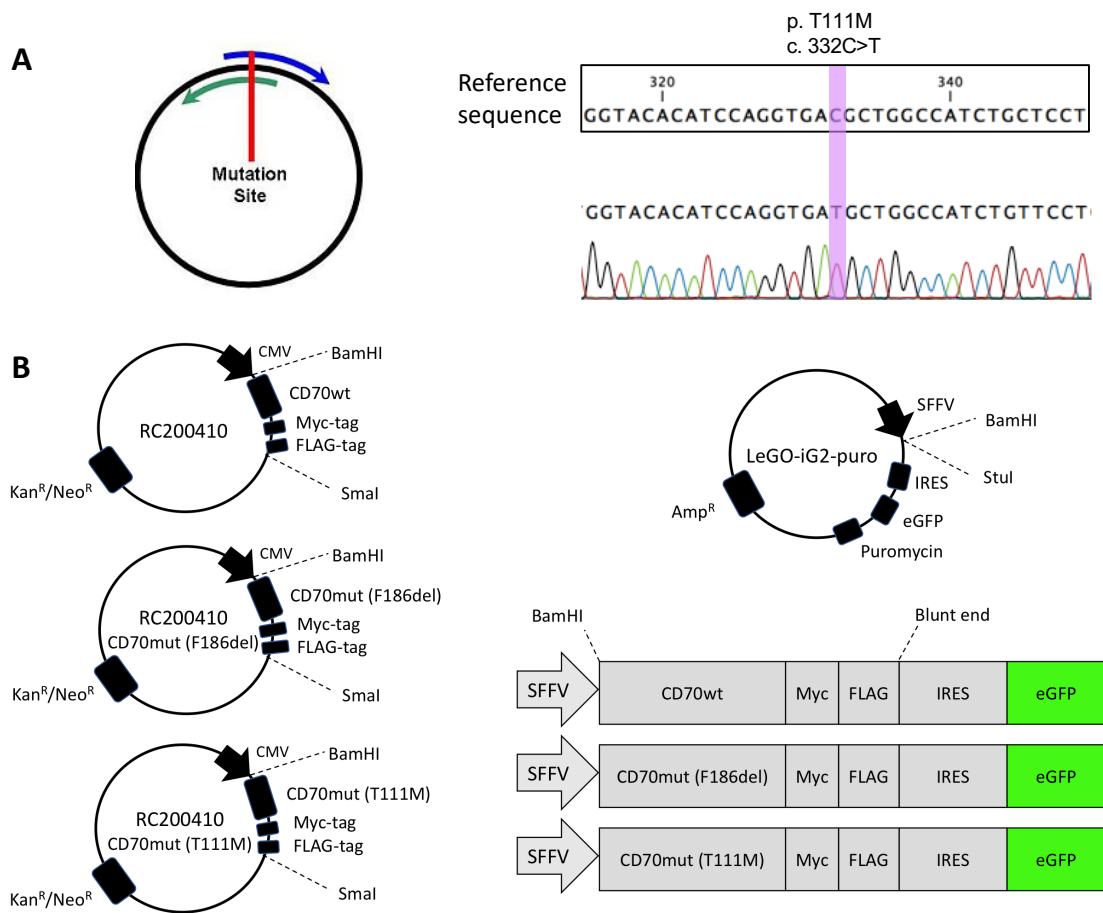


Figure 4.16 Site-directed mutagenesis, and cloning epitope-tagged CD70 expression cassettes into the LeGO-iG2-puro backbone

Schematic representation of SDM indicating primers and the mutation site (on the top-left), and Sanger sequencing result confirming that substitution was achieved by SDM (on the top-right) (A). Plasmid maps of epitope-tagged CD70wt, CD70mut (F186del) and CD70mut(T111M) with the corresponding sticky sites (at the bottom-left), plasmid map of LeGO-iG2-puro backbone, and lentiviral construct designs (at the bottom-right) (B).

Figure 4.17 shows the separated DNA fragments after double digestion with BamHI and SmaI enzymes to create compatible sticky ends with the LeGO-iG2-puro backbone. The expected DNA fragment sizes were 751 bp for all plasmids. Figure 4.17 also shows the inserts that we cloned to LeGO-iG2-puro backbone. We confirmed the presence of inserts by Sanger sequencing and diagnostic digests for cloned plasmids CD70wt-MF-LeGO-iG2-puro, CD70(F186del)-MF-LeGO-iG2-puro and CD70(T111M)-MF-LeGO-iG2-puro. These mutations will be used to test the levels of mutant CD70 molecules on the cell surface by epitope tag staining.

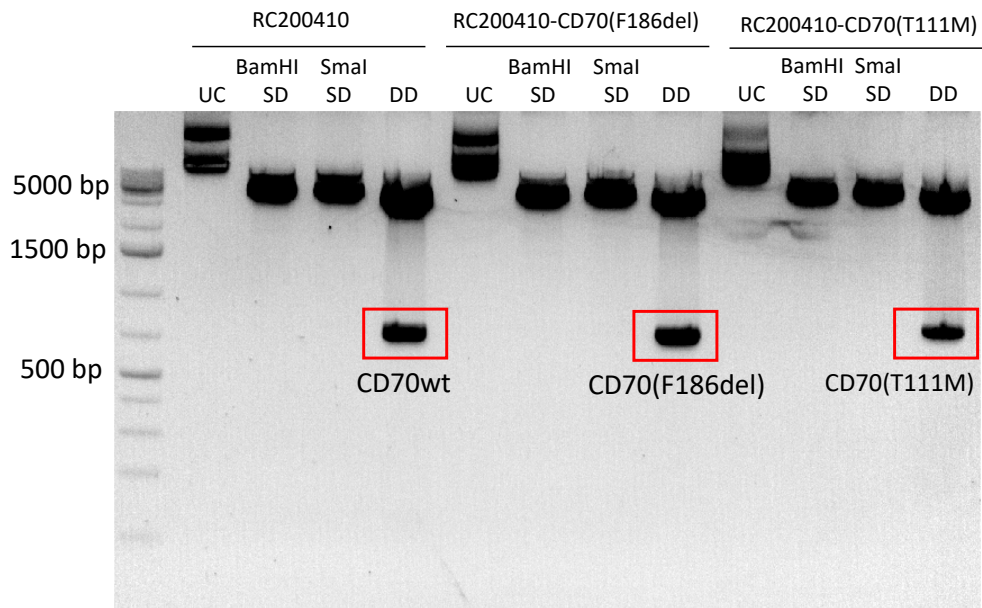


Figure 4.17 Experimental steps of lentiviral vector construction for the stable expression of epitope-tagged CD70wt, and CD70mut proteins in the LeGO-iG2-puro backbone

Agarose gel image showing the digested DNA fragments for cloning C terminus myc- and FLAG-tagged CD70wt, CD70mut (F186del), and CD70mut (T111M) into LeGO-iG2-puro lentiviral backbone. UC, uncut; DD, double digestion; SD, single digestion.

4.3. Cloning Strategy for Human CD27-Fc Chimeric Protein Production

CD70 belongs to the TNF family, and its regulation is dependent on its interaction partner CD27. CD27-CD70 signaling mainly controls effector functions of T cells and their survival. It is essential to obtain physical binding of CD27 to CD70 in order to get downstream co-stimulatory signalling. In order to test the mutant CD70 protein functionally and its interaction with CD27, we devised a cloning strategy for human CD27-Fc chimeric protein production. We aimed to assess the binding of CD27-Fc protein to CD70wt and CD70mut by detecting epitope-tagged flow cytometry antibodies. In this cloning design, we aimed to fuse the extracellular domain of CD27 to the CH1 and CH2 regions of immunoglobulin heavy chains of the IgG1 isotype as the final chimeric Fc protein. To achieve this, we designed the cloning strategy shown in Figure 4.18 A. CD27 (M1-I192) and Fc (P100-K330) were PCR amplified from CD27-LeGO-iG2-puro and

AbVec2.0-IGHG1 plasmids with the corresponding sticky sites. PCR products at the expected sizes (689 bp for CD27 EC; 719 bp for Fc region) were excised from the gel as shown in Figure 4.18 B. We cloned the excised DNA fragments into the pcDNA3.1(-)/myc-His A backbone so that the insert would be myc- and his-tagged on the C-terminus. We plan to use these constructs to express the CD27-Fc protein in eukaryotic cells and collect supernatants for functional protein analysis.

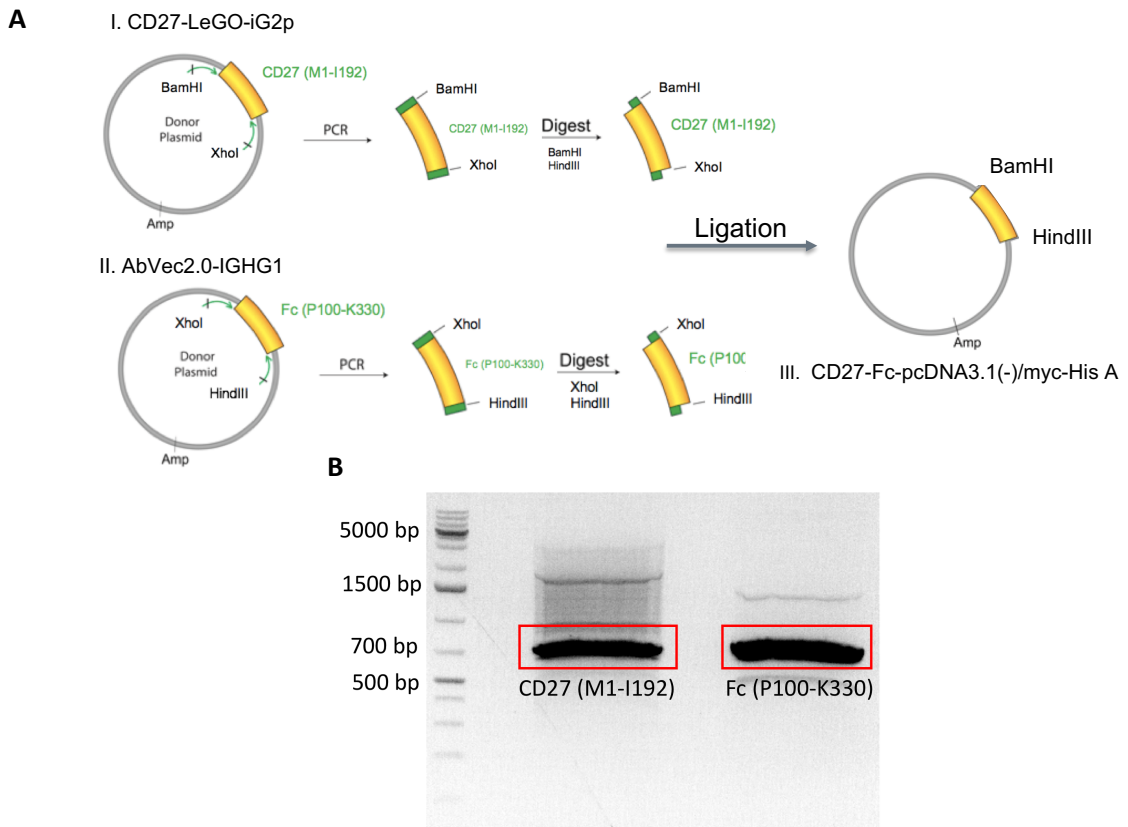


Figure 4.18 Cloning strategy for ligating two inserts in a single backbone for CD27-Fc fusion protein production

Cloning strategy for the production of human CD27-Fc protein (A). Agarose gel image of PCR-amplified inserts CD27 ED and Fc region as the experimental step for the construction of mammalian expression vector expressing CD27-Fc protein (B).

5. DISCUSSION

The immune system is a complicated network of interacting tissues, cells, and cell products that has evolved to preserve the body from invaders, and unhealthy cells. Immune system carries out this protective role through two branches: innate and adaptive systems. Typical immune responses start with innate immune responses. Innate immune responses provide robust yet non-specific interactions against pathogens as it is the first line of defense. As the second line of defense, the adaptive immune system generates strong and long-term immune responses in antigen specific manner. Innate immunity also provides time for the development of adaptive immune responses with immunological memory, which takes a longer time. Generation of immunological memory by the adaptive immune system is the basis of vaccination and provides individuals to be protected in an effective manner upon secondary infections. To achieve this great defense mechanism, adaptive immunity is mainly provided by the concerted action of B and T cells, which are in charge of humoral and cellular immunity, respectively. B cells are among APCs and responsible for antibody production. Cytotoxic activity or cytokine production are the main activities of CD8⁺ and CD4⁺ T cell subsets, respectively.

T cells have central roles for the elimination of pathogens to combat infectious diseases. To pursue this aim effectively, T cells should be fully activated. Initial studies showed T cells can only recognize antigenic peptides when they are loaded on the corresponding MHC molecules. B7/CD28 signalling axis was discovered first as the predominant co-stimulatory signalling axis, followed by the discovery of other co-stimulatory SFs (Green et al., 1994). The two-signal hypothesis for T cell activation was updated to be the three-cell hypothesis upon the discovery of crucial cytokine environments for the initiation and maintenance of immunological synapses (Corthay, 2006). T cell co-stimulatory molecules thus have positive regulatory roles for T cell effector differentiation, and they

provide a physical fulcrum for the stabilization of immunological synapses in a spatiotemporal fashion.

The CD27/CD70 signalling pathway is initiated by these TNF/TNFR superfamily members (J. Jacobs et al., 2015). CD27 is the TNFR SF member, CD70 is the TNF SF member as it is the unique ligand of CD27. Both of CD27 and CD70 function as homotrimers, and appear on cell surface. CD27 is constitutively found on B, NK and T cells, and play crucial roles in the germinal center responses. Its ligand CD70 is expressed on transiently activated lymphoid cells including predominantly on the DCs, NK and T cells. The transient availability of this ligand ensures strict regulation of this axis. The CD27/CD70 signaling pathway is involved in antibody production, T cell expansion, and memory T cell formation especially upon viral infections, however overexpression of these molecules is also associated with cancer (Ge et al., 2017; Lens et al., 1999).

Primary immunodeficiencies (PIDs) are the defects at the immune system that results in either complete or partial loss-of-function of an immune system compartment due to genetic defects (McCusker et al., 2018). This can be related to either innate and adaptive immunity. B cell and T cell immunodeficiencies are the examples of PIDs. PIDs are usually diagnosed by recurrent infections, as the individuals cannot mount appropriate immune responses. As individuals with PIDs are highly susceptible to infections, it is very critical to accurately diagnose patients to alleviate life-threatening symptoms.

Firstly, we aimed to identify the mutation that leads to PIDs in a patient and his parents. The CD70 gene was among the target genes to be analysed after whole genome sequencing analysis performed by our collaborators. We further validated the mutation (c. 3332C>T; p. T111M) with our in vitro experiments. CD70 and CD27 deficiency have been previously reported in the literature (Caorsi et al., 2018; Izawa et al., 2017; Munitic et al., 2013; Van Montfrans et al., 2012). Previous studies showed very similar clinical manifestations such as recurrent infections, EBV-associated lymphoproliferative diseases (LPDs), and B cell malignancies. This malignancies in the lack of CD27/CD70 axis stems from that this signalling pathway is crucial for the immunosurveillance of B cells through inducing antigen-specific expansion of T cells. The impairment in this axis causes significant depletion in the EBV-specific T cell expansion, and memory cells in the antiviral responses, which renders patients to undergo severe hematologic abnormalities

including EBV-associated LPD as in the case in our patient. The patient in our study also had lymphopenia, and mildly decreased levels of immunoglobulins (IgA, IgG, and IgM). The striking part is that the patient had consanguineous family members. Consanguineosity has been associated with the elevated risk to genetic abnormalities due to the inheritance of autosomal recessive traits from mutual ancestors (Shawky, Elsayed, Zaki, Nour El-Din, & Kamal, 2013). As patients with PIDs undergo serious health problems, it is very important to diagnose and perform genetic analysis of these rare diseases with very heterogenous manifestations. Recently, the developments, and increased availability of next generation sequencing technologies have positively contributed to the PID diagnostics.

In conclusion, we identify a novel mutation in the CD70 gene that leads to PID in this study. This mutation rendered patient to undergo EBV-associated lymphoproliferation because of a novel case of CD70 deficiency. As next steps, we aim to definitively determine surface expression of mutant protein using epitope-tagged CD70wt and CD70mut proteins. Additionally, we aim to express and purify CD27-Fc to be employed as an *in vitro* functionality assay for ligand binding. Furthermore, phenotypic analysis, and cytotoxicity against B cell targets of EBV-specific CD8⁺ T cells of the CD70-deficient patient could provide fundamental insights to our current study. Previous studies also demonstrated that some CD70-deficient individuals also had reduced expressions of NKG2D and 2B4, or impaired IL-2 production, which impairs NK cell functions (Abolhassani et al., 2017). Therefore, investigation on NK cell cytotoxicity in CD70-deficient individuals can also contribute to the context of CD70 deficiency.

6. BIBLIOGRAPHY

- Abolhassani, H., Edwards, E. S. J., Ikinciogullari, A., Jing, H., Borte, S., Buggert, M., ... Pan-Hammarström, Q. (2017). Combined immunodeficiency and Epstein-Barr virus-induced B cell malignancy in humans with inherited CD70 deficiency. *Journal of Experimental Medicine*, 214(1), 91–106. <https://doi.org/10.1084/jem.20160849>
- Agematsu, K., Hokibara, S., Nagumo, H., & Komiyama, A. (2000). CD27: A memory B-cell marker. *Immunology Today*, 21(5), 204–206. [https://doi.org/10.1016/S0167-5699\(00\)01605-4](https://doi.org/10.1016/S0167-5699(00)01605-4)
- Alarcón, B., Mestre, D., & Martínez-Martín, N. (2011). The immunological synapse: A cause or consequence of T-cell receptor triggering? *Immunology*, 133(4), 420–425. <https://doi.org/10.1111/j.1365-2567.2011.03458.x>
- Alkhairy, O. K., Perez-Becker, R., Driessen, G. J., Abolhassani, H., Van Montfrans, J., Borte, S., ... Hammarström, L. (2015). Novel mutations in TNFRSF7/CD27: Clinical, immunologic, and genetic characterization of human CD27 deficiency. *Journal of Allergy and Clinical Immunology*, 136(3), 703-712.e10. <https://doi.org/10.1016/j.jaci.2015.02.022>
- Allam, A., Swiecki, M., Vermi, W., Ashwell, J. D., & Colonna, M. (2014). Dual Function of CD70 in Viral Infection: Modulator of Early Cytokine Responses and Activator of Adaptive Responses. *The Journal of Immunology*, 193(2), 871–878. <https://doi.org/10.4049/jimmunol.1302429>
- Alosaimi, M. F., Hoenig, M., Jaber, F., Platt, C. D., Jones, J., Wallace, J., ... Geha, R. S. (2019). Immunodeficiency and EBV-induced lymphoproliferation caused by 4-1BB deficiency. *Journal of Allergy and Clinical Immunology*, 144(2), 574-583.e5. <https://doi.org/10.1016/j.jaci.2019.03.002>
- Arens, R., Nolte, M. A., Tesselaar, K., Heemskerk, B., Reedquist, K. A., van Lier, R. A. W., & van Oers, M. H. J. (2004). Signaling through CD70 Regulates B Cell Activation and IgG Production. *The Journal of Immunology*, 173(6), 3901–3908.

- <https://doi.org/10.4049/jimmunol.173.6.3901>
- Au, P. Y. B., & Yeh, W. C. (2007). Physiological roles and mechanisms of signaling by TRAF2 and TRAF5. *Advances in Experimental Medicine and Biology*, 597, 32–47. https://doi.org/10.1007/978-0-387-70630-6_3
- Bergbauer, M., Kalla, M., Schmeinck, A., Göbel, C., Rothbauer, U., Eck, S., ... Hammerschmidt, W. (2010). CpG-methylation regulates a class of Epstein-Barr virus promoters. *PLoS Pathogens*, 6(9). <https://doi.org/10.1371/journal.ppat.1001114>
- Bettini, M. L., Chou, P., Guy, C., Lee, T., Vignali, K. M., & Vignali, D. A. A. (2017). CD3 ITAM diversity is required for optimal T cell receptor signaling and thymocyte development. *The Journal of Immunology*, 199(5), 1555–1560. <https://doi.org/10.4049/jimmunol.1700069>
- Bhat, P., Leggatt, G., Waterhouse, N., & Frazer, I. H. (2017). Interferon- γ derived from cytotoxic lymphocytes directly enhances their motility and cytotoxicity. *Cell Death & Disease*, 8(6), e2836. <https://doi.org/10.1038/cddis.2017.67>
- Bonilla, F. A., & Oettgen, H. C. (2010). Adaptive immunity. *Journal of Allergy and Clinical Immunology*, 125(2 SUPPL. 2), S33–S40. <https://doi.org/10.1016/j.jaci.2009.09.017>
- Borg, N. A., Ely, L. K., Beddoe, T., Macdonald, W. A., Reid, H. H., Clements, C. S., ... Rossjohn, J. (2005). The CDR3 regions of an immunodominant T cell receptor dictate the “energetic landscape” of peptide-MHC recognition. *Nature Immunology*, 6(2), 171–180. <https://doi.org/10.1038/ni1155>
- Buckley, R. H. (2011). Transplantation of hematopoietic stem cells in human severe combined immunodeficiency: Longterm outcomes. *Immunologic Research*, 49(1–3), 25–43. <https://doi.org/10.1007/s12026-010-8191-9>
- Cancian, L., Bosshard, R., Lucchesi, W., Karstegl, C. E., & Farrell, P. J. (2011). C-terminal region of ebna-2 determines the superior transforming ability of type 1 Epstein-Barr virus by enhanced gene regulation of LMP-1 and CXCR7. *PLoS Pathogens*, 7(7). <https://doi.org/10.1371/journal.ppat.1002164>
- Caorsi, R., Rusmini, M., Volpi, S., Chiesa, S., Pastorino, C., Sementa, A. R., ... Gattorno, M. (2018). CD70 deficiency due to a novel mutation in a patient with severe chronic EBV infection presenting as a periodic fever. *Frontiers in Immunology*, 8(JAN). <https://doi.org/10.3389/fimmu.2017.02015>
- Casanova, J.-L., & Su, H. C. (2020). A global effort to define the human genetics of

- protective immunity to SARS-CoV-2 infection. *Cell*.
<https://doi.org/10.1016/j.cell.2020.05.016>
- Casanova, J. L., & Abel, L. (2005). Inborn errors of immunity to infection: The rule rather than the exception. *Journal of Experimental Medicine*, 202(2), 197–201.
<https://doi.org/10.1084/jem.20050854>
- Chen, L., & Flies, D. B. (2013). Molecular mechanisms of T cell co-stimulation and co-inhibition. *Nature Reviews Immunology*, 13(4), 227–242.
<https://doi.org/10.1038/nri3405>
- Chlewicki, L. K., Holler, P. D., Monti, B. C., Clutter, M. R., & Kranz, D. M. (2005). High-affinity, peptide-specific T cell receptors can be generated by mutations in CDR1, CDR2 or CDR3. *Journal of Molecular Biology*, 346(1), 223–239.
<https://doi.org/10.1016/j.jmb.2004.11.057>
- Cochet, F., & Peri, F. (2017). The role of carbohydrates in the lipopolysaccharide (LPS)/toll-like receptor 4 (TLR4) Signalling. *International Journal of Molecular Sciences*, 18(11). <https://doi.org/10.3390/ijms18112318>
- Conley, J. M., Gallagher, M. P., & Berg, L. J. (2016). T cells and gene regulation: The switching on and turning up of genes after T cell receptor stimulation in CD8 T cells. *Frontiers in Immunology*, 7(FEB), 1–7. <https://doi.org/10.3389/fimmu.2016.00076>
- Corthay, A. (2006). A three-cell model for activation of naïve T helper cells. *Scandinavian Journal of Immunology*, 64(2), 93–96. <https://doi.org/10.1111/j.1365-3083.2006.01782.x>
- Cowan, M. L. (2017). *Diseases of the respiratory system. Reptile Medicine and Surgery in Clinical Practice*. <https://doi.org/10.1002/9781118977705.ch21>
- Croft, M. (2009). The role of TNF superfamily members in T-cell function and diseases. *Nature Reviews Immunology*, 9(4), 271–285. <https://doi.org/10.1038/nri2526>
- Drutskaya, M. S., Efimov, G. A., Kruglov, A. A., Kuprash, D. V., & Nedospasov, S. A. (2010). Tumor necrosis factor, lymphotoxin and cancer. *IUBMB Life*, 62(4), 283–289. <https://doi.org/10.1002/iub.309>
- Dustin, M. L. (2002). The immunological synapse. *Arthritis Research*, 4, S119–S125.
<https://doi.org/10.1186/ar559>
- Dustin, M. L. (2014). What counts in the immunological synapse? *Molecular Cell*, 54(2), 255–262. <https://doi.org/10.1016/j.molcel.2014.04.001>
- Dustin, M. L., & Groves, J. T. (2012). Receptor Signaling Clusters in the Immune Synapse. *Annual Review of Biophysics*, 41(1), 543–556.

<https://doi.org/10.1146/annurev-biophys-042910-155238>

- Eagar, T. N., & Miller, S. D. (2013). *Helper T-cell subsets and control of the inflammatory response. Clinical Immunology: Principles and Practice: Fourth Edition* (4th ed.). Elsevier Ltd. <https://doi.org/10.1016/B978-0-7234-3691-1.00014-3>
- Epstein, M. A., Achong, B. G., Barr, Y. M., Nat ; Morgan, C., Rose, H. M., Holden, M., ... Holt, S. (1963). Cancer Inst. Monogr. (in the press). *exp. Med.* 1954, 100, 195. *J. Cell. Biol*, 19(cm), 337.
- Francisco, S., Ave, P., Francisco, S., Morena, D. La, Scott, G., Scott, P., ... State, N. Y. (2015). HHS Public Access Author manuscript 11 Screening Programs in the United States, 312(7), 729–738. <https://doi.org/10.1001/jama.2014.9132>. Newborn
- Garcia, K. C., & Adams, E. J. (2005). How the T cell receptor sees antigen - A structural view. *Cell*, 122(3), 333–336. <https://doi.org/10.1016/j.cell.2005.07.015>
- Ge, H., Mu, L., Jin, L., Yang, C., Chang, Y. E., Long, Y., ... Huang, J. (2017). Tumor associated CD70 expression is involved in promoting tumor migration and macrophage infiltration in GBM. *International Journal of Cancer*, 141(7), 1434–1444. <https://doi.org/10.1002/ijc.30830>
- Golubovskaya, V., & Wu, L. (2016). Different subsets of T cells, memory, effector functions, and CAR-T immunotherapy. *Cancers*, 8(3). <https://doi.org/10.3390/cancers8030036>
- Grakoui, A., Bromley, S. K., Sumen, C., Davis, M. M., Shaw, A. S., Allen, P. M., & Dustin, M. L. (1999). The immunological synapse: A molecular machine controlling T cell activation. *Science*, 285(5425), 221–227. <https://doi.org/10.1126/science.285.5425.221>
- Green, J. M., Noel, P. J., Sperling, A. I., Walunas, S. T. L., Gray, G. S., Bluestone, J. A., & Thompson, C. B. (1994). Absence of B7-Dependent in CD28-Deficient Mice, 1, 501–508.
- Hendriks, J., Xiao, Y., & Borst, J. (2003). CD27 Promotes Survival of Activated T Cells and Complements CD28 in Generation and Establishment of the Effector T Cell Pool. *Journal of Experimental Medicine*, 198(9), 1369–1380. <https://doi.org/10.1084/jem.20030916>
- Hivroz, C., & Saitakis, M. (2016). Biophysical aspects of T lymphocyte activation at the immune synapse. *Frontiers in Immunology*, 7(FEB), 1–12. <https://doi.org/10.3389/fimmu.2016.00046>

- Itoh, N., & Nagata, S. (1993). A novel protein domain required for apoptosis. Mutational analysis of human Fas antigen. *Journal of Biological Chemistry*, 268(15), 10932–10937.
- Izawa, K., Martin, E., Soudais, C., Bruneau, J., Boutboul, D., Rodriguez, R., ... Latour, S. (2017). Inherited CD70 deficiency in humans reveals a critical role for the CD70-CD27 pathway in immunity to Epstein-Barr virus infection. *Journal of Experimental Medicine*, 214(1), 73–89. <https://doi.org/10.1084/jem.20160784>
- Jacobs, J., Deschoolmeester, V., Zwaenepoel, K., Rolfo, C., Silence, K., Rottey, S., ... Pauwels, P. (2015). CD70: An emerging target in cancer immunotherapy. *Pharmacology and Therapeutics*, 155, 1–10. <https://doi.org/10.1016/j.pharmthera.2015.07.007>
- Jacobs, Julie, Deschoolmeester, V., Zwaenepoel, K., Flieswasser, T., Deben, C., Van den Bossche, J., ... Pauwels, P. (2018). Unveiling a CD70-positive subset of cancer-associated fibroblasts marked by pro-migratory activity and thriving regulatory T cell accumulation. *OncoImmunology*, 7(7), 1–11. <https://doi.org/10.1080/2162402X.2018.1440167>
- Janas, M. L., Groves, P., Kienzle, N., & Kelso, A. (2005). IL-2 Regulates Perforin and Granzyme Gene Expression in CD8 + T Cells Independently of Its Effects on Survival and Proliferation . *The Journal of Immunology*, 175(12), 8003–8010. <https://doi.org/10.4049/jimmunol.175.12.8003>
- Jang, J. H., Shin, H. W., Lee, J. M., Lee, H. W., Kim, E. C., & Park, S. H. (2015). An Overview of Pathogen Recognition Receptors for Innate Immunity in Dental Pulp. *Mediators of Inflammation*, 2015. <https://doi.org/10.1155/2015/794143>
- Jiang, H. Y., Xiao, R., Lian, X. R., Kanekura, T., Luo, Y. Y., Yin, Y. X., ... Lu, Q. J. (2012). Demethylation of TNFSF7 contributes to CD70 overexpression in CD4+ T cells from patients with systemic sclerosis. *Clinical Immunology*, 143(1), 39–44. <https://doi.org/10.1016/j.clim.2012.01.005>
- Jiang, S., Zhou, H., Liang, J., Gerdt, C., Wang, C., Ke, L., ... Zhao, B. (2017). The Epstein-Barr Virus Regulome in Lymphoblastoid Cells. *Cell Host and Microbe*, 22(4), 561-573.e4. <https://doi.org/10.1016/j.chom.2017.09.001>
- Jilaveanu, L. B., Sznol, J., Aziz, S. A., Duchon, D., Kluger, H. M., & Camp, R. L. (2012). CD70 expression patterns in renal cell carcinoma. *Human Pathology*, 43(9), 1394–1399. <https://doi.org/10.1016/j.humpath.2011.10.014>
- Kaempfer, R., Arad, G., Levy, R., Hillman, D., Nasie, I., & Rotfogel, Z. (2013). CD28:

- Direct and critical receptor for superantigen toxins. *Toxins*, 5(9), 1531–1542. <https://doi.org/10.3390/toxins5091531>
- Kinoshita, S., Biswas, G., Kono, T., Hikima, J., & Sakai, M. (2014). Presence of two tumor necrosis factor (tnf)- α homologs on different chromosomes of zebrafish (*Danio rerio*) and medaka (*Oryzias latipes*). *Marine Genomics*, 13, 1–9. <https://doi.org/10.1016/j.margen.2013.10.004>
- Kobrynski, L. J. (2006). Combined immune deficiencies in children. *Journal of Infusion Nursing*, 29(4), 206–213. <https://doi.org/10.1097/00129804-200607000-00007>
- La Gruta, N. L., Gras, S., Daley, S. R., Thomas, P. G., & Rossjohn, J. (2018). Understanding the drivers of MHC restriction of T cell receptors. *Nature Reviews Immunology*, 18(7), 467–478. <https://doi.org/10.1038/s41577-018-0007-5>
- Lambert, S. A., Jolma, A., Campitelli, L. F., Das, P. K., Yin, Y., Albu, M., ... Weirauch, M. T. (2018). The Human Transcription Factors. *Cell*, 172(4), 650–665. <https://doi.org/10.1016/j.cell.2018.01.029>
- Latour, S., & Fischer, A. (2019). Signaling pathways involved in the T-cell-mediated immunity against Epstein-Barr virus: Lessons from genetic diseases. *Immunological Reviews*, 291(1), 174–189. <https://doi.org/10.1111/imr.12791>
- Latour, S., & Winter, S. (2018). Inherited immunodeficiencies with high predisposition to Epstein-Barr Virus-driven lymphoproliferative diseases. *Frontiers in Immunology*, 9(JUN). <https://doi.org/10.3389/fimmu.2018.01103>
- Lee, S. H., Kwon, J. Y., Kim, S. Y., Jung, K. A., & Cho, M. La. (2017). Interferon-gamma regulates inflammatory cell death by targeting necroptosis in experimental autoimmune arthritis. *Scientific Reports*, 7(1), 2–10. <https://doi.org/10.1038/s41598-017-09767-0>
- Lee, S., & Margolin, K. (2011). Cytokines in cancer immunotherapy. *Cancers*, 3(4), 3856–3893. <https://doi.org/10.3390/cancers3043856>
- Lens, S. M. A., Drillenburg, P., Den Drijver, B. F. A., Van Schijndel, G., Pals, S. T., Van Lier, R. A. W., & Van Oers, M. H. J. (1999). Aberrant expression and reverse signalling of CD70 on malignant B cells. *British Journal of Haematology*, 106(2), 491–503. <https://doi.org/10.1046/j.1365-2141.1999.01573.x>
- Lin, J., Miller, M. J., & Shaw, A. S. (2005). The c-SMAC: Sorting it all out (or in). *Journal of Cell Biology*, 170(2), 177–182. <https://doi.org/10.1083/jcb.200503032>
- Liu, T., Zhang, L., Joo, D., & Sun, S. C. (2017). NF- κ B signaling in inflammation. *Signal Transduction and Targeted Therapy*, 2(April).

- <https://doi.org/10.1038/sigtrans.2017.23>
- Love, P. E., & Hayes, S. M. (2010). ITAM-mediated signaling by the T-cell antigen receptor. *Cold Spring Harbor Perspectives in Biology*, 2(6), 1–11. <https://doi.org/10.1101/cshperspect.a002485>
- Lovely, G. A., & Sen, R. (2016). Evolving adaptive immunity. *Genes and Development*, 30(8), 873–875. <https://doi.org/10.1101/gad.281014.116>
- Lovett-Racke, A. E., & Racke, M. K. (2018). *Role of IL-12/IL-23 in the Pathogenesis of Multiple Sclerosis. Neuroinflammation*. Elsevier Inc. <https://doi.org/10.1016/b978-0-12-811709-5.00005-3>
- Lowdell, M. W., Lamb, L., Hoyle, C., Velardi, A., & Grant Prentice, H. (2001). NON-MHC-restricted cytotoxic cells: Their roles in the control and treatment of leukaemias. *British Journal of Haematology*, 114(1), 11–24. <https://doi.org/10.1046/j.1365-2141.2001.02906.x>
- Ma, L., Yang, L., Shi, B., He, X., Peng, A., Li, Y., ... Yao, X. (2016). Analyzing the CDR3 Repertoire with respect to TCR - Beta Chain V-D-J and V-J Rearrangements in Peripheral T Cells using HTS. *Scientific Reports*, 6(June), 1–10. <https://doi.org/10.1038/srep29544>
- Mabery, E. M., & Schneider, D. S. (2010). The drosophila TNF ortholog eiger is required in the fat body for a robust immune response. *Journal of Innate Immunity*, 2(4), 371–378. <https://doi.org/10.1159/000315050>
- Martínez-Reza, I., Díaz, L., & García-Becerra, R. (2017). Preclinical and clinical aspects of TNF- α and its receptors TNFR1 and TNFR2 in breast cancer. *Journal of Biomedical Science*, 24(1), 1–8. <https://doi.org/10.1186/s12929-017-0398-9>
- McCusker, C., Upton, J., & Warrington, R. (2018). Primary immunodeficiency. *Allergy, Asthma and Clinical Immunology*, 14(s2), 1–12. <https://doi.org/10.1186/s13223-018-0290-5>
- McCusker, C., & Warrington, R. (2011). Primary immunodeficiency. *Allergy, Asthma & Clinical Immunology*, 7(S1), S11. <https://doi.org/10.1186/1710-1492-7-s1-s11>
- Morrow, J. D., & Cooper, V. S. (2012). Evolutionary effects of translocations in bacterial genomes. *Genome Biology and Evolution*, 4(12), 1256–1262. <https://doi.org/10.1093/gbe/evs099>
- Mostardinha, P., & De Abreu, F. V. (2012). Positive and negative selection, self-nonsel self discrimination and the roles of costimulation and energy. *Scientific Reports*, 2, 1–9. <https://doi.org/10.1038/srep00769>

- Mumm, J. B., & Oft, M. (2008). Cytokine-based transformation of immune surveillance into tumor-promoting inflammation. *Oncogene*, 27(45), 5913–5919. <https://doi.org/10.1038/onc.2008.275>
- Munitic, I., Kuka, M., Allam, A., Scoville, J. P., & Ashwell, J. D. (2013). CD70 Deficiency Impairs Effector CD8 T Cell Generation and Viral Clearance but Is Dispensable for the Recall Response to Lymphocytic Choriomeningitis Virus. *The Journal of Immunology*, 190(3), 1169–1179. <https://doi.org/10.4049/jimmunol.1202353>
- Nagasawa, T. (2006). Microenvironmental niches in the bone marrow required for B-cell development. *Nature Reviews Immunology*, 6(2), 107–116. <https://doi.org/10.1038/nri1780>
- Notarangelo, L. D. (2010). Primary immunodeficiencies. *Journal of Allergy and Clinical Immunology*, 125(2 SUPPL. 2), S182–S194. <https://doi.org/10.1016/j.jaci.2009.07.053>
- Notarangelo, L. D. (2016). *Human Genetic Defects Resulting in Increased Susceptibility to Viral Infections. Encyclopedia of Immunobiology* (Vol. 4). Elsevier. <https://doi.org/10.1016/B978-0-12-374279-7.14023-8>
- Nutt, S. L., & Kee, B. L. (2007). The Transcriptional Regulation of B Cell Lineage Commitment. *Immunity*, 26(6), 715–725. <https://doi.org/10.1016/j.immuni.2007.05.010>
- O’Conor, G. T. (1987). Malignant lymphoma in African children: three decades of discovery. *Princess Takamatsu Symposia*, 18, 137–147.
- Old, L. J. (1985). Tumor necrosis factor (TNF). *Science*, 230(4726), 630–632. <https://doi.org/10.1126/science.2413547>
- Onnis, A., & Baldari, C. T. (2019). Orchestration of Immunological Synapse Assembly by Vesicular Trafficking. *Frontiers in Cell and Developmental Biology*, 7(July), 1–12. <https://doi.org/10.3389/fcell.2019.00110>
- Popivanova, B. K., Kitamura, K., Wu, Y., Kondo, T., Kagaya, T., Kaneko, S., ... Mukaida, N. (2008). Blocking TNF- α in mice reduces colorectal carcinogenesis associated with chronic colitis. *Journal of Clinical Investigation*, 118(2), 560–570. <https://doi.org/10.1172/JCI32453>
- Py, B., Slomianny, C., Auberger, P., Petit, P. X., & Benichou, S. (2004). Siva-1 and an Alternative Splice Form Lacking the Death Domain, Siva-2, Similarly Induce Apoptosis in T Lymphocytes via a Caspase-Dependent Mitochondrial Pathway. *The*

- Journal of Immunology*, 172(7), 4008–4017.
<https://doi.org/10.4049/jimmunol.172.7.4008>
- Qu, Y., Zhao, G., & Li, H. (2017). Forward and reverse signaling mediated by transmembrane tumor necrosis factor- α and TNF receptor 2: Potential roles in an immunosuppressive tumor microenvironment. *Frontiers in Immunology*, 8(NOV). <https://doi.org/10.3389/fimmu.2017.01675>
- Quistad, S. D., & Traylor-Knowles, N. (2016). Precambrian origins of the TNFR superfamily. *Cell Death Discovery*, 2(1), 1–6.
<https://doi.org/10.1038/cddiscovery.2016.58>
- Radtke, F., MacDonald, H. R., & Tacchini-Cottier, F. (2013). Regulation of innate and adaptive immunity by Notch. *Nature Reviews Immunology*, 13(6), 427–437.
<https://doi.org/10.1038/nri3445>
- Raje, N., & Dinakar, C. (2015). Overview of Immunodeficiency Disorders. *Immunology and Allergy Clinics of North America*, 35(4), 599–623.
<https://doi.org/10.1016/j.iac.2015.07.001>
- Ray, A. (2016). Cytokines and their Role in Health and Disease: A Brief Overview. *MOJ Immunology*, 4(2), 1–9. <https://doi.org/10.15406/moji.2016.04.00121>
- Reinherz, E. L. (2014). Revisiting the discovery of the $\alpha\beta$ TCR complex and its co-receptors. *Frontiers in Immunology*, 5(NOV), 1–4.
<https://doi.org/10.3389/fimmu.2014.00583>
- Ribatti, D. (2017). Oncotarget 7175 www.impactjournals.com/oncotarget The concept of immune surveillance against tumors: The first theories. *Oncotarget*, 8(4), 7175–7180. Retrieved from www.impactjournals.com/oncotarget/
- Riether, C., Schürch, C. M., Flury, C., Hinterbrandner, M., Drück, L., Huguenin, A. L., ... Ochsenein, A. F. (2015). Tyrosine kinase inhibitor-induced CD70 expression mediates drug resistance in leukemia stem cells by activating Wnt signaling. *Science Translational Medicine* (Vol. 7). <https://doi.org/10.1126/scitranslmed.aab1740>
- Robinette, M. L., & Colonna, M. (2016). Immune modules shared by innate lymphoid cells and T cells. *Journal of Allergy and Clinical Immunology*, 138(5), 1243–1251.
<https://doi.org/10.1016/j.jaci.2016.09.006>
- Roca, F. J., Mulero, I., López-Muñoz, A., Sepulcre, M. P., Renshaw, S. A., Meseguer, J., & Mulero, V. (2008). Evolution of the Inflammatory Response in Vertebrates: Fish TNF- α Is a Powerful Activator of Endothelial Cells but Hardly Activates Phagocytes. *The Journal of Immunology*, 181(7), 5071–5081.

<https://doi.org/10.4049/jimmunol.181.7.5071>

- Romagnani, S. (1992). Type 1 T helper and type 2 T helper cells: Functions, regulation and role in protection and disease. *International Journal of Clinical & Laboratory Research*, 21(2–4), 152–158. <https://doi.org/10.1007/BF02591635>
- Rosenzweig, S. D., & Holland, S. M. (2004). Phagocyte immunodeficiencies and their infections. *Journal of Allergy and Clinical Immunology*, 113(4), 620–626. <https://doi.org/10.1016/j.jaci.2004.02.001>
- Rosenzweig, S. D., & Holland, S. M. (2011). Recent insights into the pathobiology of innate immune deficiencies. *Current Allergy and Asthma Reports*, 11(5), 369–377. <https://doi.org/10.1007/s11882-011-0212-9>
- Salzer, E., Daschkey, S., Choo, S., Gombert, M., Santos-Valente, E., Ginzel, S., ... Seidel, M. G. (2013). Combined immunodeficiency with life-threatening EBV-associated lymphoproliferative disorder in patients lacking functional CD27. *Haematologica*, 98(3), 473–478. <https://doi.org/10.3324/haematol.2012.068791>
- Skisiel, G. D., Bouchlaka, M. N., Monjazebe, A. M., Crittenden, M., Curti, B. D., Wilkins, D. E. C., ... Murphy, W. J. (2015). Out-of-Sequence Signal 3 Paralyzes Primary CD4+ T-Cell-Dependent Immunity. *Immunity*, 43(2), 240–250. <https://doi.org/10.1016/j.immuni.2015.06.023>
- Shabani, M., Nichols, K. E., & Rezaei, N. (2016). Primary immunodeficiencies associated with EBV-Induced lymphoproliferative disorders. *Critical Reviews in Oncology/Hematology*, 108, 109–127. <https://doi.org/10.1016/j.critrevonc.2016.10.014>
- Shannon-Lowe, C., & Rickinson, A. (2019). The Global Landscape of EBV-Associated Tumors. *Frontiers in Oncology*, 9(August), 1–23. <https://doi.org/10.3389/fonc.2019.00713>
- Sharpe, A. H. (2009). Mechanisms of costimulation. *Immunological Reviews*, 229(1), 5–11. <https://doi.org/10.1111/j.1600-065X.2009.00784.x>
- Shawky, R. M., Elsayed, S. M., Zaki, M. E., Nour El-Din, S. M., & Kamal, F. M. (2013). Consanguinity and its relevance to clinical genetics. *Egyptian Journal of Medical Human Genetics*, 14(2), 157–164. <https://doi.org/10.1016/j.ejmhg.2013.01.002>
- Simons, K. H., de Jong, A., Jukema, J. W., de Vries, M. R., Arens, R., & Quax, P. H. A. (2019). T cell co-stimulation and co-inhibition in cardiovascular disease: a double-edged sword. *Nature Reviews Cardiology*, 16(6), 325–343. <https://doi.org/10.1038/s41569-019-0164-7>

- Spits, H. (2002). Development of $\alpha\beta$ T cells in the human thymus. *Nature Reviews Immunology*, 2(10), 760–772. <https://doi.org/10.1038/nri913>
- Starzer, A. M., & Berghoff, A. S. (2020). New emerging targets in cancer immunotherapy: CD27 (TNFRSF7). *ESMO Open*, 4. <https://doi.org/10.1136/esmoopen-2019-000629>
- Sun, M., & Fink, P. J. (2007). A New Class of Reverse Signaling Costimulators Belongs to the TNF Family. *The Journal of Immunology*, 179(7), 4307–4312. <https://doi.org/10.4049/jimmunol.179.7.4307>
- Takeuchi, A., & Saito, T. (2017). CD4 CTL, a cytotoxic subset of CD4⁺ T cells, their differentiation and function. *Frontiers in Immunology*, 8(FEB), 1–7. <https://doi.org/10.3389/fimmu.2017.00194>
- Takeuchi, O., & Akira, S. (2010). Pattern Recognition Receptors and Inflammation. *Cell*, 140(6), 805–820. <https://doi.org/10.1016/j.cell.2010.01.022>
- Thakur, A., Mikkelsen, H., & Jungersen, G. (2019). Intracellular pathogens: Host immunity and microbial persistence strategies. *Journal of Immunology Research*, 2019. <https://doi.org/10.1155/2019/1356540>
- Van Montfrans, J. M., Hoepelman, A. I. M., Otto, S., Van Gijn, M., Van De Corput, L., De Weger, R. A., ... Tesselaar, K. (2012). CD27 deficiency is associated with combined immunodeficiency and persistent symptomatic EBV viremia. *Journal of Allergy and Clinical Immunology*, 129(3), 787-793.e6. <https://doi.org/10.1016/j.jaci.2011.11.013>
- van Schoonhoven, A., Huylebroeck, D., Hendriks, R. W., & Stadhouders, R. (2020). 3D genome organization during lymphocyte development and activation. *Briefings in Functional Genomics*, 19(2), 71–82. <https://doi.org/10.1093/bfpg/elz030>
- Vidal, M. (2010). The dark side of fly TNF: An ancient developmental proof reading mechanism turned into tumor promoter. *Cell Cycle*, 9(19), 3851–3856. <https://doi.org/10.4161/cc.9.19.13280>
- Wajant, H. (2003). Death receptors. *Essays in Biochemistry*, 39, 53–71. <https://doi.org/10.1042/bse0390053>
- Wälchli, S., Løset, G. Å., Kumari, S., Johansen, J. N., Yang, W., Sandlie, I., & Olweus, J. (2011). A practical approach to T-cell receptor cloning and expression. *PLoS ONE*, 6(11). <https://doi.org/10.1371/journal.pone.0027930>
- Walling, B. L., & Kim, M. (2018). LFA-1 in T cell migration and differentiation. *Frontiers in Immunology*, 9(MAY). <https://doi.org/10.3389/fimmu.2018.00952>

- Wasiuk, A., Testa, J., Weidlick, J., Sisson, C., Vitale, L., Widger, J., ... He, L.-Z. (2017). CD27-Mediated Regulatory T Cell Depletion and Effector T Cell Costimulation Both Contribute to Antitumor Efficacy. *The Journal of Immunology*, 199(12), 4110–4123. <https://doi.org/10.4049/jimmunol.1700606>
- Watts, T. H. (2005). Tnf/Tnfr Family Members in Costimulation of T Cell Responses. *Annual Review of Immunology*, 23(1), 23–68. <https://doi.org/10.1146/annurev.immunol.23.021704.115839>
- Wu, Y., Anasetti, C., & Yu, X.-Z. (2019). *T-Cell Costimulation and Coinhibition in Graft-Versus-Host Disease and Graft-Versus-Leukemia Effect. Immune Biology of Allogeneic Hematopoietic Stem Cell Transplantation*. Elsevier Inc. <https://doi.org/10.1016/b978-0-12-812630-1.00011-6>
- Xie, P. (2013). TRAF molecules in cell signaling and in human diseases. *Journal of Molecular Signaling*, 8(1), 1. <https://doi.org/10.1186/1750-2187-8-7>
- Xu, Y., Chang, L., Huang, A., Liu, X., Liu, X., Zhou, H., ... Liang, P. (2017). Functional Detection of TNF Receptor Family Members by Affinity-Labeled Ligands. *Scientific Reports*, 7(1), 1–7. <https://doi.org/10.1038/s41598-017-06343-4>
- Yamamoto, T., Hattori, M., & Yoshida, T. (2007). Induction of T-cell activation or anergy determined by the combination of intensity and duration of T-cell receptor stimulation, and sequential induction in an individual cell. *Immunology*, 121(3), 383–391. <https://doi.org/10.1111/j.1365-2567.2007.02586.x>
- Yang, S., Xie, C., Chen, Y., Wang, J., Chen, X., Lu, Z., ... Zheng, S. G. (2019). Differential roles of TNF α -TNFR1 and TNF α -TNFR2 in the differentiation and function of CD4 + Foxp3 + induced Treg cells in vitro and in vivo periphery in autoimmune diseases. *Cell Death and Disease*, 10(1). <https://doi.org/10.1038/s41419-018-1266-6>
- Yasmin, R., Siraj, S., Hassan, A., Khan, A. R., Abbasi, R., & Ahmad, N. (2015). Epigenetic regulation of inflammatory cytokines and associated genes in human malignancies. *Mediators of Inflammation*, 2015. <https://doi.org/10.1155/2015/201703>
- Yel, L. (2010). Selective IgA Deficiency. *Journal of Clinical Immunology*, 30(1), 10–16. <https://doi.org/10.1007/s10875-009-9357-x>
- Yokosuka, T., Kobayashi, W., Sakata-Sogawa, K., Takamatsu, M., Hashimoto-Tane, A., Dustin, M. L., ... Saito, T. (2008). Spatiotemporal Regulation of T Cell Costimulation by TCR-CD28 Microclusters and Protein Kinase C θ Translocation.

- Immunity*, 29(4), 589–601. <https://doi.org/10.1016/j.immuni.2008.08.011>
- Zhao, Y., Niu, C., & Cui, J. (2018). Gamma-delta ($\gamma\delta$) T Cells: Friend or Foe in Cancer Development. *Journal of Translational Medicine*, 16(1), 1–13. <https://doi.org/10.1186/s12967-017-1378-2>
- Zheng, Y., Zha, Y., & Gajewski, T. F. (2008). Molecular regulation of T-cell anergy. *EMBO Reports*, 9(1), 50–55. <https://doi.org/10.1038/sj.embor.7401138>
- Zhou, X., Ramachandran, S., Mann, M., & Popkin, D. L. (2012). Role of lymphocytic choriomeningitis virus (LCMV) in understanding viral immunology: Past, present and future. *Viruses*, 4(11), 2650–2669. <https://doi.org/10.3390/v4112650>
- Zinkernagel, R. M., & Doherty, P. C. (1997). The discovery of MHC restriction. *Immunology Today*, 18(1), 14–17. [https://doi.org/10.1016/S0167-5699\(97\)80008-4](https://doi.org/10.1016/S0167-5699(97)80008-4)

APPENDIX A - Chemicals

Chemicals and Media Components	Supplier Company
Acetic acid (glacial)	Merck Millipore, USA
Agarose	Sigma, Germany
Ampicillin Sodium Salt	Cellgro, USA
Boric acid	Molekula France
Chloroquine	Sigma, Germany
Distilled water	Merck Millipore, USA
DMEM	Gibco, USA
DNA Gel Loading Dye, 6X	NEB, USA
DPBS	Sigma, Germany
EDTA	Sigma, Germany
Ethanol	Sigma, Germany
Ethidium Bromide	Sigma, Germany
Fetal Bovine Serum	Thermo Fischer Scientific, USA
Glycerol	Sigma, Germany
HEPES Solution, 1M	Sigma, Germany
Histopaque®-1077	Sigma, Germany
Hydrochloric acid	Sigma, Germany
Isopropanol	Sigma, Germany
L-glutamine	Thermo Fischer Scientific, USA
LB Agar	Sigma, Germany
LB Broth	Invitrogen, USA
MEM Non-Essential Amino Acid Solution	Thermo Fischer Scientific, USA
Methanol	Sigma, Germany
Paraformaldehyde (PFA)	BioLegend, USA
PBS	Thermo Fischer Scientific, USA
Penicillin/Streptomycin	Thermo Fischer Scientific, USA
pH (4.0) Buffer Solution	Merck Millipore, USA
pH (7.0) Buffer Solution	Merck Millipore, USA
PIPES	Sigma, Germany
Poly-L-Lysine	Sigma, Germany
Proteamine Sulfate	Sigma, Germany
Potassium Acetate	Merck Millipore, USA
Potassium Chloride	Sigma, Germany
RNase A	Roche, Germany
RPMI 1640	Thermo Fischer Scientific, USA
Saponin	Sigma, Germany
Sodium Chloride	Amresco, USA
Tris Base	Sigma, Germany
Tris Hydrochloride	Amresco, USA
TRIzol Reagent	Invitrogen, USA
Trypan Blue Solution	Thermo Fischer Scientific, USA
Trypsin EDTA	Invitrogen, USA

APPENDIX B – Equipments

Equipment	Supplier Company
Autoclave	HiClave HV-110, Hirayama, Japan
Balance	Isolab, Germany
Centrifuge	5418R, Eppendorf, Germany 5702, Eppendorf, Germany 5415R Eppendorf, Germany Allegra X-15R Beckman Coulter, USA
CO ₂ Incubator	Binder, Germany
Deepfreeze	-80, Forma 88000 Series, Thermo Fischer Scientific, USA
Electrophoresis Apparatus	VWR, USA
Filters (0.22 µm and 0.45 µm)	Merck Millipore, USA
Flow Cytometer	BD LSR Fortessa, USA
Freezing Container	Mr. Frosty, Thermo Fischer Scientific, USA
Gel Documentation	Gel Doc EZ, Biorad, USA
Heater	Thermomixer Comfort, Eppendorf, Germany
Hemocytometer	Neubauer Improved, Isolab, Germany
Ice Machine	Hausser Scientific, Blue Bell Pa., USA
Incubator	AF20, Scotsman Inc., USA BE300, Memmert, Germany
Incubator Shaker	Memmert, Modell 300, Germany
Laminar Flow	Memmert, Modell 600, Germany Innova 44, New Brunswick Scientific, USA
Liquid Nitrogen Tank	HeraSafe HS15, Heraeus, Germany
Magnetic Stirrer	HeraSafe HS12, Heraeus, Germany
Microliter Pipettes	Heraeus, HeraSafe KS, Germany Taylor-Wharton, 300RS, USA SB162, Stuart, UK
Microscope	Thermo Fischer Scientific, USA Gilson, Pipetman, France
Microvawe Oven	Isolab, Germany
pH Meter	Primover, Zeiss, Germany
Refrigerator	CK40, Olympus, Japan Bosch, Germany SevenCompact, Mettler Toledo, USA Bosch, Germany Arcelik, Turkey Panasonic, Japan
Spectrophotometer	NanoDrop 2000, Thermo Fischer Scientific, USA UltraSpec 2100 pro, Amersham Biosciences, UK
Thermal Cycler	C1000 Touch, Biorad, USA

Vortex	PTC-200, MJ Research Inc., Canada
Water Bath	VWR, USA Innova 3100, New Brunswick Scientific

APPENDIX C - Molecular Biology Kits

Commercial Kit	Supplier Company
NucleoSpin Gel and PCR Clean-up	Macharey-Nagel, USA
Plasmid DNA purification (NucleoBond® Xtra Midi/Maxi)	Macharey-Nagel, USA
PureLink Genomic DNA Mini Kit	Invitrogen, USA
RevertAid First Strand cDNA Synthesis Kit	Fermantas
Q5 Site-Directed Mutagenesis Kit	NEB, USA
Zero Blunt TOPO PCR Cloning Kit for Sequencing	Thermo Fischer Scientific, USA

APPENDIX D – Antibodies

Antibody	Supplier Company	Clone
APC mouse IgG1, κ isotype control	BioLegend (400119)	MOPC-21
APC mouse anti-human CD70 antibody	BioLegend (355101)	113-16
PE mouse anti-human CD70 antibody	BD Biosciences (555835)	Ki-24

APPENDIX E - DNA Ladder

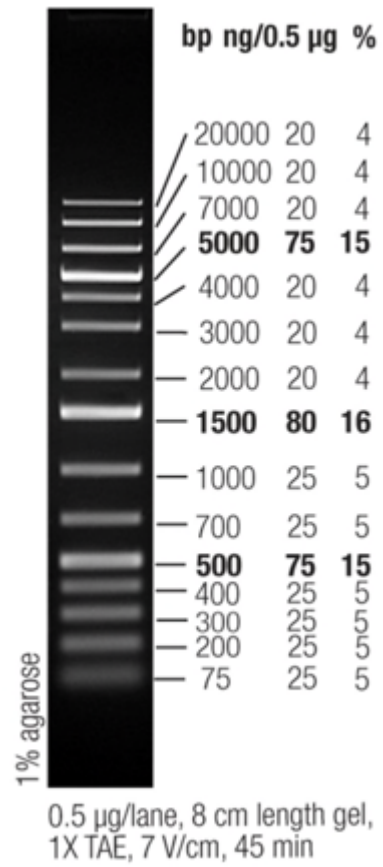


**Figure D1. GeneRuler DNA Ladder Mix (SM1331),
Thermo Fischer Scientific, USA**

APPENDIX F - Plasmid Maps

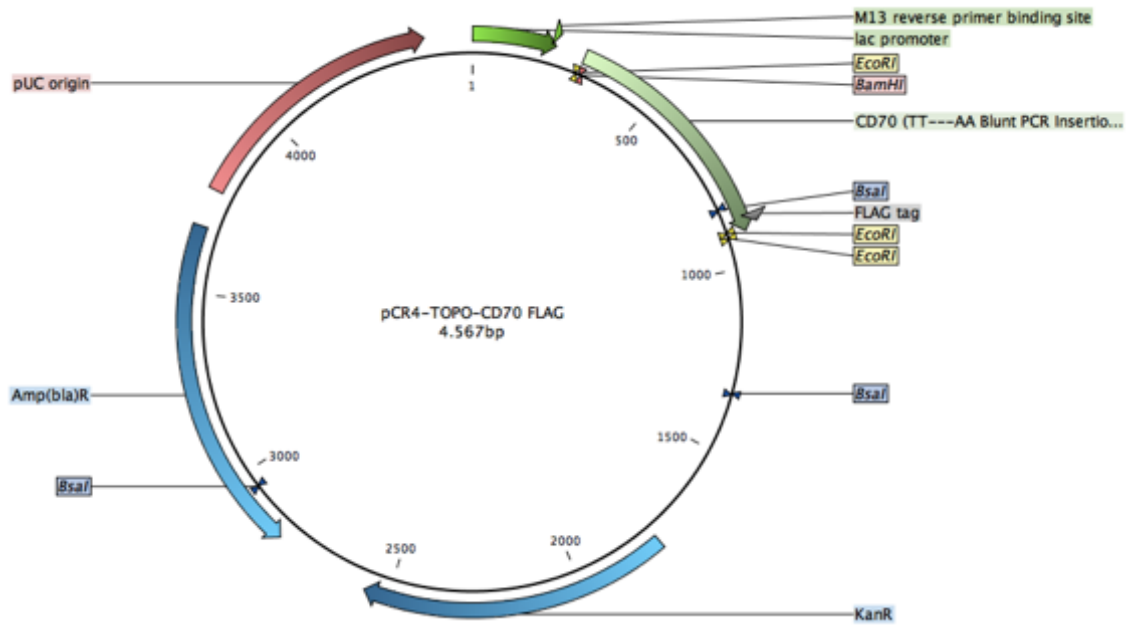


Figure F1. The plasmid map of pCR4-TOPO-CD70 FLAG

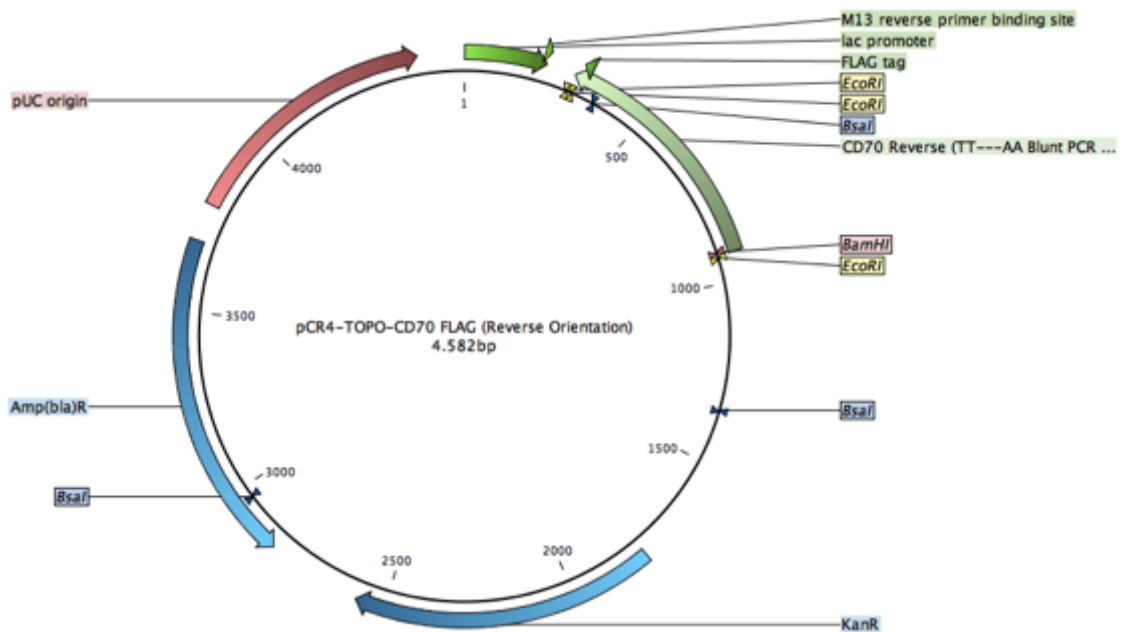


Figure F2. The plasmid map of pCR4-TOPO-CD70 FLAG (Reverse Orientation)

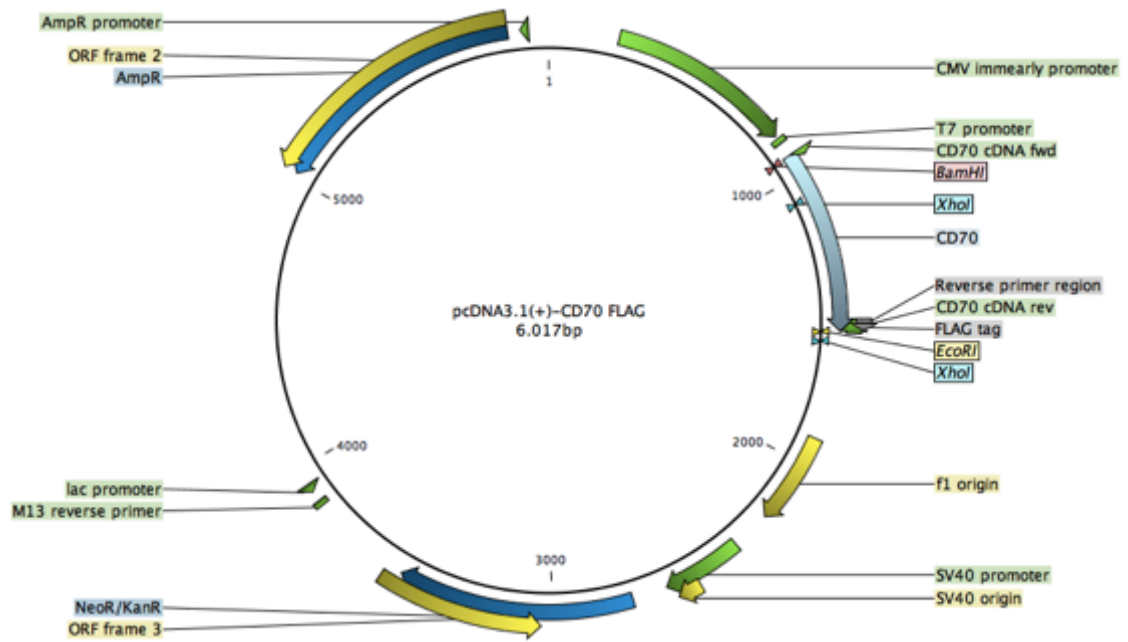


Figure F3. The plasmid map of pcDNA3.1(+)-CD70 FLAG

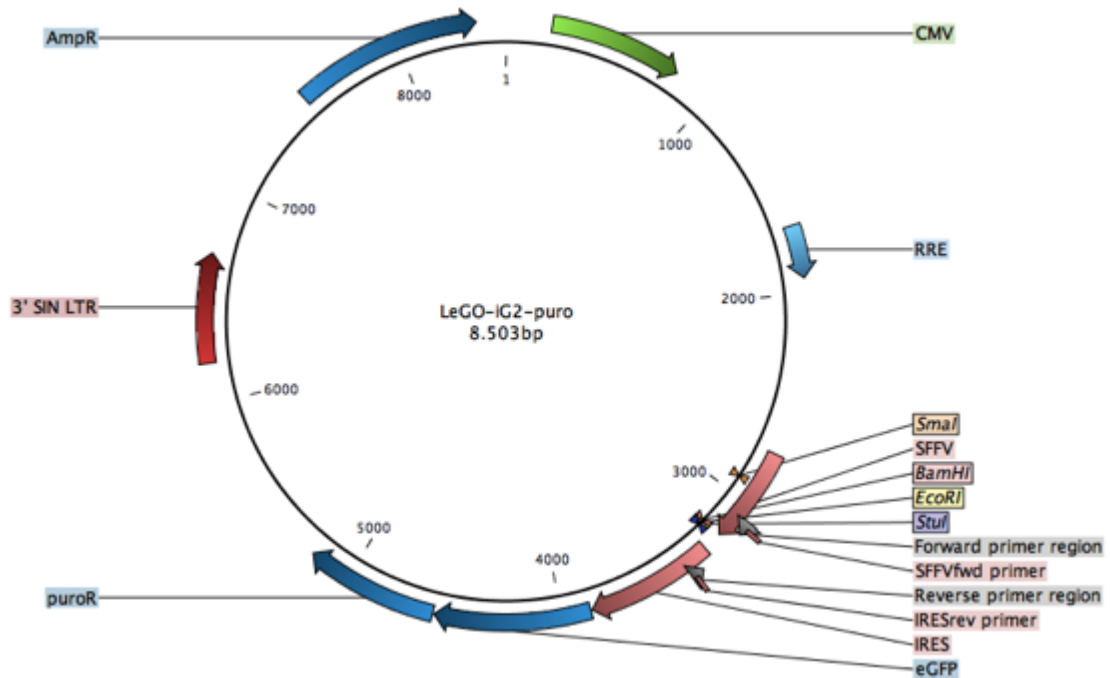


Figure F4. The plasmid map of LeGO-iG2-puro

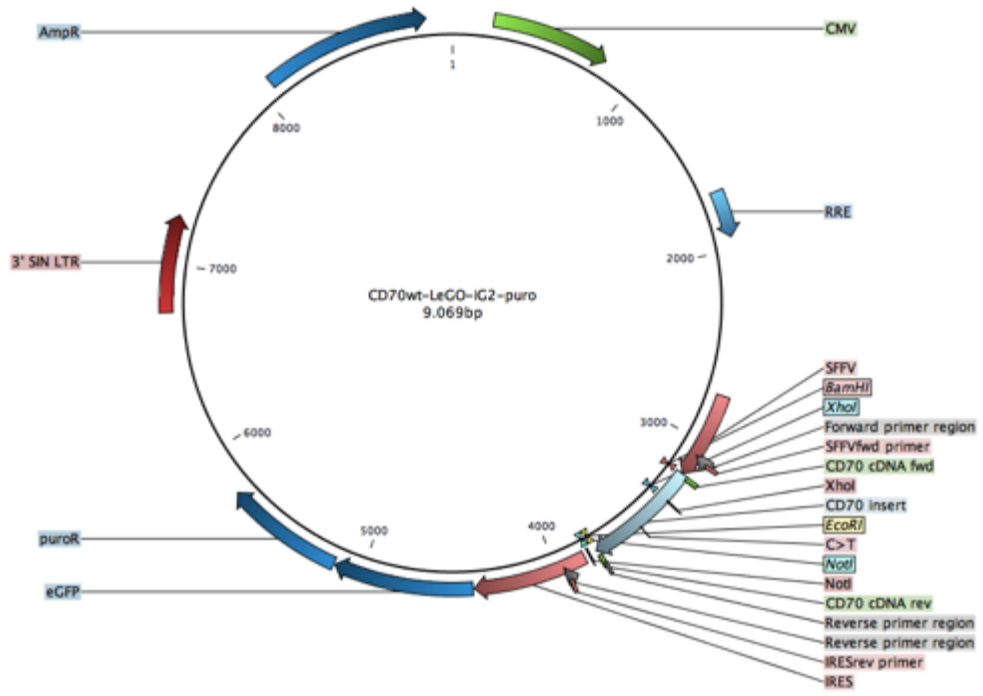


Figure F5. The plasmid map of CD70wt-LeGO-iG2-puro

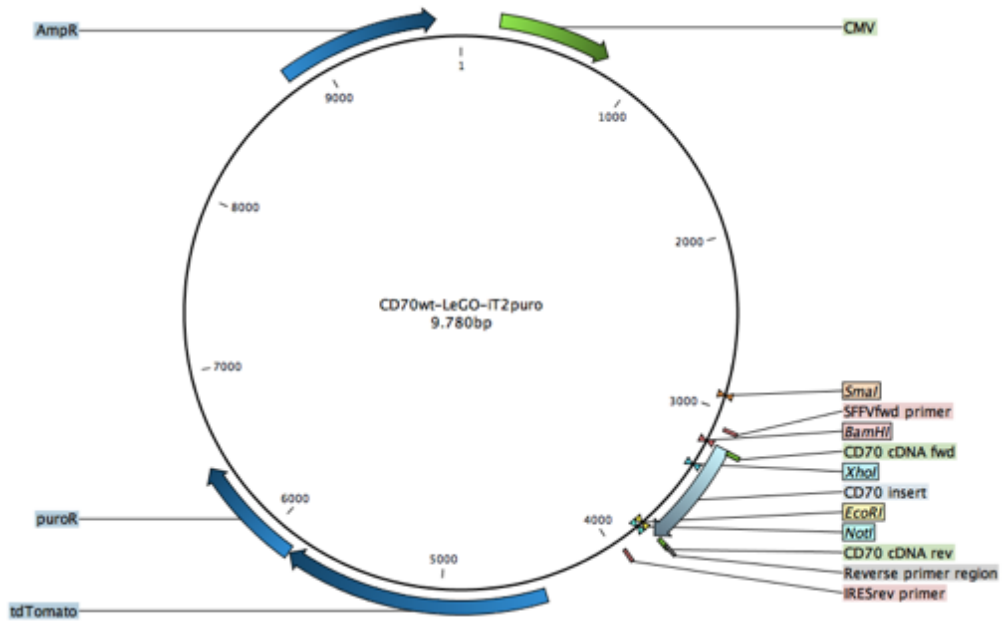


Figure F6. The plasmid map of CD70wt-LeGO-iT2-puro

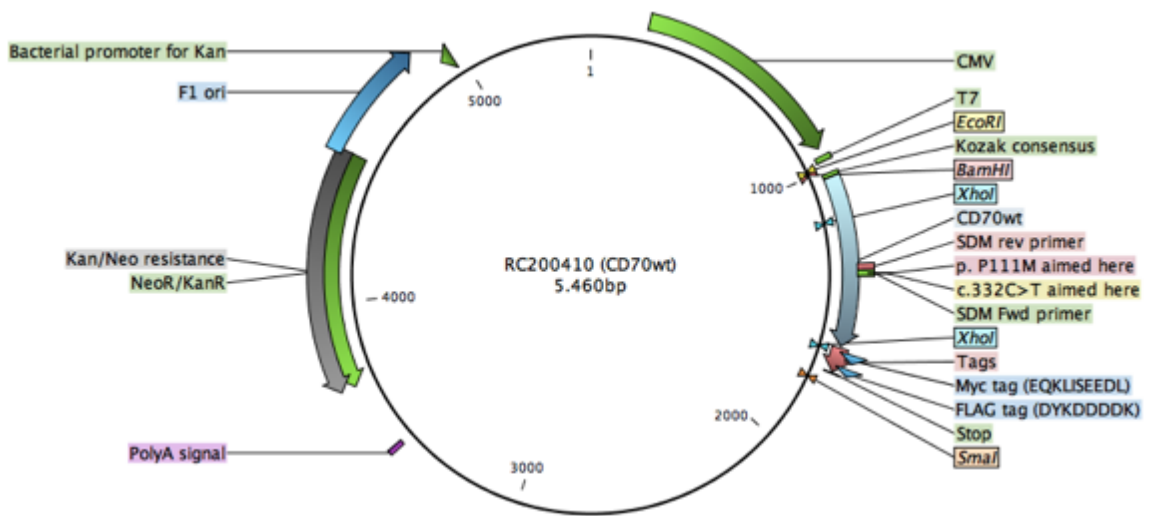


Figure F7. The plasmid map of RC200410 (CD70wt)

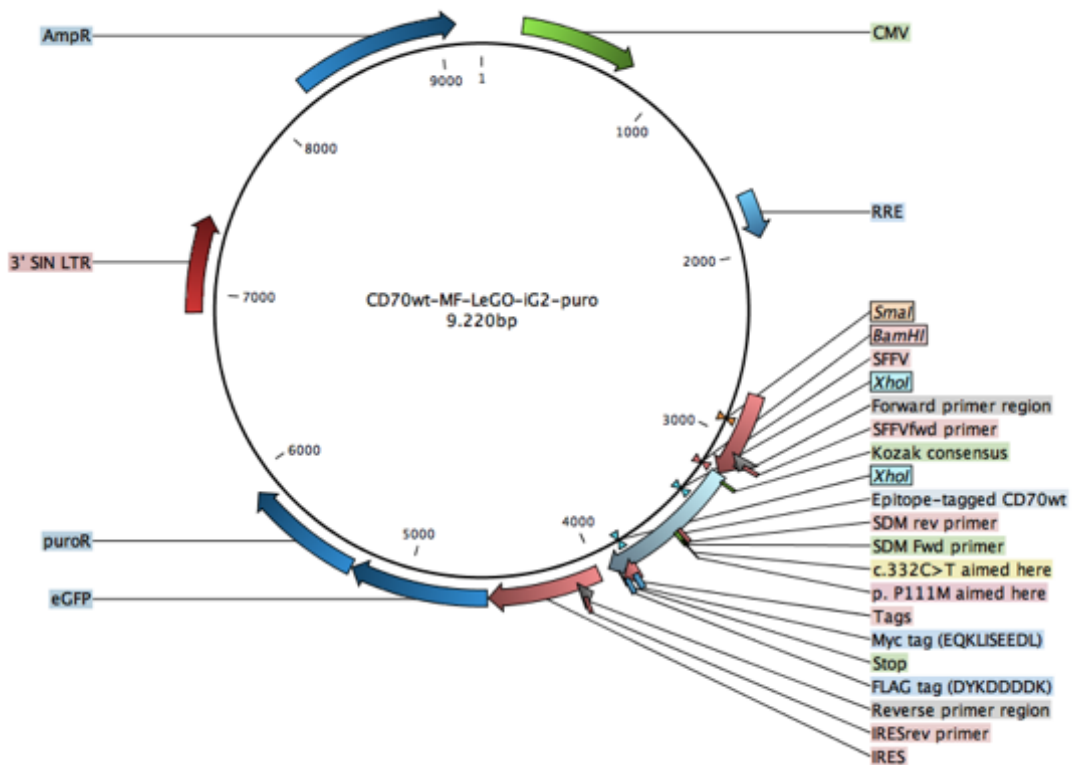


Figure F8. The plasmid map of CD70wt-MF-LeGO-iG2-puro

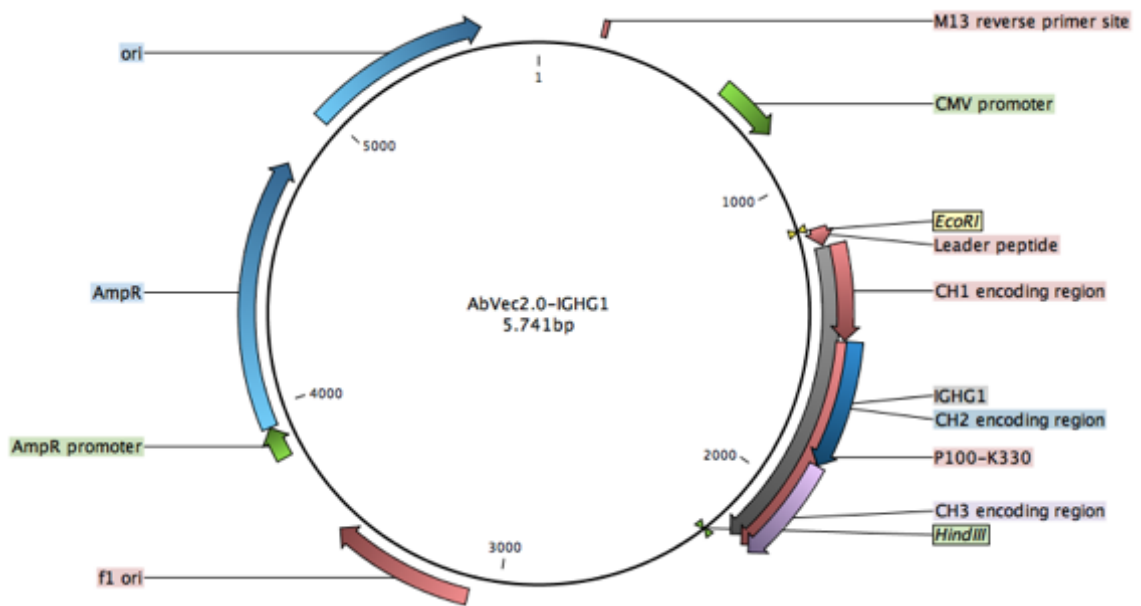


Figure F9. The plasmid map of Abvec2.0-IGHG1

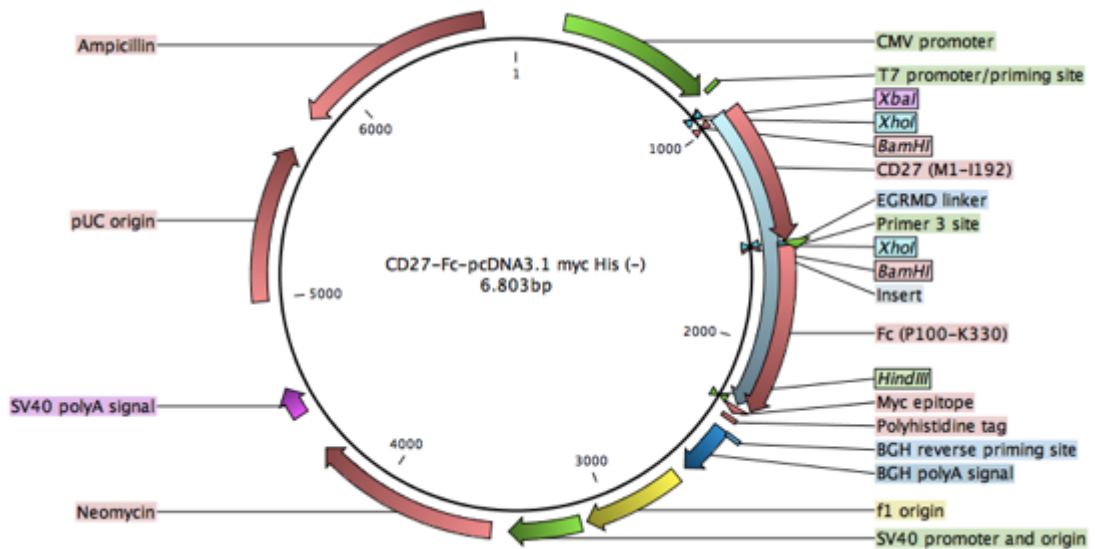


Figure F10. The plasmid map of CD27-Fc-pcDNA3.1 myc His (-)

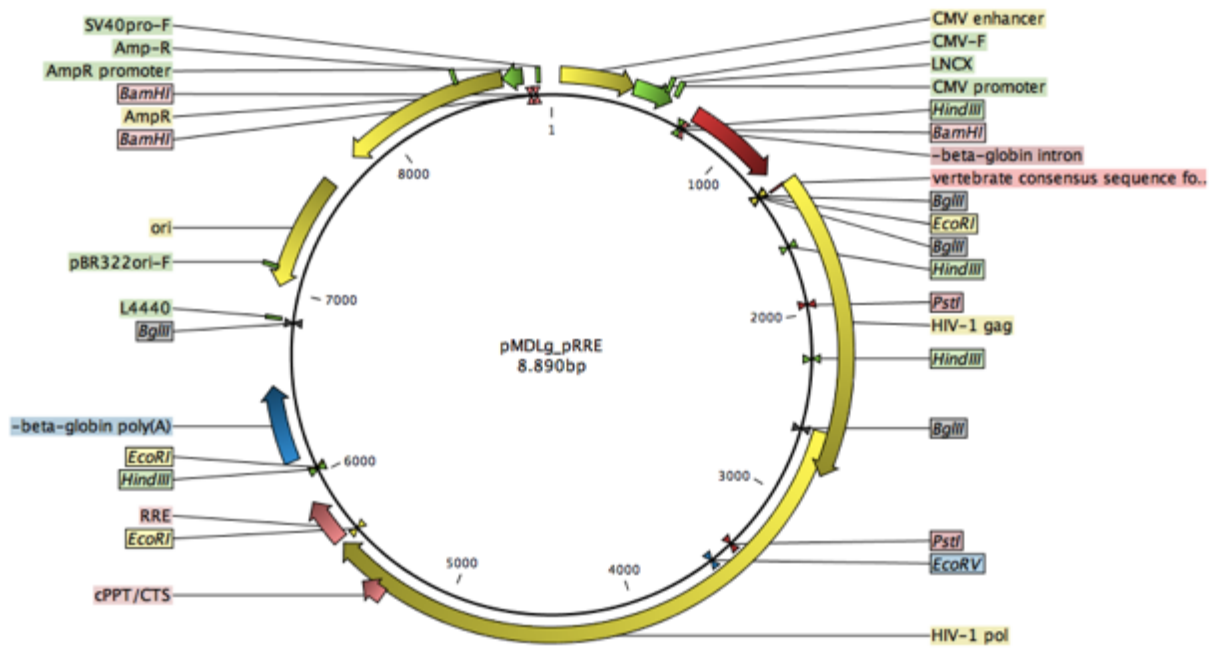


Figure F10. The plasmid map of pMDLg/pRRE

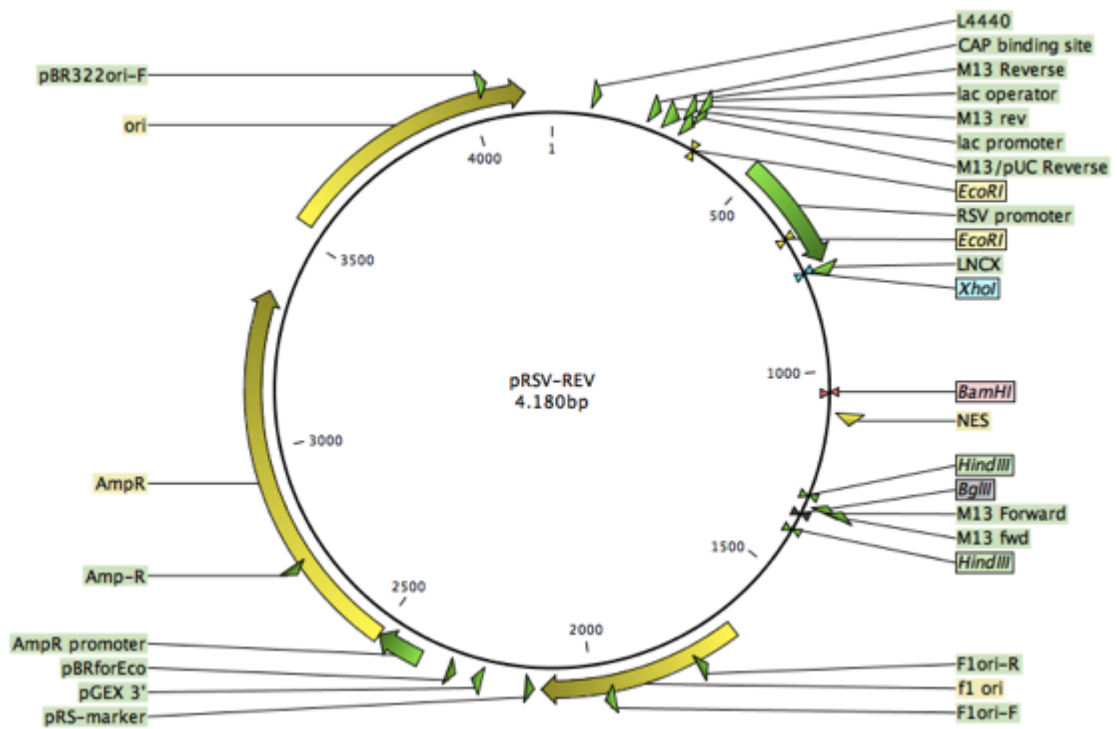


Figure F9. The plasmid map of pRSV-REV

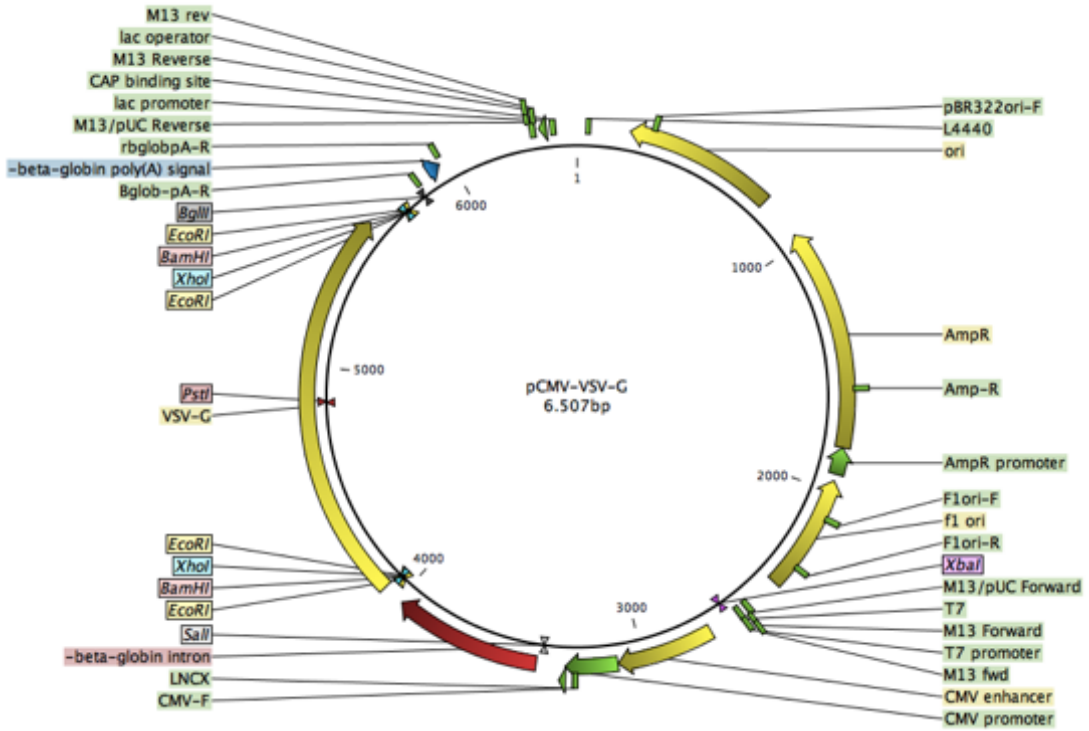


Figure F9. The plasmid map of pCMV-VSV-G